

https://dspace.org/

Isolation and characterisation of novel broadly neutralising antibodies from rabbits immunised with the HIV-1 Env/2dCD4S60C immune complex

Smith, Simone

2020
https://hdl.handle.net/10539/31974

Downloaded from a DSpace repository. https://dspace.org/

Isolation and characterisation of novel broadly neutralising antibodies from rabbits immunised with the HIV-1 Env/2dCD4^{S60C} immune complex.

Simone Smith (806594)



A dissertation submitted to the Faculty of Health Sciences, University of the Witwatersrand, Johannesburg, in fulfilment of the requirements for the degree of Master of Science in Medicine.

November 2020

Declaration

I, Simone Ashleigh Smith declare that this dissertation is my own work. It is being submitted for the degree of Master of Science in Medicine in the University of the Witwatersrand, Johannesburg. It has not been submitted before for any degree or examination at this or any other University.



Simone Ashleigh Smith

19th day of November 2020

Conference presentations arising from this study

1. Smith, S.A., Tumba, N.L., Killick, M.A., Papathanasopoulos, M.A., Isolation and Characterisation of Novel Broadly Neutralising Antibodies from Rabbits Immunised with the HIV-1 Env/2dCD4^{S60C} Immunogen Complex. June 2019, 9th SA AIDS conference, Durban ICC, Durban, SA. Poster Presentation.
2. Smith, S.A., Tumba, N.L., Killick, M.A., Papathanasopoulos, M.A., Isolation and Characterisation of Novel Broadly Neutralising Antibodies from Rabbits Immunised with the HIV-1 Env/2dCD4^{S60C} Immunogen Complex. September 2019, 10th Cross-faculty postgraduate symposium, Wits University, Johannesburg, SA. Oral presentation.

Abstract

Developing a safe and effective prophylactic vaccine against HIV-1 still remains the most effective strategy for controlling and eliminating the worldwide health burden of HIV infection. In order for an HIV-1 vaccine to be effective, it would need to elicit "long-lasting" broadly neutralizing antibody (bNAb) responses capable of providing protection against a large number of globally circulating HIV-1 subtypes. The development of effective vaccines by previous human clinical trials have failed to elicit protective immunity, and this may be due to the many challenges of HIV-1 vaccine design including the conformation-dependent exposure of critical epitopes in an immunogen. The viral envelope glycoprotein (Env; the target of bNAbs) binding to CD4 exposes epitopes which are masked in the unbound Env conformation, such as CD4 induced epitopes that are subsequently exposed during the open Env conformation. A preliminary study performed by our laboratory testing various HIV-1 Env/2dCD4^{S60C} immune complexes in rabbit immunisations have demonstrated that it is possible to generate antibodies capable of neutralising tier-2 (harder to neutralise) HIV-1 pseudoviruses *in vitro*. The aim of this study was to delineate the neutralising responses observed in these Env/2dCD4^{S60C} immunised rabbits by isolating and characterising the monoclonal antibodies from these sera. The first objective was to confirm the presence of neutralising antibody responses elicited by the immunized New Zealand white rabbits in response to a booster with the immunogen complex using the TZM-bl based neutralising assays. The trimeric gp140$_{GCN4}$ and 2dCD4^{S60C} were expressed, purified, and complexed for use in the rabbit booster immunizations. Next, we sought to sort for single antigen-specific memory B cells using a multi-parameter Flow Cytometry and Fluorescence Activated Cell Sorting (FACS) technique. Following single cell sorting, transcriptionally active linear expression cassettes (TAPs) were assembled by PCR. The linear cassettes containing a promoter, the antibodies variable and constant regions and a terminator sequence were assembled in a mammalian expression vector system as TAPs. Matched linear cassettes pairs (heavy- and light-chains) were co-transfected in HEK 293T mammalian cells and tissue culture supernatants were collected, concentrated and evaluated for monoclonal antibody expression. Concentrated culture supernatants were tested to determine the binding activity of the expressed antibodies, and confirm size and identity using ELISAs and SDS-PAGE/western blot analyses, respectively. Using the TZM-bl neutralization assay, our results confirmed the persistence of circulating neutralizing antibody responses two years after the last

immunization (new baseline) against a heterologous, tier-2 clinically relevant pseudovirus, ZM53M.PB12. In addition, we demonstrated that these specific neutralization titres (ID_{50}) could once again be elevated in three rabbits following a single boosting immunization with the Env/2dCD4^{S60C} complex. Anti-HIV-1 specific B cells from rabbit PMBCs post booster were successfully isolated and sorted as single cells using multi-parameter Flow Cytometry and FACS techniques. All elements of the TAP cassette were successfully PCR amplified from the sorted B cells, however, subsequent analysis showed that the antibody variable fragments were missing from the assembled TAP cassettes. As such, the expressed proteins failed to bind the Env, 2dCD4^{S60C} and Env/2dCD4^{S60C} antigens in an ELISA, and the presence of truncated antibody fragments was confirmed in the immunoblot assays. Overall, the durability of the bNAb response elicited by immunization with the Env-2dCD4^{S60C} complex were confirmed, highlighting the importance of isolating and characterizing the monoclonal antibodies responsible for neutralization, and future strategies can optimize the protocols described here.

Acknowledgements

Firstly, and most importantly, I would thank and give God glory, for the guidance, wisdom, strength and grace I have been granted to complete my degree.

I would also like to express my utmost gratitude and sincerest appreciation to everyone that contributed to journey of completing my research project;

To my supervisors, Mrs. Nancy Meulenburg, Dr. Mark Killick, and Prof. Maria Papathanasopoulos, thank you for all of your unconditional support, and for all of the opportunities that you have offered me throughout the years. Thank you for your patience with me, your motivation and for always calming me down when I felt overwhelmed. Thank you for your scientific expertise, wisdom and guidance. I am extremely grateful to have had you all as my supervisors.

To Nazma Mansoor and Rozanne Adams from BD Biosciences, thank you for giving up your time to train and assist me with the use of FACS Aria II, your assistance was highly appreciated.

To my friends and colleagues at the HIV Pathogenesis Research Unit (HPRU), thank you for the advice, support and willingness to always help me. To Thulile, Gavin, and Adriaan, thank you for your support and mentorship which assisted my scientific journey. To Roberto, Melanie, and Dominic, thank you for all of the silly conversations, and for your overall contribution to making the long hours worth it. To Tumelo, thank you for your selfless help in the laboratory and encouraging advice, to Nelia, thank you for all of the long morning discussions, and to Ashlyn who I have been on this journey with since our Honours degree, thank you for the encouragement, support and friendship over the past few years.

To my parents, sister, niece, and extended family, thank you for the opportunity and thank you for every selfless sacrifice made for me to pursue this degree. Thank you always being my pillar of strength, and for all of the encouragement, I definitely would have never been able to complete this degree without your support.

Table of Contents

Declaration ii

Conference presentations arising from this study iii

Abstract iv

Acknowledgements vi

List of figures xi

List of tables xii

List of abbreviations xiii

1. Introduction 1

1.1. The HIV-1 pandemic 1

1.2. HIV-1 life cycle 3

1.3. HIV-1 life cycle inhibitors 7

1.4. Immune responses to HIV-1 infection 7

1.4.1. Acute infection 7

1.4.2. Chronic infection 8

1.4.3. Innate Immune system 9

1.4.4. Adaptive immune system 10

1.5. HIV-1 Phase IIb/III vaccine trials 12

1.6. HIV-1 specific broadly neutralising antibodies 17

1.6.1. Antibody structure 18

1.6.2. Broadly neutralising antibody epitopes 20

1.7. Broadly neutralising antibodies and their role in HIV-1 vaccine development 25

1.8. Rationale for study 28

2. Materials and Methods 30

2.1. Reagents used in this study 30
2.1.1. Reagents used for TZM-bl-based neutralisation assays 30
2.2. General mammalian cell culture 31
2.2.1. Reviving frozen rabbit Peripheral Blood Mononuclear Cells (PBMCs) 31
2.3. Recombinant protein expression 32
2.3.1. 2dCD4 expression and purification 32
2.3.2. CAP45 GCN4(+) gp140 expression 32
2.3.3. CAP45 GCN4 (+) gp140 purification 33
2.4. Confirmation and boosting of anti- HIV-1 neutralising antibodies in rabbit sera 35
2.4.1. Neutralising antibody assay 36
2.5. Rabbit antigen specific B memory cell isolation 37
2.5.1. Peripheral Blood Mononuclear Cells (PBMCs) Isolation 37
2.5.2. Antigen-specific memory B-cell isolation by Fluorescence activated cell sorting (FACS) 38
2.6. PCR amplification of the transcriptionally active linear cassette 42
2.7. Recombinant protein expression 47
2.7.1. Small-scale antibody expression studies from the transcriptionally active linear expression cassettes 47
2.7.2. Binding activity of the expressed antibodies to $gp140_{GCN4}$ Env and $2dCD4^{WT}$ using Enzyme Linked Immunosorbent Assay (ELISA) 48
2.7.3. Determining monoclonal antibody expression using Sodium dodecyl sulphate-polyacrylamide gel electrophoresis (SDS-PAGE) and western blot 49
3. Results 52
3.1. CAP45GCN4 expression and purification 52
3.1.1. Expression of $gp140_{GCN4}$ Env 52
3.1.2. Purification of trimeric $gp140_{GCN4}$ 53

3.2. Confirmation of the $gp140_{GCN4}$ Env/2dCD4^{S60C} neutralising responses 53
3.3. Antigen-specific memory B cell isolation 56
3.4. PCR amplification of the transcriptionally active linear cassette (TAP) 59
3.4.1. Heavy and light chain antibody variable region amplification 59
3.4.2. Amplification of the individual transcriptionally active linear cassette (TAP) constituents 60
3.4.3. Transcriptionally active linear cassette assembly 62
3.5. Evaluation of rabbit monoclonal antibody expression 65
3.5.1. Enzyme-linked immunosorbent assay (ELISA) for the detection of recombinantly expressed monoclonal antibodies in culture supernatants 65
3.5.2. Confirmation of antibody expression by SDS-PAGE and western blot analysis ... 66
4. Discussion 71
4.1. Confirmation of the elicitation of broadly neutralizing responses by the HIV-1 $gp140_{GCN4}$ Env/2dCD4^{S60C} immunogen complex 72
4.2. Antigen-specific rabbit memory B-cell isolation 73
4.3. Antibody expression of transcriptionally active linear cassettes 76
4.4. Conclusion and future work 79
References 80
Appendix A: Supplementary figures 96
Appendix B: Human Ethics waiver 100
Appendix C: Animal ethics approval 101
Appendix D: Recipes 105
B1) Agarose gel electrophoresis 105
B1.1) Preparation of 0.8% agarose gels 105
B1.2) Agarose gel electrophoresis procedure 105
B2) SDS-PAGE 105

B2.1) Monomer Solution: 30% Acrylamide/ 0.8% Bisacrylamide 105
B2.2) Stacking Gel Buffer: 4X Tris-HCl, pH 6.8 (0.5 M Tris) 106
B2.3) Separating Gel Buffer: 4X Tris-HCl, pH 8.8 (1.5 M Tris) 106
B2.5) 10% Ammonium Persulphate (APS) 106
B2.6) 10×Tank Buffer 106
Appendix E: Plagiarism form 107

List of figures

Figure 1.1: HIV-1 statistics for East and Southern Africa at the end of 2018. Image obtained from [2]. ... 2
Figure 1.2: Schematic representation of the HIV-1 trimeric envelope glycoprotein made up of the non-covalently bound gp120 and gp41 subunits. Image obtained from [22]. ... 4
Figure 1.3: The HIV-1 viral life cycle, showing the seven stages of infection of a CD4 positive T cell. Image obtained from [24]. ... 6
Figure 1.4: Schematic representation of the structure of an antibody. Image obtained from [149]. ... 19
Figure 1.5: Sites of broadly neutralising antibody epitopes on the HIV-1 envelope glycoprotein. Image obtained from [156]. ... 21
Figure 1.6: The high mannose patch broadly neutralizing antibody binding site on the HIV-1 envelope glycoprotein. Image obtained from [181]. ... 24
Figure 1.7: The native-like, soluble, trimeric conformation of SOSIP.664 gp140. Image obtained from [202]. ... 27
Figure 3.1: Western blot analysis of the expressed HIV-1 $gp140_{GCN4}$ envelope glycoprotein. ... 52
Figure 3.2: The purification of trimeric $gp140_{GCN4}$ using size exclusion chromatography. ... 53
Figure 3.3: Determination of elicited HIV-1 neutralising antibody titres in $gp140_{GCN4}$ Env/$2dCD4^{S60C}$ immunised rabbits. ... 55
Figure 3.4: The gating strategy for identification of rabbit antigen-specific memory B cells from immunised rabbits. ... 58
Figure 3.5: PCR amplification of rabbit heavy- and light-chain antibody variable regions. ... 59
Figure 3.6: PCR amplification of rabbit antibody variable fragments, heavy- and light-chain secondary PCRs. ... 61
Figure 3.7: PCR amplification of the CMV promotor, and the antibody constant regions including the polyA tail. ... 62
Figure 3.8: Assembled heavy- and light-chain transcriptionally active linear cassettes. ... 64
Figure 3.9: Evaluation of the binding activity of the TAP-expressed rabbit antibodies against $gp140_{GCN4}$ and 2dCD4WT using ELISAs**.** ... 66
Figure 3.10: Evaluation of the antibody controls used to confirm monoclonal antibody expression by SDS-PAGE. ... 67
Figure 3.11: Confirmation of the 2G12 antibody expression by western blot. ... 68
Figure 3.12: Evaluation of the rabbit monoclonal antibody expression by western blot analysis. ... 70
Supplementary Figure 1: The VRC_4196 and VRC_4197 plasmid vector maps. ... 96
Supplementary Figure 2: The heavy- and light-chain constant and polyA fragments inserts for the plasmid vectors. ... 97
Supplementary Figure 3: Optimisation of PCR protocols for the primary PCR reaction. ... 98
Supplementary Figure 4: Western blots used for confirmation of antibody expression. ... 99

List of tables

Table 2.1: Summary of the antibodies and fluorophore conjugates required for rabbit antigen-specific memory B cell isolation. 39
Table 2.2: Primers used for the amplification of the transcriptionally active linear expression cassette containing the heavy-chain antibody fragment. 44
Table 2.3: Primers used for the amplification of the transcriptionally active linear expression cassette containing the light-chain antibody fragment. 45

List of abbreviations

2dCD4	Two domain CD4
ADCC	Antibody-dependent cellular cytotoxicity
AIDS	Acquired Immunodeficiency Syndrome
APC-Cy7	Allophycocyanin-cyanine7
APS	Ammonium Persulphate
ART	Antiretroviral therapy
BCA assay	Bicinchoninic acid assay
bNAbs	Broadly neutralising antibodies
BN-PAGE	Blue native polyacrylamide gel electrophoresis
bp	base pair
BSA	Bovine serum albumin
CD4bs	CD4 binding site
CD4i	CD4 induced
cDNA	complementary DNA
CDRs	Complementary determining regions
CSR	Class switch recombination
CTL	Cytotoxic T-lymphocyte
DEAE Dextran	Diethylaminoethyl dextran
DEPC	Diethyl Pyrocarbonate
DMEM	Dulbecco's Modified Eagle's Medium
DMSO	Dimethyl sulfoxide
DNA	Deoxyribonucleic acid

dsDNA	double stranded DNA
DTT	Dithiothreitol
EDTA	Ethylenediaminetetraacetic acid
ELISA	Enzyme linked immunosorbent assay
Env	Envelope glycoprotein
Env_{FVC}	HIV-1 subtype C consensus Founder Virus Env
Fab	Antigen-binding fragment
FACS	Fluorescence activated cell sorting
Fc	Fragment cystallizable region
FCS	Foetal Calf Serum
FITC	Fluorescein isothiocyanate
FPLC	Fast protein liquid chromatography
FSC	Forward scatter
FV	Founder virus
GALT	Gut associated lymphoid tissue
GC	Germinal center
GSH	Glutathione
GSSG	Glutathione disulphide
HAART	Highly active antiretroviral therapy
HC	Heavy-chain
HCMV	Human Cytomegalovirus
HEK 293T cells	Human embryonic kidney 293T cells
HIV	Human Immunodeficiency Virus

HRP	Horse radish peroxidase
ID_{50}	50% Infectious Dose
IFN	Interferon
Ig	Immunoglobulins
IL-2	Interleukin-2
IPTG	Isopropyl β- d-1-thiogalactopyranoside
INSTIs	Integrase strand transfer inhibitors
kDa	Kilo Dalton
KIRs	Killer cell immunoglobulin-like receptors
LB	Luria broth
LC	Light-chain
LPS	Lipopolysaccharides
MMP	Methyl α-D-manno-pyranoside
MPER	Membrane proximal external region
mRNA	messenger ribonucleic acid
MSM	Men who have sex with men
MWM	Molecular weight marker
NAbs	Neutralising antibodies
NHP	Non-human primates
NNRTIs	Non-nucleotide reverse transcriptase inhibitors
NRTIs	Nucleotide reverse transcriptase inhibitors
NZW	New Zealand white
PAMPs	Pathogen-associated molecular pattern molecules

PBMCs	Peripheral blood mononuclear cells
PCR	Polymerase chain reaction
PE	Phycoerythrin
PEI	Polyethylenimine
PIs	Protease inhibitors
PMT	Photomultiplier tubes
PMTCT	Prevention of mother to child transmission
PRRs	Pattern recognition receptors
PBS	Phosphate buffered saline
PBS-T	Phosphate buffered saline-tween
PCR	Polymerase chain reaction
PEI	Polyethylenimine
PEP	Post exposure prophylaxis
polyA	poly-adenylation
PrEP	Pre-exposure prophylaxis
Rpm	Revolutions per minute
RNA	Ribonucleic acid
RT	Reverse transcriptase
RT-PCR	Reverse transcription polymerase chain reaction
SDS-PAGE	Sodium dodecyl sulfate polyacrylamide gel electrophoresis
SEC	Size exclusion chromatography
SHM	Somatic hypermutation
SSIV	Superscript IV

SSC	Side scatter
ssRNA	single stranded RNA
TAE	Tris-Acetate EDTA
TAPs	Transcriptionally active linear expression cassettes
$TCID_{50}$	50 % Tissue Culture Infectious Dose
TEMED	N,N,N',N'-tetramethylethane-1,2-diamine
Tfh	T follicular helper cells
TBS-T	Tris buffered saline-tween
TMB substrate solution	3,3',5,5'-Tetramethylbenzidine substrate solution
UV	Ultraviolet
WT	Wild type

1. Introduction

1.1. The HIV-1 pandemic

The human immunodeficiency virus type 1 (HIV-1), a lentivirus of the retrovirus family, is responsible for the global acquired immunodeficiency syndrome (AIDS) pandemic [1]. Since HIV and AIDS was first discovered in the 1980s, an estimated 74.9 million individuals have been infected with HIV-1, which has resulted in approximately 32 million AIDS-related deaths by the end of 2018 [2]. Research into combating the virus and the development of antiretroviral therapy has significantly led to the decrease in AIDS related deaths and the number of new infections [3]. The UNAIDS reported that an estimated 37.9 million people worldwide were living with HIV-1 at the end of 2018. In the year 2018, an estimated 1.7 million people became newly infected with HIV-1, and approximately 770 000 people died due to AIDS-related illnesses [2]. East and Southern Africa remain the most severely affected, accounting for approximately 54% of all infections (Figure 1.1) [2]. East and Southern Africa accounted for an estimated 800 000 individuals newly infected with HIV-1, just less than half the estimated number of newly infected individuals worldwide of 1.7 million people as reported for the end of 2018 (Figure. 1.1) [2]. Despite the high numbers of infections, the overall number of new infections in the East and Southern African regions has decreased by approximately 28% since 2010 [2]. The number of deaths in these regions, has also decreased by 44%, which is widely attributed to an increase in individuals knowing their status to an estimated 85% of infected individuals, and an estimated 67% of people knowing their status being on treatment, and 58% of the people on treatment being virally suppressed at the end of 2018 [2].

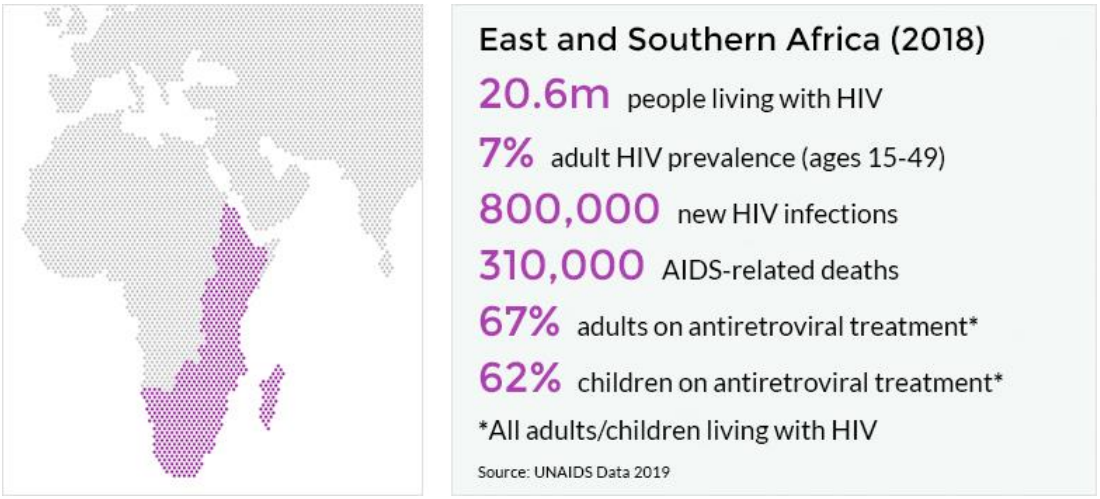


Figure 1.1: HIV-1 statistics for East and Southern Africa at the end of 2018. Image obtained from [2].

In June 2019, the UNAIDS reported an estimated 24.5 million people living with HIV/AIDS had access to antiretroviral therapy (ART) worldwide [2]. The increase in ART administration to individuals living with HIV-1 from 7.7 million people in 2010 to 24.5 million people in 2019 has been a contributing factor to the decrease in the amount of new infections as well as recorded deaths observed worldwide [2], [4]. Despite decreased infection rates, HIV-1 infections remain a health burden globally, particularly in the East and Southern African region, therefore novel and effective prevention strategies need to be implemented.

Prevention and treatment strategies are currently a combination of social and biomedical interventions. The social strategies aim to reduce the transmission of HIV-1 by targeting risky behaviours [5]. These social strategies include educating the public on practicing safe sexual behaviour, the importance of proper condom usage, the rapid treatment of sexually transmitted infections, counselling and psychological support, safe infant feeding, the reduction of stigma and discrimination as well as safe needle usage [6]–[8]. Social interventions also aim to improve adherence to ART for individuals living with HIV-1.

The biomedical strategies make use of both clinical and medical methods in the hope of reducing the transmission of HIV-1. The biomedical interventions include voluntary medical male circumcision, where research has shown a reduction in the risk of HIV-1 transmission in circumcised heterosexual males by approximately 60% [9], [10]. Other biomedical interventions include HIV-1 testing and counselling, needle and syringe programmes providing education on

safe needle usage, blood screening, increased access to sexual and reproductive health services, preventing mother-to-child transmission (PMTCT), and the administration and usage of ART-based treatments including pre-exposure prophylaxis (PrEP), and post-exposure prophylaxis (PEP) [6], [7]. ART is currently the most effective treatment method for individuals infected with HIV-1, however, there are many limitations to ART [11], [12]. Some of the limitations include the development of resistance mutations that occur leading to virological failure of treatment regimens due to sub-optimal drug levels or prolonged usage; individuals having restricted access to ART in certain areas; and the inability of currently available antiretroviral drugs to target and eliminate latent viral reservoirs which ultimately leads to failure to fully restore the immune system of the infected individual, and the absence of an HIV cure [12].

Studies focused on prevention strategies such as the development and administration of pre-exposure prophylaxis (PrEP) [13], the development of ART as treatment to prevent HIV-1 infection [14], and the development of preventative HIV-1 vaccines are crucial for the eradication of HIV-1 and require significant investment in research [15]. Mathematic modelling has shown that combined preventative strategies such as the increase in medical male circumcision and the early administration of ART and PrEP has contributed significantly to the reduced incidence of HIV-1 infections [16]. The development of a safe and effective prophylactic vaccine against HIV-1 still remains the most effective goal for controlling and eliminating the worldwide health burden of HIV infection [17]. In order for an HIV-1 vaccine to be effective, it would need to elicit long-lasting broadly neutralizing antibody (bNAb) responses capable of providing protection against a large number of globally circulating HIV-1 subtypes.

1.2. HIV-1 life cycle

For a better understanding of HIV prevention and treatment strategies, the life cycle of HIV needs to be explained since many effective treatment regimens and vaccine strategies target different stages of the HIV life cycle. In the first stage, during viral infection of a host CD4 cell, virus to host cell adhesion takes place when the gp120 component of the virus envelope glycoprotein (Env) resulting in conformational changes which allows for coreceptor binding. Env is a glycosylated trimeric conformation made up of two heterodimeric subunits, gp120 and gp41 [18] (Figure 1.2) (the structure of Env will be explained in more detail in section 1.8). The gp120 subunit attaches

sequentially to the CD4 receptors and to either of the CCR5 or CXCR4 host cell co-receptors (Figure. 1.3) [19]–[21].

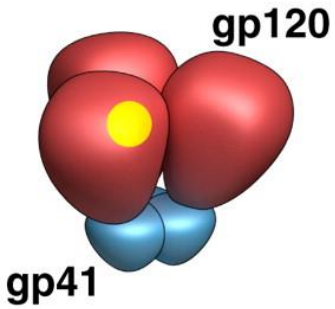


Figure 1.2: Schematic representation of the HIV-1 trimeric envelope glycoprotein made up of the non-covalently bound gp120 and gp41 subunits. Image obtained from [22].

The gp120 subunit of Env attaches first to the host receptor CD4 which allows for conformational rearrangements that facilitate gp120 binding to a coreceptor (either CCR5 or CXCR4) that has a higher binding affinity for gp120 (Figure. 1.3) [21]. Once gp120 has bound to the receptors/coreceptors, Env undergoes conformational changes inducing the exposure of the gp41 subunit, formation of the six helix bundle in gp41, and insertion of the fusion peptide into the membrane of the host cell leading to viral-host membrane fusion (stage 2) [20], [23]. During membrane fusion, the viral capsid is released into the cytoplasm of the host cell and uncoats, releasing two viral single positive strands of RNA (ssRNA) and the essential enzymes needed for replication, namely; reverse transcriptase, integrase, and protease (Figure. 1.3) [24], [25]. During the third stage, the viral ssRNA is reverse transcribed into linear double-stranded DNA (dsDNA) by the reverse transcriptase (RT), which is also responsible for initiating and catalysing the reaction (Figure. 1.3) [23], [25]. During the fourth stage, integrase cleaves the ends of the dsDNA creating two sticky ends, allowing the viral DNA to aggregate with other viral and host proteins into a pre-integration complex, to be trafficked to the nucleus of the host cell and integrated into the host cell genome (Figure. 1.3) [23], [26]. Once the viral DNA is integrated into the host genome, transcription of the viral DNA into messenger RNA (mRNA) takes place (Figure. 1.3).

During stages five to seven, the transcribed mRNA migrates to the cytoplasm of the cell where structural proteins are generated for the synthesis of a new viral particle (Figure. 1.3) [23], [27]. The newly generated viral RNA and proteins migrate towards the host cell surface forming an immature HIV-1 (non-infectious) virion (Figure. 1.3) [28]. In the cytoplasm, large proteins are

cleaved by viral and host proteases into smaller core proteins [24]. In order for a virus to be infectious, partial maturation takes place in the cytoplasm, which involves the cleavage of the Gag-Pol polyprotein precursors by HIV-1 proteases (Figure. 1.3) [21]. The Gag polyprotein is not completely cleaved in the cytoplasm. The core proteins then assemble around two new RNA strands and enzymes responsible for replication, forming a capsid for the generation of a new HIV-1 molecule (Figure. 1.3) [24]. During Env synthesis, gp160 precursors are transported to the golgi apparatus where they undergo oligomerisation into trimers and are cleaved into gp120 and gp41 subunits by the host protease furin, forming functional Env [29]. Trimers of Env make up approximately 72 knobs [30] anchored on the outer lipid membrane making up the envelope surface. Neutralising epitopes that are conformation-dependent, are located on the trimeric Env. These conformation-dependent neutralising epitopes are found on native protein, or are created following conformational changes during viral entry, however, on the unfolded denatured proteins, they are only partially expressed. Once Env has been synthesised and the Gag and Pol proteins are cleaved or partially cleaved, an immature virion is released by budding from the cell surface, taking components of the cell membrane with it. Complete cleavage of the Gag proteins into their subunits by the viral protease then results in a fully infectious virion, capable of a new cycle of infection of CD4+ T cells (Figure. 1.3) [21]. This replication process occurs every two to three days, destroying infected CD4+ T cells, and ultimately leading to the destruction of the hosts' immune system. Trimeric Env has been the sole target for vaccine-strategies aimed towards the generation of bNAbs to target and prevent HIV-1 infection.

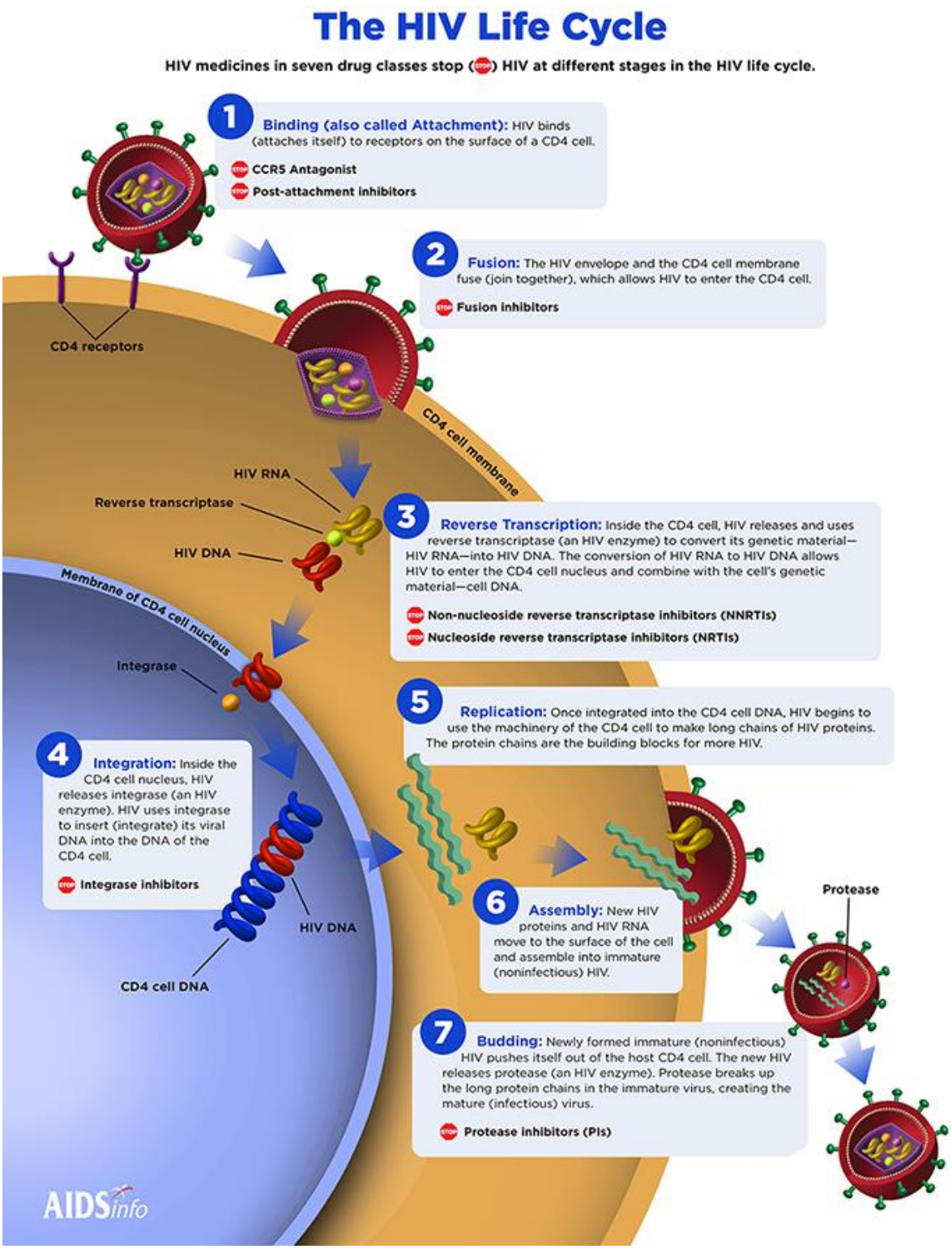


Figure 1.3: The HIV-1 viral life cycle, showing the seven stages of infection of a CD4 positive T cell. The targets of FDA approved antiretroviral drugs are also highlighted. Image obtained from [24].

1.3. HIV-1 life cycle inhibitors

Different classes of drugs used for ART are used to target and inhibit various stages in the viral replication cycle. Entry and fusion inhibitors- such as Maraviroc which is a coreceptor antagonist- selectively bind to the CCR5 coreceptor, preventing the attachment of the viral gp120 to the CD4+ T cell thus preventing fusion and viral entry [31]. Nucleoside/tide Reverse Transcriptase Inhibitors (NRTIs) and Non-Nucleoside Reverse Transcriptase Inhibitors (NNRTIs) target the second stage of the replication cycle through distinct mechanisms. The NRTIs such as Tenofovir Disoproxil Fumarate, act as analogs of the DNA nucleotides, therefore, when the analogs are incorporated by the viral reverse transcriptase enzyme during reverse transcription, DNA chain elongation is terminated [32]. NNRTIs such as Efavirenz, bind directly to the reverse transcriptase resulting in conformational changes leading to the inability of the enzyme to perform its function of transcribing the viral RNA strands into double-stranded DNA [33], [34]. Integrase Strand Transfer Inhibitors (INSTIs) such as Raltegravir, block the integration of the viral cDNA into the host cell genome [35], and Protease inhibitors (PIs) such as Ritonavir, inhibit viral maturation by preventing cleavage of the viral proteins into smaller core proteins for viral assembly [36].

1.4. Immune responses to HIV-1 infection

The majority of early transmission and acute HIV-1 studies in humans have shown that productive infection arises from a single viral variant, known as the founder virus (FV), despite the transmission of a diverse viral quasispecies [37]. Transmission studies reveal that the FV phenotype may be moulded by the transmission bottlenecks and the selective pressure placed on the virus [37]. HIV-1 is primarily transmitted by sexual activity occurring through mucosal surfaces. HIV-1 can be transmitted vertically by mother-to-child exposure and directly through intravenous means. HIV-1 targets CD4+ T cells, ultimately leading to the depletion of these cells, which are required for protective adaptive immune responses to pathogenic infections. The depleting effect of HIV-1 on CD4+ T cells lead to immunodeficiency which results in AIDS-related opportunistic infections, and ultimately death if left untreated.

1.4.1. Acute infection

Acute HIV-1 infection is the time of transmission, and covers the period of infection from HIV-1 RNA detection until the generation of antibodies against HIV-1 (seroconversion) which occurs 3

to 4 weeks post infection [38]. Studies have shown that acute HIV-1 infection results in depletion of CD4+ memory T cells, mostly in the mucosal tissues, which is due to the high expression of CCR5, and the activated state of mucosal CD4+ T cells [39]–[41]. During the early period of infection, the innate immune system is activated which recruits granulocytes, macrophages, and lymphocytes. The macrophages and lymphocytes, specifically T-cells, are also cellular targets of the virus. The activated CD4+ CCR5+ T cells are presented as targets cells for additional infection once the virus and infected cells move to the draining lymph nodes [42], [43]. Viral replication and dissemination to the secondary lymphoid tissue then occurs, particularly in the gut-associated lymphoid tissue (GALT), where there is an increased number of activated CD4+ CCR5+ T cells present [39]. During the acute stage of infection, naïve and resting central memory T cells which do not express CCR5 are not targeted, therefore, providing the potential for regeneration of the T cell populations during this period [44].

Peak plasma viraemia (measured as viral load; RNA copies/ml) is reached after 21-28 days of infection, along with a decreased number of peripheral CD4+ T cells. At this point, the emergence of anti-HIV-1 CD8+ Cytotoxic T lymphocytes (CTL) brings viral replication under control, however, the number of CD4+ T cells in the GALT remain severely reduced, and the peripheral CD4+ T cells slowly increase, but never reach pre-infection levels [40], [45]. The early loss of CD4+ CCR5+ memory T cells has great immunological consequences, eventually leading to a failing host immune defence system, and the progression to AIDS at a later stage of infection [46]. At the time of peak viremia, viral reservoirs are already established in resting memory CD4+ T cells with a lower decay rate, which suggests that highly active antiretroviral treatment (HAART) cannot fully neutralise the virus for the duration of the patient's lifespan [47].

1.4.2. Chronic infection

Post-infection, after 12-20 weeks the viral load decreases to a stable viral set point [48], initiating the chronic stage of infection. Studies have demonstrated that in the absence of HIV specific CD8+ CTL responses, there is no decline in virus levels from peak viremia for a prolonged period which indicates that CD8+ CTL activity is significant to the control in viremia [49], [50]. Regardless of the presence of circulating CD4+ T cells, and the majority of infected individuals being asymptomatic for long periods of time following peak viremia, an immune activation and an accelerated cell turnover occurs during chronic infection [51], [52]. In the gut, increased numbers

of naïve and central memory T cells are present, and although these cells have a short half-life, they play a role in partially substituting for the depleted CD4+ effector memory T cells during acute infection [44], [53]. In contrast, stimulating the naïve and central memory CD4+ T cell repertoire generates more cell targets expressing CCR5, which provides additional viral targets for infection [46].

Immunological damage to the gastrointestinal tract results in mucosal barrier breakage which leads to translocation of microbial products, which includes bacterial lipopolysaccharide (LPS), into the peripheral circulation. Studies have demonstrated that HIV infection, bacterial translocation and elevated plasma LPS levels correlate with the high levels of immune system activation seen during HIV infection [54]. Bacterial translocation plays a critical role in chronic immune activation, however, it is not responsible as the sole microbial burden. HIV-1 also plays a crucial role in chronic immune activation since during viral replication the production of gp120 and Nef, or viral nucleic acids results in the activation of proinflammatory cytokines and type I interferon (IFN), including IFN-α and IFN-β [38], [44], [55]. Immune activation ultimately results in the depletion of CD4+ T cells through multiple mechanisms, a decrease in the half-life of CD4+ and CD8+ T cells, abnormal T cell trafficking, clonal exhaustion of T cells, and drainage of memory T cell pools [56]–[58]. During chronic infection, a minority of activated CD4+ T cells are infected with HIV-1 [46], [58]. Viral evolution at this stage of infection is accelerated by the high viral mutation rate and alteration in cellular tropism, which leads to the emergence of dual tropic or predominantly CXCR4 tropic strains from a pool of CCR5-tropic strains, with increased virulence and improved breadth of target cell tropism [44]. Additionally, lymphoid tissue damage leads to thymic dysfunction, the transformation of growth factor-β-dependent fibrosis and alterations in lymphoid follicle architecture [57], [59]. HIV-1 infection has a significant impact on blood and tissue B cells resulting in induced early class switching in polyclonal B cells, B cell apoptosis, and loss of germinal centers (GC) in lymphoid tissue [60], [61]. Along with adaptive immune system damage, there is a significant dysregulation of the innate immune system [38].

1.4.3. Innate Immune system

The innate immune system is responsible for the initial responses to HIV-1 infection. The innate immune system functions by either directly inactivating the invading pathogen, or primes the adaptive immune system for the generation of the necessary effector responses. Innate immune

cells, such as macrophages, monocytes, and dendritic cells interact with pathogen-associated molecular patterns (PAMPs) through pattern recognition receptors (PRRs) (reviewed in [62]). These PRRs evolve as substrate-specific receptors that are able to identify self- and non-self and persistently monitor the intra- and extracellular environment (reviewed in [62]). The innate immune system detects HIV-1 by recognizing the viral nucleic acids present in the cytosol of infected cells during replication and in the endosomes of phagocytosing cells. The majority of the PAMP/PRR interactions result in the activation of signaling pathways that lead to pro-inflammatory cytokines and type-1 interferons (IFNs) transcriptional activation. Type 1 IFNs induce the expression of IFN-stimulated genes by binding to receptors of infected and neighbouring cells, that results in the inhibition of viral replication and spread [63].

The innate-like lymphocytes, natural killer cells, are crucial to the control of viral infections through interactions with other host immune cells, through secreting chemokines and cytokines or through direct cellular cytotoxicity against infected target cells (reviewed in [64]). Natural killer cells identify infected cells through interactions with antibodies that are bound to the target cell surface through antibody-dependent cellular cytotoxicity (ADCC) or through interactions as a result of inhibition and activation of surface cell receptors with the ligands on infected cell. Natural killer cells are often activated by the decreased levels of expression of the MHC-class-1 molecules on the surface of HIV-1 infected cells by signaling inhibitory killer cell Ig-like receptors (KIRs), which is a crucial complementary mechanism to MHC-class-1 recognition dependent CD8 T-cell responses (reviewed in [65]).

1.4.4. Adaptive immune system

Research studies have shown that HIV-1 specific CD8+ CTLs are crucial to the control of viral replication [50], [66]. Towards the end of the acute stage of infection, the rapid decrease in the viral load is correlated with the emergence of HIV-1 specific CD8+ CTLs [50], [66], [67]. Cytotoxic CD8+ T cells bind to infected cells through their T-cell receptors when they recognise viral proteins on the surface of the cell using MHC-class1 molecules. The HLA-class-I type has an effect on the disease progression rate, where certain HLA alleles such as *HLA-B35* correlate with faster disease progression to AIDS, however, certain HLA molecules such as HLA-B57 and HLA-B27 can assist with viral control and delay progression to AIDS [68]. The peptide binding specificity is critical for the protectiveness provided by the alleles, which allows CD8+ T cells to

target epitopes that are located within the Gag region, where immune response is evaded by escape mutations resulting in a high cost of viral fitness [69], [70]. The transmission of viral variants with disadvantageous escape mutations that lead to reduced viral replication assists with the control of HIV-1 in the new host and plays a role in reducing the viral load and the depletion of CD4+ T cells [71], [72].

1.4.4.1. CD4+ T cells

CD4+ T cells facilitate the maintenance of functional CD8+ T cell responses with the same antigen-specificity [73], [74]. The major target for HIV-1 is CD4+ T cells leading to depletion of these cells throughout the infection period [45], [75] while persistent infection of activated and HIV-1 specific CD4+ T cells occurs during the chronic infection stage [76]. The depletion of HIV-1 specific CD4+ T helper cells is suggested to be the main attribute to the failure of successful viraemic control, because of the role these cells have in directing various cellular and humoral immune functions [77].

HIV-1 specific CD4+ T cells have intrinsic direct cytotoxic activity against infected cells [78]. A study using a large cohort of ART-naïve HIV-1-clade-C infected adults demonstrated that the increased amounts of Gag-specific CD4+ T cell responses correlates with increased CD4 numbers and a decreased viral load [79]. IL-2 has a key immunoregulatory role in CD4+ T cells during immune response as it plays a significant role in differentiation, activation, and proliferation of NK cells, Th1 and Th2 CD4+ T cells, B cells, regulatory T cells, and memory CD8+ T cells [80].

1.4.4.2. B cells

The focus on the elicitation of bNAbs, which are potent antibodies that are able to neutralise a wide range of HIV-1 strains from various HIV-1 subtypes in vaccine research is of extreme significance, as these antibodies could prevent infection and ideally provide sterilising immunity [81]. These bNAbs only occur naturally in approximately 10-30% of HIV-1 infected individuals over several years [82]–[86] through a process of extensive somatic hypermutation (SHM) [87]. Although circulating bNAbs are generated in infected individuals, the presence of these bNAbs is not directly associated with viremia control *in vivo*, however, passive infusion studies in NHPs have revealed that bNAbs possess a protective role against challenge infections. CD4+ T follicular helper (Tfh) cells are a special subset of cells that help B cells in the GCs to assist in antibody

maturation [88]. Tfh cells are important as they provide the needed cognate interactions (CD40-CD40L, MHCII-peptide-TCR) and secrete soluble mediators at the interface of zone borders of the T and B cells, which results in B cell GC formation, immunoglobulin (Ig) class-switch recombination (CSR), SHM and differentiation of B cells into long-lived memory B cells and plasma cells [89]–[93]. The GCs are structures within the follicles of B cells where SHM of the immunoglobulin (Ig) variable region occurs to improve the affinity for antigen binding leading to an improved protective efficacy [94]–[99]. The role Tfh cells play is significant to the generation of high affinity antibodies.

Due to the critical responsibilities of Tfh in the GC B cell responses, several research groups have studied the impact of HIV-1 infection on Tfh cell frequency and function [100], [101]. The frequency of Tfh cells is associated with plasma viremia, which suggests that Tfh cells may be a target for HIV-1 infection [100]. Tfh cells in infected lymph nodes have an increased concentration of HIV-1 DNA in comparison to non-Tfh cells [101] and are a reservoir of latent virus in infected individuals receiving ART [102], [103]. Studies have shown an expansion of Tfh in HIV-1 infected individuals which is associated with an increased frequency of GC B cells and antibody production [100], [101]. However, regardless of the increased frequency of the Tfh cells, studies have shown that Tfh cells from HIV-1 infected individuals are functionally impaired and do not provide the required help to B cells [104]. This is suggested to be partially due to increased expression of PD-L1 by B cells resulting in PD-1 ligation which inhibits proliferation of Tfh cells, reduces induced T cell co-stimulator ICOS expression and IL-21 cytokine secretion [104]. Exogenous administration of IL-21 is shown to improve the frequency of B cells which indicates that a reduced secretion of IL-21, may in part, impair memory B cell response formation [105], [106]. It therefore seems that the function of Tfh cells is affected by the lymph nodes of HIV-1 infected individuals, and Tfh cells may arise based on microenvironmental signals which result in abnormal inhibitory molecule expression.

1.5. HIV-1 Phase IIb/III vaccine trials

Through early research into vaccine design using non-human primate (NHP) models that made use of various *nef* or multiple gene deleted viral strains, it became obvious that using live-attenuated vaccine would not generate an effective, safe vaccine, since the virus showcased deletion repair and enhanced viral fitness resulting in antibody escape and increased viral infection

[107]–[109]. The area of interest in vaccine development strategies turned next to the development of Env subunit vaccines, which was considered safer than the traditional live-attenuated and heat-killed whole virus vaccines. The focus was mainly on the generations of various Env gp160 or gp120 recombinant proteins from a variety of viral strains and subtypes, and assessing the immunogenicity of the recombinant proteins produced from various viral gene expression systems (reviewed in [110]). Pre-clinical studies have investigated a number of potential combinations for vaccine regimens, including prime-boost strategies, consisting of combinations of expression vectors, recombinant proteins, various delivery schedules and methods and routes of administration (reviewed in [110]). The findings of subsequent clinical trials confirmed the elicitation of an antibody mediated immune response in humans is possible by Env vaccination, however, the immune responses by the first or second generation Env immunogens lack potency and neutralisation breadth.

Researchers face many challenges with vaccine development, such as the high variability rate of the virus. Between the two HIV types (HIV-1 and HIV-2) and the various groups and subtypes of HIV-1, the Env amino acid sequences differ significantly, and HIV-1 continues to evolve within an infected individual. The high genetic diversity is as a result of the high error rate of reverse transcriptase and the high replication rate of HIV-1 [111], [112], and leads to the generation of multiple quasi-species of related genomes with 5-10% divergence in a single infected individual. The variability of the virus allows quasispecies and/or mutated viruses to escape selective pressure generated by the immune system and antiviral drugs. HIV-1 also evades the immune system is through the structural modifications of the native Env spikes on the viral envelope. As mentioned, Env mediates infection through receptor binding and fusion, and as the only virally-encoded protein on the viral surface, it is the major target for neutralising antibodies [20], [113]. The gp120 and gp41 components of the trimeric glycoprotein spikes are non-covalently linked and unstable. Post binding, the gp120 monomeric components are shed into the peripheral blood, and act as immune decoy, so that the non-native monomeric gp120 “deceives” the host immune system which results in the generation of antibodies targeting non-functional forms of Env. Initial vaccine trials were based on soluble monomeric gp120, which due to its non-native conformation proved unsuitable for the elicitation of bNAbs in humans. These previously used vaccines were able to, at best elicit neutralising antibodies against autologous HIV-1 strains. Great strides were made in vaccine research after the rational vaccine design of recombinant, soluble native-like Env proteins

based on the comprehensive analysis of the native Env structure (tertiary and quaternary) and function with the most well characterized native-like trimeric Env spike to date being the gp140 SOSIP.664 trimer [114]–[117].

During recent years, the immunogens have been optimised, however, despite the multitude of vaccine candidates being pre-clinically tested as HIV-1 vaccines, including the gp140 SOSIP.664 trimer, bNAbs targeting various heterologous strains have not been induced. The two first Phase III clinical trials testing the efficacy of HIV vaccines were based on recombinant Env. The VAX004 trial started in 1998 was a randomised, double-blind, placebo controlled study of AIDSVAX B/B using subtype B recombinant gp120 in alum [118]. The VAX004 trial took place in North America and the Netherlands and enrolled 5403 men who have sex with men (MSM) and women at high risk of infection [118]. The VAX004 immunogen generated some neutralising and CD4-blocking antibodies in all vaccinees, however, the estimated vaccine efficacy was only 6% [118]. A randomised, double blind, placebo-controlled efficacy trial of AIDSVAX B/E (VAX003) began in 1999 in Thailand and a 2546 injection drug user (IDU) cohort was enrolled [119]. Two recombinant gp120 HIV-1 Env antigens from a CXCR4 lab-adapted clade B strain and a CCR5 primary subtype CRF01_AE isolate adjuvanted in alum were used for the AIDSVAX B/E vaccine [119]. The VAX003 study failed to produce protection against infection, with an estimated efficacy at 0.1% [119]. Overall, the VAX003 and VAX004 recombinant Env-based vaccines were immunogenic however, both failed to generate protective immune responses against infection.

A randomized, placebo-controlled efficacy trial consisting of priming with a recombinant canarypox vector expressing Env, Gag and Pol (ALVAC), followed by two recombinant gp120 boosts (AIDSVAX B/E) was evaluated in 2003 [120]. The trial enrolled 16402 healthy heterosexual individuals at risk of acquiring HIV-1 in Thailand [120]. This RV144 trial had an overall estimated efficacy of 31.2% [120]. Unexpectedly, the observed protection was attributed to the generation of non-neutralising IgG against the V1/V2 region of HIV-1 Env and not due to low-level neutralising antibodies arising [120]. A sieve analysis performed for a comparison of the breakthrough viruses in the vaccine recipients showed that HIV-1 from the infected individuals had genetic signatures of vaccine-induced immune pressure within the V1/V2 region [121]. Env-specific plasma IgA antibodies were observed to be directly correlated to protection [122]. Since other clinical trials aimed at generating protective cellular immune responses were also

unsuccessful (reviewed in [123]–[125]), the data obtained from RV144, which combined vaccine immunogens aimed at eliciting cellular and humoral immune responses suggests that Env played a crucial role towards generating protective antibody responses against mucosal acquisition of HIV-1.

Looking at Phase IIb safety and efficacy trials, the STEP (HIV Vaccine Trials Network 502, HVTN502, started in 2004) and Phambili (HVTN503, started in 2007) trials were devised to elicit protective cellular immune responses against HIV-1. These vaccines were designed based on research suggesting cell mediated immunity was crucial towards controlling both the replication of HIV-1 and the progression of disease in long term non-progressors [126]–[128]. STEP was a phase II, double-blind, randomized, and placebo-controlled study using the MRKAd5 HIV-1 Gag/Pol/Nef vaccine in HIV-1 seronegative women and MSM at high-risk of infection [129]. The trial enrolled 3000 participants with study sites in South America, North America, Australia, and the Caribbean. The phase II Phambili trial included the same MRKAd5 clade B Gag/Pol/Nef vaccine in a cohort of 801 heterosexual men and women from South Africa [130]. Both vaccines were demonstrated to be immunogenic and well-tolerated, however, an exploratory multivariate interim analysis from the STEP trial showed an increase in the incidence of HIV-1 acquisition in vaccinated males versus placebo recipients and because of these findings, both trials were terminated early [131]. A sieve analysis was performed on HIV-1 genome sequences from 68 of the newly infected individuals as a follow up to assess whether selective pressure was applied on virus by the vaccine [132]. As expected, a genetic imprint was observed on the founder viral strains. The sieve effect was only observed in the proteins components that made up the vaccine and epitopes predicted to be affected, indicating possible T cell pressure post-infection [132]. The vaccine induced HIV-1 specific CD8+ T cell responses were weak and a limited number of T cell epitopes were targeted.

The HVTN505 Phase IIb trial began in 2009, using a DNA/Ad5 prime boost regimen, and was designed to evaluate whether the vaccine could prevent HIV infection and/or reduce the amount of HIV-1 in the blood of vaccine recipients who became infected with HIV [133]. The trial enrolled 2504 MSM and transgender people who have sex with men in the USA [133]. In this study, the men were required to be circumcised and the baseline Ad5 serum neutralizing antibody titre had to be less than 1:18 [133]. The DNA vaccine was formulated to express the clade B gag/pol/nef

and the clade A, B, and C Env while the recombinant Ad5 expressed clade B gag-pol and clade A, B, and C Env [133]. The HVTN505 trial was stopped early due to a lack of efficacy. Moreover, by the end of the trial, 41 participants in the vaccine arm had become infected with HIV-1, while 31 participants in the placebo arm acquired HIV-1, although there was a non-statistically significant increase in HIV acquisition in the vaccine group versus the placebo group [133]. Sieve analysis of breakthrough viral genomes revealed a significantly lower HIV-1 diversity in the *gag*, *pol*, *vif*, and *env* genes, and the *env* sequences were considerably more distant from the subtype B vaccine insert in vaccinees [134]. Due to the sieve analysis primarily being identified in Env, with regards to vaccinees, it is suggested that the selective pressure exerted on the breakthrough virus was in the Env regions correlated to infectivity, indicating that antibodies may have played a partial role [134]. Although the vaccine did not provide protection against HIV-1 infection, it is suggested that rapid Env diversification after the acquisition of HIV-1 was induced by the elicited immune pressure, or protection was provided against HIV-1 infection by the vaccine against viral strains more closely related to the vaccine strains [134].

The HVTN702 trial launched in 2016 was a Phase IIb/III placebo-controlled, randomized clinical trial based on the RV144 clinical trial [135]. The vaccine regimen consisted of two experimental vaccines; ALVAC-HIV, a canarypox-vector based vaccine, and a two-component gp120 protein subunit. The ALVAC-HIV and the protein subunit were both modified to be specific against HIV-1 subtype C, and the MF59 adjuvant was combined with the protein subunit to hopefully elicit a more robust immune response. At the one-year mark of the study the participants received booster shots to prolong the early protective effect that was observed in the RV144 trial. The HVTN702 was the largest and most advanced HIV-1 vaccine clinical trial initiated thus far and took place in South Africa. The study enrolled 5400 healthy, sexually active men and women from ages 18 to 35 years old [136]. The participants received five injections over a period of one year and thereafter were monitored for two years. The study was stopped in February 2020 as the vaccine was not shown to provide protection against HIV-1 transmission. Upon analysis of the individuals taking part in the study, 129 of those receiving the vaccine, and 123 of the individuals receiving the placebo became infected with HIV-1 [136].

Imbokodo/HVTN705 is a Phase IIb placebo controlled, randomized, double blind study started in 2017, using mosaic vaccine immunogens engineered using bioinformatic tools to elicit subtype-

independent immune responses against global circulating HIV-1 strains. The study involves a combination of two vaccine candidates, Ad26.Mos4.HIV which will be administered four times over 12 months, and HIV-1 Clade C gp140 protein and adjuvant which will be administered twice, in combination with Ad26.Mos4.HIV. The study has enrolled 2600 HIV-1 negative women from five sub-Saharan African countries. The participants will be followed over two years, and the results from the study are expected to be released in February 2022.

1.6. HIV-1 specific broadly neutralising antibodies

Numerous vaccine candidates have been developed and tested in small animal models, non-human primates and even human clinical trials [110], [120], [129], [131], [133], [136]–[140], however, these studies have shown less than ideal outcomes. Thus, the major challenge in HIV-1 vaccine development is identifying the correct antigen, which when presented to the host immune system will generate protective immunity, including bNAbs able to neutralise a broad diversity of circulating HIV-1 subtypes.

During natural disease progression, binding, non-neutralising antibodies are detected within eight days of infection. Initially antibody responses are only detectable as immune complexes and after approximately 2 to 4 weeks post infection, free antibodies to gp41 and gp120 develop. It usually takes 3 to 12 months for neutralising antibodies (antibodies that directly eliminate the virus) to develop. These antibodies are usually targeted against the Env variable regions such as the variable V1/V2 or V3 loops, however, they possess limited breadth. The slow generation of neutralising antibodies allows the virus to escape the selective pressure applied by these strain-specific antibody responses, which results in the development of circulating virus resistant to the present neutralising antibodies. Only approximately 10% to 25% of infected individuals generate bNAb responses with potency and breadth. The reason that this low number of individuals are able to develop a more neutralising response than other individuals is complex and involves a number of features including the infecting and evolving virus, viral load, and the quality and efficiency of both the CD4+ and CD8+ T cell responses.

HIV-1 bNAbs have been shown to have an unusually high degree of somatic hypermutations which suggests that in order to acquire breadth the antibodies undergo multiple rounds of affinity maturation [141]. Affinity maturation is a process whereby antigen specific antibodies undergo

iterative selection in the germinal centre, resulting in increased affinity of the antibodies for the antigen. Studies have demonstrated that individuals with higher viral loads have an improved breadth of neutralising antibody responses, suggesting that greater amounts of viral antigenic stimulation may possibly improve the antibody breadth [142]. It is well known that bNAbs consist of a great deal of mutations. SHM and B cell selection enable fast and high affinity antibody production within a few weeks of infection under normal circumstances. As the antibody response develops, a small number of variable region mutations occur, which may result in an up to 5% change from the germline sequences. The development of mutations observed in certain bNAbs has amounted to over 30% nucleotides divergence of the variable region from the germline sequences, in addition to nucleotide insertions and deletions. This partly explains the rarity of these bNAbs in HIV-1 infected individuals. Genetic and structural characterisations of bNAbs have shown that the HIV-1 bNAbs possess high levels of somatic hypermutations within the CDR3 domain [141]. The CDR3 loops of antibodies play a role in the diversity of antibody structures which is critical to antigen binding [143]. The results of long-lived antigen persistence and B cell evolution and how this can be obtained by the administration of a prophylactic HIV-1 vaccine is still to be determined. Numerous pre-clinical studies looking at various sequential immunisation strategies using multiple Env immunogens that mimic the genetic variability seen in natural infection over time are ongoing [144]–[146].

1.6.1. Antibody structure

Antibodies have an approximate molecular weight of 150 kDa. Antibodies are made up of a duplicate of two subunits, a heavy chain (50 kDa) and a light chain (23 kDa), linked together by disulphide bonds and non-covalent interactions (Figure. 1.4). Antibodies are Y-shaped molecules, with the two branched fragments making up the Fab (fragments of antigen binding) regions which have the ability to recognise and bind to an antigen. The third fragment is called the Fc (fragment crystallisable) portion which mediates interactions with effector functions of the immune system after antigen binding. The light chain contains a large region known as the constant region since the sequence is similar in different types of antibodies. The light chain is made up of either a kappa or lambda chain. The constant region has amino acid sequences in the carboxyl terminal end (residues 109 to 214) of the kappa or lambda chains that are conserved. The amino acid residues 1 to 108 (amino-terminal) show a high level of variability between the different antibodies and this

region is known as the variable region. The heavy chain also consists of constant and variable regions, with the first 113 amino acids being the variable region and the remaining amino acids making up the constant region.

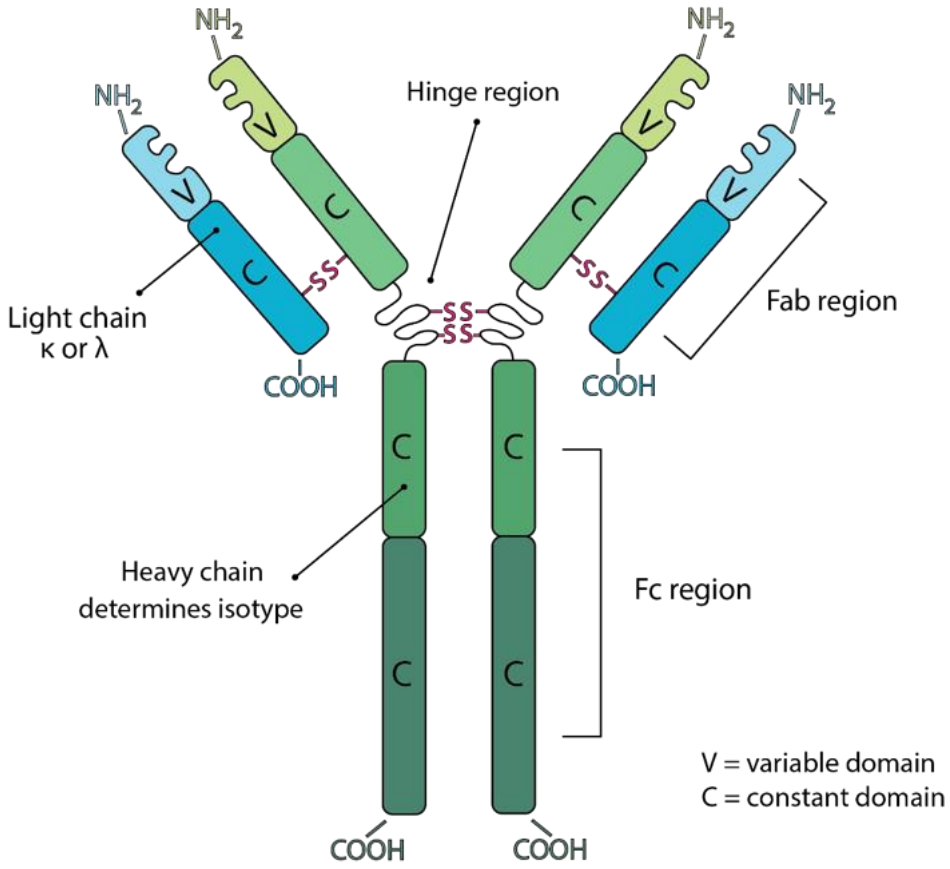


Figure 1.4: Schematic representation of the structure of an antibody. Image obtained from *[147]*.

The variability of the amino acid sequences in the variable region is perfectly positioned and does not arise randomly. Most of the variability is located around residues 30, 55 and 95 in the light chain [148]. These areas are known as the complementarity-determining regions (CDRs). In the direction moving from the amino-terminal end of an antibody heavy- and light-chains, the three regions are called CDR1, CDR2, and CDR3 [149]. The CDRs are each approximately 10 amino acids long [149]. Invariant segments known as framework residues [150] make up approximately 85% of the variable region [149]. Framework residues are intervening sequences found between the CDRs which have limited variability between chains. The framework residues are responsible for the placement of the CDRs. The variable region folds in a manner that exposes the CDRs on the surface of the chain. The CDRs form a cleft when the light and heavy chains are connected

which acts as the antigen-binding site of an antibody [150]. Since the amino acid sequences of the CDRs are responsible for determining the shape and ionic properties of the antigen-binding site, the CDRs are therefore responsible for the specificity of the antibody [149]. These features are significant for the elicitation of antibodies by immunisation because longer and charged IgG CDR3 regions are needed for the production of antibodies that are able to penetrate the HIV-1 envelope glycan shield [151] which, to date, has not been possible in the context of vaccination. Studies of the emergence of the VRC01 bNAb lineage, HIV-specific antibodies which target the CD4 binding site, together with the evolution of the viral Env sequences, revealed that bNAb evolution occurred quickly to an autologous gp120 molecule, then the rate of evolution slowed down after 11 years as the evolution of the VRC01 bNAb was monitored for a period of 15 years [152]. Despite this deceleration of the mutation rate, the antibody continued to evolve as a result of the persisting antigen which enabled the continuation of SHM.

1.6.2. Broadly neutralising antibody epitopes

The progression of isolating, characterising and understanding broadly neutralising antibodies from HIV-1 infected patients has been important in identifying vulnerable epitopes on the Env trimer, and improving immunogen development. The vulnerable epitopes currently identified by broadly neutralising antibodies include the gp41 membrane proximal external region (MPER), the gp120-gp41 cleavage interface, the CD4-binding site on gp120, the N332 glycan on gp120 V3 and the N160 glycan on gp120 V1/V2 (Figure. 1.5). The discovery of these epitopes has also provided valuable insight into the underlying mechanisms of antibody development, thereby identifying the course of antibody-virus coevolution (which is the the reciprocal interaction and maturation between antibodies and viruses) required for their maturation. In addition, several unique characteristics of bNAbs make them particularly attractive in therapeutic and preventative strategies over existing ART and bNAbs are currently being explored in human clinical trials [153].

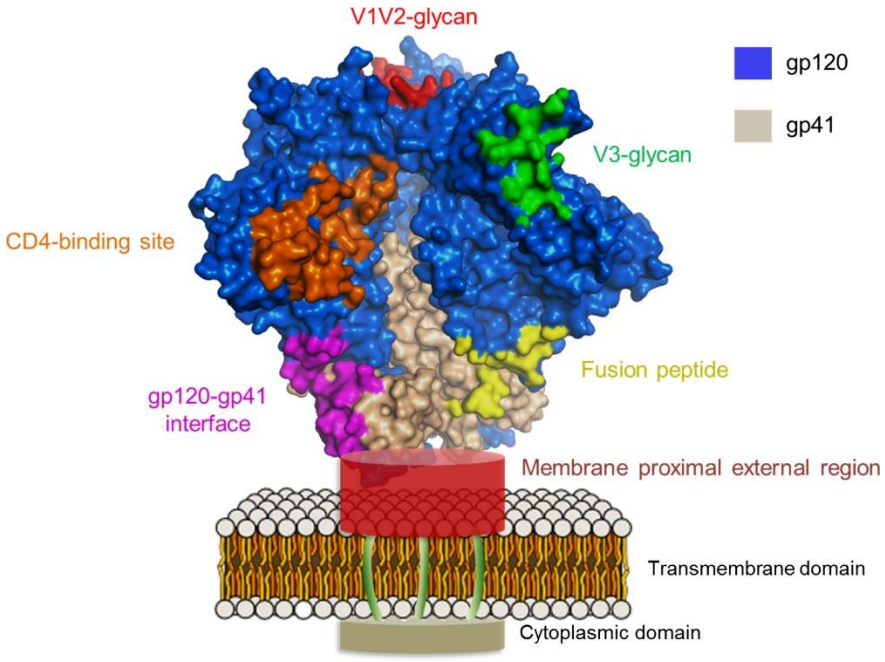


Figure 1.5: Sites of broadly neutralising antibody epitopes on the HIV-1 envelope glycoprotein. Image obtained from *[154]*.

1.6.2.1. The MPER bNAbs

Key characteristics of MPER bNAbs are the highly conserved sequences of these antibodies and that these antibodies contain long HCDR3 loops with hydrophobic residues at the tips, which neutralise the virus when bound to the membrane [155]–[158]. These MPER bNAbs insert the long HCDR3 into the viral membrane and simultaneously interact with the first turn of the gp41 α-helical transmembrane and lipids using at least two lipid-binding pockets. The membrane therefore makes up a two-part epitope which improves the binding affinity [159] and some variants of the MPER bNAbs bind better following conformational changes induced after HIV-1 binding to co-receptors of the host cell [160]. One of the main targets for MPER bNAbs is the gp41 fusion intermediate [161], [162], where some of these antibodies prevent refolding into the fusion-active conformation [163]. MPER bNAbs such as 10e8 and ln01 [164], [165] show various levels of autoreactivity such as lipid binding which plays a role in the maturation of MPER bNAbs, further providing evidence that the generation of these antibodies is linked to the succession of immune tolerance mechanisms through the engagement of antibody lineages induced by host proteins and microbiota [166], [167]. The MPER bNAbs, 10e8 and 4e10, have shown the broadest neutralisation breadth with 98% neutralisation of different viral strains during infectivity testing [164], [168].

1.6.2.2. The gp120-gp41 interface bNAbs

The gp160 Env is highly glycosylated and trimerized in the endoplasmic reticulum, where furin is responsible for its cleavage into the gp120 and gp41 subunits [169]. Gp120-gp41 interface bNAbs such as PGT151 and 35022, usually target specific glycan epitopes that overlap with gp41and are highly quaternary conformation-dependent. The neutralisation ability of the antibody 35022 requires binding to the N88, N230, and N241 glycans on gp120, and the neutralisation potential of PGT151 requires binding to the N611 and N637 gp41 glycans [164], [170]. By proximity, PGT151 is suggested to also bind to some gp120 glycans, however, these interactions are not crucial for neutralisation by the antibody [171].The heterogeneity of glycans results in various levels of neutralisation plateaus (maximum inhibition) of the gp120-gp41 interface bNAbs.

1.6.2.3. The CD4 binding site bNAbs

CD4 is required for functional infectivity of HIV-1 and therefore the CD4 binding site has a highly conserved structure. The isolation of CD4 binding site (CD4bs) bNAbs has occurred from multiple HIV-1 infected individuals, which suggests that these antibodies are commonly induced and are an achievable goal during the development of a vaccine. Two classes of bNAbs recognise the CD4 binding site (CD4bs), namely; CD4 mimicking CD4bs bNAbs, which mimic CD4 in its approach to gp120 and are predicted to neutralise the virus through steric hindrance. An example of CD4 mimicking CD4bs bNAbs are CH235, VRC01, and the class of bNAbs known as VRC01-like antibodies [172]. The CD4 mimicking CD4bs class is the most potent of the CD4bs bNAbs, and they possess a number of common properties that enable them to bind with high affinity to the CD4bs. One of the common features of this class of antibodies is that they have a variable region heavy chain from the V_H1-2 family, that with the necessary mutations, enables the antibodies to bind to the CD4bs in a similar way that the conserved CD4 receptor binds gp120. The second common feature is a very short LCDR3 consisting of five amino acids and several mutations including a few in the framework region, that accommodate a glycan at N276 that is in close proximity to the CD4bs.

Loop binders are another class of CD4bs bNAbs, where the binding of these antibodies is largely due to the long HCDR3 loop, and these antibodies interfere with the binding of gp120 to CD4. Examples of loop binders include CH103 and IgG1b12 [173], [174]. These antibodies have high

levels of SHM and a relatively long HCDR3, required for the penetration of the Env glycan shield. Loop binders' features are less restricted than VRC01-like antibodies and they are not as potent.

1.6.2.4. The high-mannose patch (V3-glycan) bNAbs

The high-mannose patch is located on the side of the outer domain of Env trimer in monomeric gp120 and contains a great deal of Man8/Man9 glycans in a dense region of the glycan shield [175]. This region was first identified with the 2G12 bNAb, which has a unique domain exchanged structure that is used to recognise a cluster of mannose glycans on N332 [176]–[178] (Figure. 1.6). This region has been described as a "supersite of vulnerability". A number of bNAbs were identified that bind to overlapping sites on the region around and including N332, however, they make use of long HCDR3s to penetrate through the glycan shield thus accessing the protein surface around the base of the V3 loop. BNAbs that target the glycan supersites on the V3 region of Env are PGT121 and PGT128 [175]. The breadth of these bNAbs is most likely as a result of their tolerance for glycan heterogeneity and the phenomenon known as glycan promiscuity, that can be described as the ability of the bNAbs to bind alternate glycans in certain circumstances. As a result of glycan promiscuity, these antibodies are able to recognise virus isolates that lack the N332 glycan.

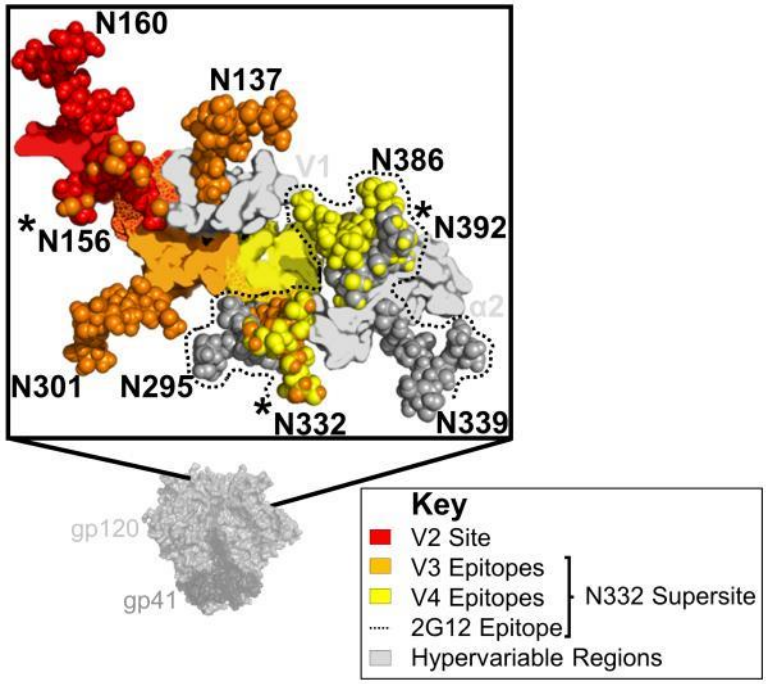


Figure 1.6: The high mannose patch broadly neutralizing antibody binding site on the HIV-1 envelope glycoprotein. The image shows the positions of the targeted glycans and the variable regions on which they are positioned. The red represents the V2 site, the orange represents the V3 epitopes, and the yellow represents the V4 epitopes. The N332 supersite is found on the V3 and V4 epitopes. Image obtained from *[179]*.

1.6.2.5. The Apex (V1/V2-glycan) bNAbs

The trimeric apex is formed from the converging, sequence conserved regions of the V1/V2 domain and the V3 loop [18], [180], [181]. The densely packed glycan at positions N160, and N156, as well as the hypervariable loops V1 and V2 provide protection to the virus against neutralisation [182]. For antibodies to access these apex epitopes, antibodies require unusually long anionic HCDR3 regions [183], [184]. The apex bNAbs are quaternary conformation dependent [183], [184], such as PG9 which bind to N160 glycans from two separate protomers [185], [186]. Some antibodies, such as CAP256-VRC26 which target a similar epitope to PG9 are not dependent on the N160 glycan for neutralisation [183]. The actual peptide epitope determined by mutagenesis is minimal for both of the above-mentioned antibodies and is made up mostly of a short stretch of cationic amino acids. For PG9, the peptide makes up less than 25% of the epitope while the rest of the epitope is made up of glycans [182]–[184], [187]. The conserved glycans form an essential component of these bNAbs-targeted epitopes and are required for the neutralising activity.

1.6.2.6. The Fusion peptide bNAbs

The fusion peptide is located at the N terminus of the gp41 subunit of Env, and is composed of 15 to 20 hydrophobic amino acids that are vital for the entry of virus into the host cell [188]–[190]. The N123-VRC34.01 antibody is directed against the fusion peptide and inhibits the conformational changes of Env required for virus-cell entry [190]. The glycans in the N-terminal region of the fusion peptide have been shown to be solvent exposed and are therefore a target for neutralising antibodies [191], [192].

1.7. Broadly neutralising antibodies and their role in HIV-1 vaccine development

The design of an immunogen able to elicit bNAbs remains the primary goal of HIV-1 vaccine development strategies. Numerous challenges need to be overcome, including the extensive viral diversity as a result of the HIV-1 error-prone DNA-dependent RNA polymerase and recombination resulting in unique recombinants and circulating recombinant forms [193], the low spike density of Env displayed on the surface of the virus which reduces the efficiency of cross-linking and antibody avidity and masking of critical epitopes that are crucial for neutralisation but are often protected by the high carbohydrate content of the virus [194]. Moreover, non-neutralising antibody responses are induced by the conformational flexibility of the virus, the strain-specific amino acid variability, and decoy forms of the HIV-1 Env, such as floating monomers [195]. As mentioned previously, several approaches to vaccine immunogen design have proven unsuccessful in generating bNAbs.

Strategies using Env-based vaccines have focused on developing antigenically correct immunogens, and have included gp120 monomers, resurfaced stabilised gp120 cores, gp120 outer domain, gp140 trimers, and various scaffolds that display specific epitopes (reviewed in [196]). These strategies were tested in small animal models and NHP and although these immunogens were all able to elicit antibodies with autologous Nab activity, none of them induced bNAb production. These challenges led researchers to focus more on understanding the immunobiology of HIV-1 Env, with a particular interest on the structural and functional basis for the neutralisation of HIV-1 Env.

The native HIV-1 Env spike is comprised of three gp120 and gp41 heterodimers that assemble via non-covalent interactions into a trimeric structure on the surface of the virus, and are the only virally-encoded exposed targets for antibodies. Consequently, a trimer-based immunogen design seems the most natural, native-like immunisation strategy. Of the most successfully strategies, was the introduction of SOSIP mutations that allow expression of soluble, cleaved forms of trimeric gp140 (gp160 with the transmembrane and cytoplasmic domain of gp41 deleted) which improves their stability and homogeneity [18]. For this purpose, a disulphide bond was introduced between gp120 and gp41, termed SOS, which links the subunits covalently therefore strengthening their interaction [114], [117], [197], [198]. The disulphide bond was formed specifically through a mutation on gp120, where there is Ala-to-Cys change at residue 501, and a mutation on gp41, where there is a Thr-to-Cys change at residue 605 [18] (Figure. 1.7). At position 559 of gp41 there was an Ile-to-Pro change, termed IP, which strengthens the gp41-gp41 associations and results in an improvement in trimer formation [114], [115] (Figure. 1.7). A type of SOSIP gp140 trimer was generated, based on the HIV-1 subtype A virus BG505 to remove all except five of the residues of the membrane proximal external region (MPER) until residue 664 of gp41 [199]. Due to the above-mentioned modifications, the expression of a thermostable, non-aggregating and homogenous soluble Env trimer, BG505 SOSIP.664 gp140 was successful. These trimers are compact, properly folded and mimic the native trimers on the surface of the HIV-1 virus [18]. The trimers are reactive with a wide variety of diverse bNAbs except MPER antibodies because the full MPER is not present in the construct [200]. The modifications made to develop SOSIP.664 gp140 trimeric immunogens in order to replicate the native Env have induced autologous NAb responses in small animals and NHP models, however, have failed to elicit strong bNAb responses [201]–[203]. The weak NAb responses observed are because the present and exposed conserved NAb epitopes on these native-like immunogens are not able to elicit a broad and potent immune response in the context of vaccination. Evidence of this is partly attributed to the fact that current Env-based immunogens and/or immunisation regimens are not able to direct the evolution of antibody affinity maturation required for the elicitation of effective NAb responses [173].

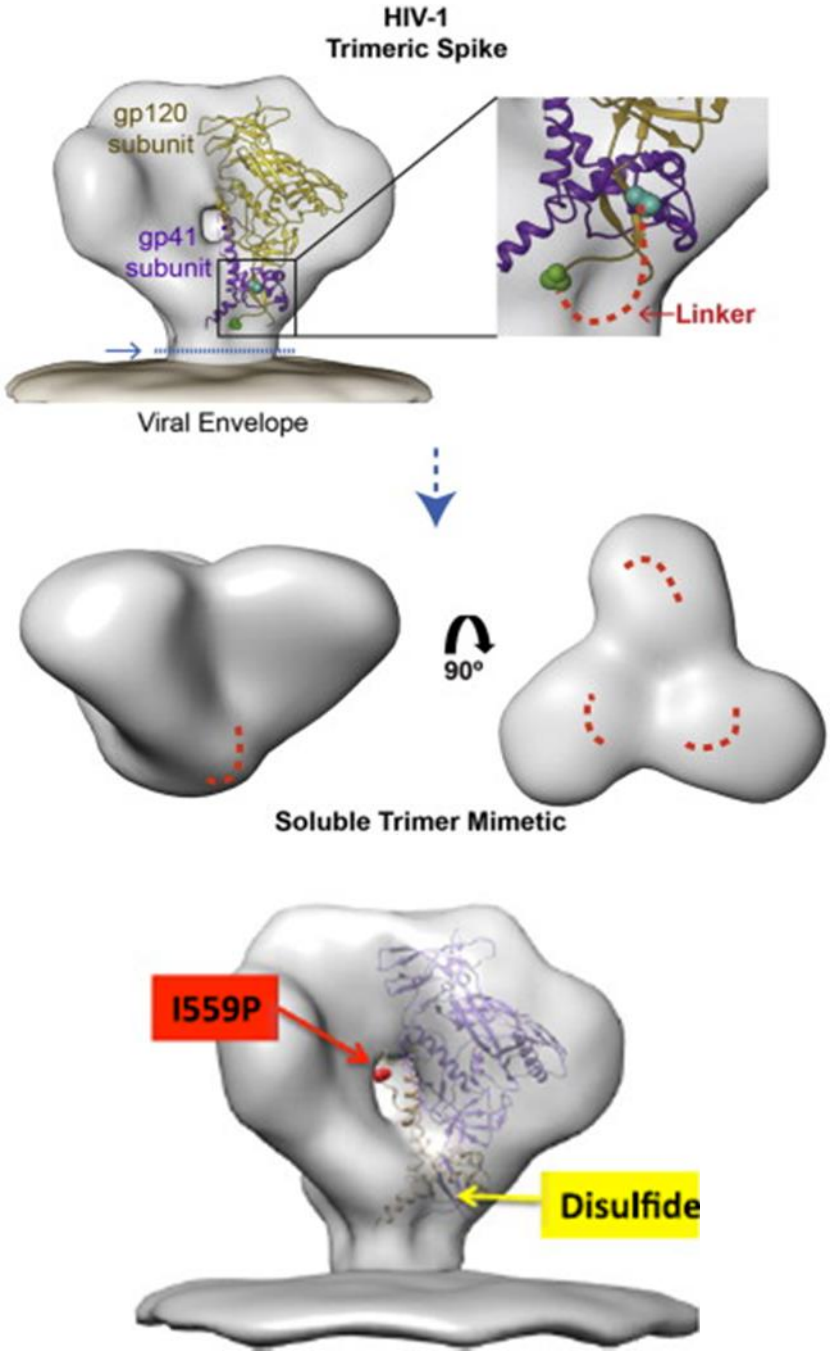


Figure 1.7: The native-like, soluble, trimeric conformation of SOSIP.664 gp140. The gp140 glycoprotein is cleaved into the gp120 and truncated gp41 subunits which are linked together through disuphide bonding. At residue 559 of gp41 there is a Ile-to-Pro change which improves trimerisation of Env. The MPER was cleaved until residue 664 increasing the solubility of Env. Image obtained from *[200]*.

In pre-clinical studies, it has proven possible to elicit cross-reactive bNAbs using alternative Env-based subunit immunogens. One of these Env-based immunogen ideas shown to elicit bNAbs makes use of the concept of driving the closed Env trimeric conformation to the more open conformation by complexing Env to the CD4 host receptor which results in conformational changes exposing otherwise hidden, CD4-induced (CD4i) epitopes [204]–[210]. In the closed quaternary Env structure the CD4i epitopes are poorly accessible due to the weakly immunogenic glycosylated Env surface [168], [211], [212]. Since the CD4i epitopes are composed of highly conserved sequences of Env [172], [213], this suggests that the associated target antibodies are highly cross-reactive across viral strains. These antibodies bind epitopes that include or are proximal to the bridging sheet where they compete with coreceptor binding and broadly although not potently are able to neutralise various HIV-1 strains [214]–[216]. The coreceptor binding epitopes are suggested to be immunogenic in humans based on the antibodies directed against CD4i epitopes isolated from HIV-1 infected individuals [213]. Several research groups are exploring the use of Env complexed to CD4 in the context of a vaccine to elicit bNAbs.

1.8. Rationale for study

A preliminary study performed by our laboratory testing various HIV-1 Env-2dCD4^{S60C} vaccine immunogens in New Zealand white rabbits demonstrated that it is possible to generate potent antibodies that are capable of neutralising a broad range of tier-2 (harder to neutralise) HIV-1 pseudoviruses *in vitro* [217]. The immunogen rationale was based on a previous study done by our laboratory, where recombinant 2-domain CD4 with a Ser/Cys mutation (2dCD4^{S60C}) was produced which bound gp120 with higher affinity through the formation of a targeted intermolecular disulphide bond [218]. On the CD4 domain 1 α-helix a substitution of Ser^{60} with Cys positions a thiol in proximity of the gp120 V1/V2 loop disulphide (Cys^{126}-Cys^{196}) resulting in the required sterochemical and geometric conditions for redox exhange between CD4 Cys^{60} and gp120^{126}, which subsequently leads to the interchain disulphide bond formation [218]. The study demonstrated that the functional mutated recombinant 2dCD4^{S60C} protein has a higher binding affinity to gp120 than wild-type 2dCD4 (2dCD4^{WT}) and the enhanced affinity is attributed to the disulphide exchange [218]. It was also demonstrated that between 2dCD4^{S60C}, 2dCD4^{WT} and soluble CD4 for binding to recombinant gp120 *in vitro*, 2dCD4^{S60C} bound better as the interaction was the most stable which potentially produces a more potent antiviral in cell culture [218].

Additionally, we described the generation and characterisation of an inferred HIV-1 subtype C Env sequence (Env_{FVC}) based on transmitted founder virus sequences from South Africa, Malawi, and Zambia [219]. Proteolytically cleaved $gp140_{GCN4(+)}$ trimers based on the Env_{FVC} sequences were stabilised through $2dCD4^{S60C}$ complexing to stimulate an immune reponse directed towards novel CD4i exposed epitopes [217]. The introduction of the GCN4-trimerisation motif coding sequence in gp140 sufficiently generated stable trimeric Env. GCN4 encodes a conserved zipper protein that functions as a transcription factor.

Findings from the preclinical study showed that the $gp140_{GCN4(+)}$ Env_{FVC} complexed to $2dCD4^{S60C}$ induced potent bNAbs, the extent of which has not been reported previously. The bNAbs likely target novel CD4i epitopes on the Env_{FVC}, novel $2dCD4^{S60C}$ epitopes, or a combination of both. Thus, this study aimed to isolate monoclonal antibodies from the immunised rabbits in an attempt to characterise the immune responses to the Env-$2dCD4^{S60C}$ and delineate the bNAb epitopes.

The objectives of the study are:

- To confirm the presence of bNAb responses in rabbits boosted with the Env-$2dCD4^{S60C}$ complex two years post the initial immunisations.
- To sort and isolate anti-HIV-1 specific B cells from rabbit peripheral blood mononuclear cells (PBMCs) using Flow Cytometry and FACS (Fluorescent Activated Cell Sorting) techniques, and PCR amplify the relevant antibodies' heavy- and light- chain variable (Fab) regions to create transcriptionally active linear cassettes.
- To express rabbit monoclonal antibodies using the heavy- and light- chain linear cassettes in HEK293T mammalian cells, and characterise their binding activity using ELISA, SDS-PAGE and Western blot analysis.

2. Materials and Methods

2.1. Reagents used in this study

The following recombinant plasmids, proteins and cell lines were available in our laboratory for the purposes of this study: expressed and purified 2dCD4^{S60C} recombinant protein used for the immunogen and the 2dCD4^{WT} recombinant protein used for the memory B cell isolation and the characterisation studies, expressed using the recombinant pET15-2dCD4$^{(S60C/WT)}$ vectors [218]; the CAP45 GCN4(+) stable expressing Freestyle human embryonic kidney (HEK) derived 293F cell line (Thermo Fisher Scientific, Waltham, MA, USA) used for the expression of recombinant CAP45 GCN4(+) (gp140$_{GCN4}$ Env) [217]; HIV-1 antibody expression vectors (heavy and light chain) for the 2G12 (VRC_4196 and the VRC_4197 plasmid vectors, Appendix A, Supplementary Figure. 1A, and 1B, gifted by Dr Peter Kwong of the NIH National Institute of Allergy and Infectious Disease); the 10e8 antibody expression vectors (contributed by Dr Mark Connors; obtained through the NIH AIDS Research and Reagent Program, Division of AIDS, NIAID) and the purified 10e8 antibody for use as a positive control for the SDS-PAGE and western blot analyses [220]; protein-A, affinity chromatography purified total rabbit IgG antibodies from sera (rabbit 63 – immunized with Env/2dCD4^{S60C} complex) as a suitable positive control for the SDS-PAGE and western blot analyses; HEK 293T mammalian cells used for recombinant protein and antibody expression; stored serum samples obtained from three rabbits (rabbit ID 24, 31 and 83) two-weeks after their last boosting immunisation with Env/2dCD4^{S60C} complex (16th December 2016), and served as Baseline 0 (B0) samples for the neutralization assays.

A human ethics waiver was obtained from the University of the Witwatersrand Committee for Research on Human Subjects (Appendix B).

2.1.1. Reagents used for TZM-bl-based neutralisation assays

The following reagents were obtained through the NIH AIDS Research and Reference Reagent Program, Division of AIDS, NIAID: the TZM-bl (JC53-bl) reporter cell line (Drs John C. Kappes, Xiayun Wu and Transzyme Inc.); ZM53M.PB12 envelope expression plasmid (Drs E. Hunter and C. Derdeyn) and the pSG3$^{\Delta Env}$ plasmid (Drs. John C. Kappes and Xiaoyun Wu).

2.2. General mammalian cell culture

2.2.1. Reviving frozen rabbit Peripheral Blood Mononuclear Cells (PBMCs)

For the fluorescence activated cell sorting (FACS), frozen PBMCs were thawed on ice and revived in pre-warmed complete RPMI media ((10% Foetal Calf Serum (FCS) (Gibco, Life Technologies, Carlsbad, CA, USA), 2 mM L-glutamine (GlutaMax, Gibco, Life Technologies, Carlsbad, CA, USA), and penicillin (100 µg/ ml) and streptomycin (100 µg/ ml) (Sigma-Aldrich, St. Louis, MO, USA), 2mM sodium pyruvate (Gibco, Life Technologies, Carlsbad, CA, USA), 10mM HEPES (Thermo Fisher Scientific, Waltham, MA, USA), 0.05mM 2-mercaptoethanol (Thermo Fisher Scientific, Waltham, MA, USA)) for 24 hours at 37℃, in T75 tissue culture flasks (Nunc, Roskilde, Denmark).

2.2.2. Maintenance of TZM-bl cells, HEK 293T cells, and 293F cells

TZM-bl (JC53-bl) cells and HEK 293T cells were maintained in 15 ml Dulbecco's Modified Eagle Medium (DMEM) supplemented with 10% FCS (Gibco, Life Technologies, Carlsbad, CA, USA), 2 mM L-glutamine (GlutaMax, Gibco, Life Technologies, Carlsbad, CA, USA), and penicillin (100 µg/ ml) and streptomycin (100 µg/ ml) (Sigma-Aldrich, St. Louis, MO, USA) in a 75 cm^2 Corning Cell Culture Flask (Sigma-Aldrich, St Louis, MO, USA). Once the cells reached 70% to 80% confluency, the cells were washed with 5 ml of 1× Dulbecco's Phosphate Buffered Saline (PBS), and 2 ml of Tryple (Thermo Fisher Scientific, Waltham, MA, USA) was added to the cells for 45 seconds at room temperature. The Tryple was aspirated and the cells were incubated for 5 min at 37℃ with 5% CO_2 to allow the adherent monolayer of cells to detach from the culture cell flask. The cells were stained using 0.4% trypan blue solution (Sigma-Aldrich, St. Louis, MO, USA) at a ratio of 1:1 to the cell suspension. Thereafter, viable cells were counted microscopically from the stained cell suspension using the Countess II FL cell counter (Life Technologies, Carlsbad, CA, USA). The cells were re-seeded in 15 ml of complete DMEM at a concentration of 3×10^5 cells/ml. The cells were passaged every 48 hours or at optimal confluency.

Stable FreeStyle (293F) cells expressing $gp140_{GCN4}$ Env were subcultured every 48 hours in serum-free Freestyle™ Expression Media (Thermo Fisher Scientific, Waltham, MA, USA) supplemented with a final concentration of 250 µg/ml Geneticin (G418, Gibco, Thermo Fisher,

Waltham, MA, USA) in one fifth of the total volume of an Erlenmeyer flask (Sigma-Aldrich, St Louis, MO, USA). The cells were stained using 0.4% trypan blue solution at a ratio of 1:1 to the cell suspension. Thereafter, viable cells were counted and the viability was established microscopically from the stained cell suspension using the Countess II FL cell counter and seeded at a cell number of between 0.2-0.5×10^6 cells/ml. The cells were incubated at 37°C with 5% CO_2 on a shaker flask system at a rotational speed of 130 rpm.

2.3. Recombinant protein expression

For immunization studies, subsequent B cell isolation and characterization, adequate amounts of the $gp140_{GCN4}$, $2dCD4^{S60C}$, and $2dCD4^{WT}$ proteins were expressed and purified using the protocols described below.

2.3.1. 2dCD4 expression and purification

The $2dCD4^{S60C}$ protein, one of the components of the immunogen used for this study, and $2dCD4^{WT}$ protein were expressed and purified as described previously [218]. Briefly, the recombinant pET15-2dCD4($^{S60C, WT}$) vector was used to transform BL21 (DE3) *E. coli*. For protein expression freshly transformed BL21 (DE3) colonies were expanded in standard LB media at 37˚C on high rotation until optical density ~ 0.6 at 600nm was achieved. Protein expression was carried out in the absence of the IPTG-induction by transferring the culture to 20˚C shaking incubator culturing for a further 20 hours. The recombinant $2dCD4^{S60C/WT}$ was purified from insoluble inclusion bodies using a denaturing purification protocol and refolded in glutathione-containing refolding buffers, and analysed by SDS-PAGE and western blot analyses (see section 2.7.3). Using this method, between 0.5 and 1.0 mg of functional recombinant $2dCD4^{S60C/WT}$ (per litre of bacterial cell culture) were routinely purified.

2.3.2. CAP45 GCN4(+) gp140 expression

$Gp140_{GCN4}$ Env, one of two protein components for immunisations and B cell isolation, was expressed as follows: The supernatant containing the expressed $gp140_{GCN4}$ Env was harvested every 48 hours simultaneously as the 293F cells were passaged. The supernatant was harvested by centrifugation, using the Eppendorf centrifuge 5804R (Thermo Fisher Scientific, Waltham, MA, USA) at 1000 ×g for 10 minutes and thereafter stored at -20°C until purification.

2.3.3. CAP45 GCN4 (+) gp140 purification

2.3.3.1. Lectin affinity chromatography for the purification of CAP45 GCN4 (+) gp140

The supernatant from the stably transfected cells was filtered through an Acrodisc syringe filter with a 0.45 μm Supor® membrane (PALL Life Sciences, Port Washington, NY, USA). The equivalent of 1 ml packed agarose-conjugated *Galanthus nivalis* (snowdrop) lectin resin (Sigma, St Louis, MO, USA) was added to the supernatant and incubated overnight at 4℃ while stirring. The suspended resin was harvested from the culture supernatant by passing it through a Luer-lock, non-jacketed liquid chromatography column (Dimensions: internal diameter (i.d.) 2.5 × 10 cm) (Sigma-Aldrich, St. Louis, MO, USA). The collected flow-through was reserved in order to perform an additional round of lectin purification to maximize protein yields. The harvested resin was washed with 100 ml of 1 M $NaCl_2$ solution prepared in 1×PBS (Thermo Fisher Scientific, Waltham, MA, USA), followed by 100 ml of 0.5 M $NaCl_2$, 1×PBS solution and finally re-equilibrated with 100 ml of 1×PBS. Twenty millilitres of 1 M methyl α-D-manno-pyranoside (MMP) (Sigma-Aldrich, St. Louis, MO, USA) prepared in 1×PBS was added to the resin and incubated for 30 min to elute the recombinant CAP45 GCN4(+) gp140 Env protein, this step was repeated. The lectin resin was reconstituted by passing through 100 ml of 1M $NaCl_2$ prepared in 1×PBS, and then 100 ml of 1×PBS through the column. After the second round of lectin purification, the eluted protein fractions were combined and filtered through an Acrodisc syringe filter with a 0.45 μm Supor® membrane. An Amicon® Ultra-50kDa (MilliporeSigma, Burlington, MA, USA) centrifugation filter unit was used to concentrated the protein to an approximate final volume of 1 ml. The concentrated protein was washed with 1×PBS to remove the residual MMP. Aliquots of the filtered supernatant, the flow-through, and the wash steps were collected to run on an 10% SDS-PAGE gel, and analysed by western blot for visualisation of the protein.

2.3.3.2. Determination of protein concentration

The concentrated $gp140_{GCN4}$ Env was quantified using a BCA™ Protein Determination Kit (Pierce, Thermo Fisher Scientific, Waltham, MA, USA) and the protocol was followed as per the manufacturer's instructions. Bovine serum albumin (BSA) standards ranging from 25 – 2500 μg/ml were prepared in 1×PBS and used to determine the standard curve from which the concentration of the expressed and purified proteins was calculated. Ten microliters of the BSA

standards and unknown samples were each added to a flat-bottomed, 96-well, polysorp Immuno plate (Nunc, Thermo Fisher Scientific, Waltham, MA, USA) in duplicate. Thereafter, 200 µl of the BCA working reagent was added to each sample and incubated at 37°C on an orbital shaker (THERMOstar Microplate incubator, BMG Labtech, Ortenberg, Germany) at 1500 rpm for 30 minutes. Following incubation and allowing the plate to cool to room temperature the absorbance at 570 nm was determined using the BioRad iMark™ microplate reader (BioRad, Hercules, CA, USA). The unknown sample protein concentrations were determined from a standard curve plotted from absorbance values of blank corrected protein standards.

2.3.3.3. Size exclusion chromatography of $gp140_{GCN4}$ Env for the isolation of the trimeric conformation

Size exclusion chromatography (SEC) was performed to separate proteins based on size and isolate the trimeric $gp140_{GCN4}$ conformation. The trimer conformation is representative of the native envelope spike on the surface of HIV-1 and is used to recapitulate the native antigenicity/immunogenicity of the native Env spike in soluble trimer conformation. SEC was performed using the HiLoad 16/600 Superdex 200 PG column (GE Healthcare, Chicago, IL, USA) which separates proteins of approximately 10 to 600 kDa in size. Separations were performed on the AKTA FPLC (fast protein liquid chromatography platform) (GE Healthcare, Chicago, IL, USA). Prior to protein conformation separation, the column was washed by passing 50 ml of 0.5 M NaOH, followed by 50 ml of 70% ethanol, and then 120 ml of 20% ethanol through the AKTA purification system. All of the solutions used to wash the column was passed through the AKTA purification system at a flow rate of 1 ml/min. The column was then equilibrated with filtered and sterile 1×PBS for 120 min at a flow rate of 1 ml/min. The $gp140_{GCN4}$ protein sample was prepared by centrifuging the sample at 16 000 ×g for 5 minutes to remove aggregated proteins from the sample. One millilitre of the lectin-purified and concentrated recombinant $gp140_{GCN4}$ Env protein was loaded on to the column resolved at 1 ml/min flow rate. Eluted protein was fractionated into 2 ml volumes and the corresponding trimeric conformation peaks and the presence of recombinant $gp140_{GCN4}$ Env protein was confirmed by SDS-PAGE and western blot analysis. The fractions that confirmed for the presence of recombinant proteins were combined and concentrated using an Amicon® Ultra-50kDa centrifugation unit. The concentration of the $gp140_{GCN4}$ Env was then determined using the BCA kit as described in section 2.3.3.2.

2.4. Confirmation and boosting of anti- HIV-1 neutralising antibodies in rabbit sera

The three New Zealand White (NZW) (*Oryctolagus cuniculus*) rabbits (Rabbit ID 24, 31 and 83) used in this study were last immunised two years prior to the initiation of the current study, on 16th December 2016, and were observed to elicit a broadly neutralising response against clinically relevant HIV-1 strains [217]. For this study, the three rabbits were boosted with the same $gp140_{GCN4}$ Env/$2dCD4^{S60C}$ immunogen complex, and the blood was used to isolate antigen-specific memory B cells. Animal immunisations were performed following University of the Witwatersrand Animal Ethics Screening Committee approval (AESC clearance no: 2014 51 B; Appendix C).

The $gp140_{GCN4}$ Env/$2dCD4^{S60C}$ immunogen complex was generated by incubating equimolar amounts of $gp140_{GCN4}$ Env with $2dCD4^{S60C}$ in the presence of 1 mM β-mercaptoethanol for 1 h, and further purified by SEC [217]. For the immunisations, the $gp140_{GCN4}$ Env/$2dCD4^{S60C}$ immunogen complex was formulated in Adjuplex™ (Advanced BioAdjuvants Omaha, Nebraska, USA) according to manufacturer's instructions. Adjuplex™ adjuvant is a nanoliposomal mixture of carbomer homopolymer and highly purified natural phospholipids and is used to boost the immune response generated by the antigens [221]. Each animal received 20 µg of total $gp140_{GCN4}$ Env/$2dCD4^{S60C}$ protein-immunogen in a final volume of 500 µl. Immunisations were administered intramuscularly, alternating right and left hind legs [217].

At the start of this study (11 April 2018) a baseline bleed was performed (Baseline 1; B1), where 10 ml of blood in total was collected from each rabbit, 5 ml of blood was collected into clot activator serum Vacutainer Blood collection tubes (BD Biosciences, Franklin Lakes, N.J., USA) for serum isolation, and the other 5 ml of blood into ethylenediaminetetraacetic acid (EDTA) Vacutainer Blood collection tubes (BD Biosciences, Franklin Lakes, N.J., USA) for the isolation of PBMCs. Two weeks later, rabbits received boosting immunisations according to the procedure described above [217], and two weeks post boost, (10 May 2018), the rabbits were bled where 5 ml of blood from each rabbit was collected into clot activator serum tubes and 5 ml of blood was collected into EDTA tubes (Vaccine Boost 1; VB1). The sera from each blood sample collected in

the clot activator serum tubes was isolated by centrifugation at 1000 ×g for 10 minutes. The sera were aspirated and stored at -80 ℃ until use.

2.4.1. Neutralising antibody assay

Prior to evaluating the baseline and boosted neutralizing sera titres, frozen rabbit sera samples were thawed to room temperature and then heat inactivated to remove complement proteins, by heating each sample at 56 ℃ for one hour. Neutralizing antibody responses were assessed against a tier-2 clinically-relevant pseudovirus, ZM53M.PB12, using an HIV-1 pseudovirus infectivity assay in the TZM-bl reporter cell line. The neutralization assay was performed using Nunc™ Edge 2.0 96-Well Plates (Thermo Fisher Scientific, Waltham, MA, USA) as follows, 150 µl of complete DMEM (DMEM (Thermo Fisher Scientific, Waltham, MA, USA), 10% FCS, 1% penicillin/streptomycin, 0.05% glutamine (Thermo Fisher Scientific, Waltham, MA, USA)) was added to the cell control wells, and 100 µl of complete DMEM was added to the virus control wells. For the sera samples, 100 µl of complete DMEM was added to each well, thereafter undiluted sera were added to the first row and 3-fold serial dilution performed in order to produce a dilution range from 1:20 to 43,740. Fifty microlitres of 4,000 $TCID_{50}$ (50 % Tissue Culture Infectious Dose) pseudovirus, ZM53M.PB12, was added to the sample wells and the virus control wells. The $TCID_{50}$ was calculated using the standardized calculation published by the Los Alamos HIV Database [222] which determines the pseudovirus concentration based on positive infection. The plate was incubated at 37℃ in 5% CO_2 for 1 hour. Following incubation, 100 µl of TZM-bl cells (1×10^5 cells/ml in complete DMEM supplemented with DEAE Dextran (Sigma-Aldrich, St Louis, MO, USA)) was added to each sample well, the virus control wells, and the cell control wells. The plates were incubated at 37℃ in 5% CO_2 for 48 hours. The DEAE Dextran was added at a final concentration of 20 µg/ml.

Following the 48-hour incubation, luciferase expression was determined as follows: The media was aspirated from the wells, and 80 µl of Glo lysis buffer (Promega, Madison, WI, USA) was added to each well and incubated at room temperature for 5 minutes, 50 µl of the cell lysate was aspirated and transferred to a Corning™ 96-Well Solid White Polystyrene Microplate (Thermo Fisher Scientific, Waltham, MA, USA), and 50 µl of BrightGlo luciferase (Promega, Madison, WI, USA) was added to each well. Luminescence was quantified within 15 minutes using the Promega Glomax Explorer luminometer (Promega, Madison, WI, USA). Using the luminescence

readings generated by the Promega Glomax Explorer lumimometer, the percentage of pseudovirus inhibited from infecting the TZM-bl cells was calculated. GraphPad Prism 8 v. 8.0.2. (GraphPad Software, La Jolla, CA, USA) was used to generate a graph showing the percentage inhibition against the sera dilution, and from the graph, the ID_{50} values were calculated using the non-linear regression function. The ID_{50} values represent the sera dilution required to inhibit 50% of virus infection. The data was normalized to the cell control and virus control.

2.5. Rabbit antigen specific B memory cell isolation

2.5.1. Peripheral Blood Mononuclear Cells (PBMCs) Isolation

To further characterize the rabbit neutralising antibody response elicited as a result of the $gp140_{GCN4}$ Env/$2dCD4^{S60C}$ immunogen complex, antigen-specific memory B cells were required to be isolated from the rabbit PBMCs using FACS sorting. Ficoll-Paque density gradient centrifugation was used to purify PBMCs from the peripheral blood of the three immunised rabbits, according to the manufacturer's instructions (GE Healthcare, Chicago, IL, USA). Briefly, the rabbit blood collected in the EDTA-tubes were diluted with an equal volume of with 1×PBS. Fifteen millilitres of Ficoll-Paque (GE Healthcare, Chicago, IL, USA) was added to the bottom of a 50 ml tube, and the diluted rabbit blood was layered on top of the 15 ml of Ficoll-Paque. The tubes were centrifuged at 350 ×g for 30 min (with no brake). The PBMCs layer was carefully collected and transferred into a new tube to which 15ml of 1×PBS was added to wash the PBMCs. Washing was done by gently pipetting up and down the PBS followed by centrifugation at 210 ×g for 10 minutes. This wash step was repeated a total of three times. After the third wash the PBMCs were resuspended in 10 ml of 1×PBS and cell viability was determined and the cells were enumerated using the ReadyProbes™ Cell Viability Imaging Kit (Blue/Green) (Invitrogen, Thermo Fisher Scientific, Waltham, MA, USA) according to the manufacturer's instructions using the Countess II FL cell counter (Life Technologies, Carlsbad, CA, USA). Briefly, the ReadyProbes® Cell Viability Imaging Kit (Blue/Green) makes use of fluorescence to determine cell viability and contains a NucBlue® Live reagent which binds the nuclei of live cells and can be detected using a DAPI filter, and a NucGreen® Dead reagent which binds to the nuclei of dead cells and can be detected using a FITC/GFP filter. Following enumeration, PBMCs were harvested by centrifugation and diluted to 1×10^6 cells/ml in freezing mix (10% Dimethyl Sulfoxide (DMSO) (Sigma-Aldrich, St Louis, MO, USA), 90% Fetal Calf Serum (FCS)). Five hundred

microliter aliquots were prepared and frozen using the Mr. Frosty™ Freezing Container (Thermo Fisher Scientific, Waltham, MA, USA) and stored at -80°C until usage.

2.5.2. Antigen-specific memory B-cell isolation by Fluorescence activated cell sorting (FACS)

FACS is a specialized form of flow cytometry. The method sorts a heterogenous mixture of biological cells into desired containers, one cell at a time, based on light scattering and their fluorescent characteristics. The light scatter determines the size of the cells (forward scatter), and the granularity and complexity of the cells (side scatter). To sort for the antigen-specific memory B cells from the PBMCs, antibodies conjugated to fluorochromes (Table 2.1) were used to detect the appropriate surface cellular markers. When the conjugated antibodies find antigens on cell surface markers, the fluorescence of the fluorochromes can be monitored as these cells pass through a laser beam. The fluorochrome panel was based on the panel used in a previous study by Starkie, *et al* [223], however, the panel was optimised for this study as follows: the spectral overlap of the emission spectrum of each fluorochrome, and the lasers included in the FACS Aria I available to the laboratory were considered. The entire panel of fluorochromes were analysed, ensuring that the spectral overlap was minimal. Any residual fluorescence spillover was corrected for using the compensation controls.

Table 2.1: Summary of the antibodies and fluorophore conjugates required for rabbit antigen-specific memory B cell isolation.

Target cell	Cell marker	Conjugates (concentration used for conjugation reaction)		
		Antibody	**Fluorophore**	**Fluorophore maximum emission spectrum**
Live/dead cells	Genetic material	None	Hoechst 33342	461 nm
T cells	CD3	Rat anti-rabbit CD3 IgG*	FITC	525 nm
Naïve B cells	IgM	Mouse anti-rabbit IgM (100 µg)	APC-Cy7 (12 µg)	785 nm
Memory B cells	IgG	Goat anti-rabbit IgG*	PE	578 nm
Antigen-specific memory B cells	2dCD4^{WT}-antigen	2dCD4^{WT} protein (100 µg)	DyLight 680 (12 µg)	715 nm
	Env (gp140$_{GCN4}$) -antigen	Env (gp140$_{GCN4}$) protein (100 µg)	Alexa Fluor 647 (40.5 µg)	668 nm

* The antibodies were purchased as fluorophore conjugates therefore no conjugation step was required.

2.5.2.1. Preparation of the antibody and fluorophore conjugates required for FACS

The following experimental procedures were used to conjugate the necessary antibodies and proteins to the fluorophores: The APC/Cy7® Conjugation Kit - Lightning-Link® (Abcam, Cambridge, UK) was used to conjugate 100 µg of mouse anti-rabbit IgM (Bio-Rad, Hercules, CA, USA) to 12 µg of Allophycocyanin–Cy7 (APC-Cy7), and the Lightning-Link® DyLight® 680 Conjugation Kit (Fast) - Lightning-Link® (Abcam, Cambridge, UK) was used to conjugate 100 µg of 2dCD4^{WT} to 12 µg of DyLight 680. The conjugation protocol for the above-mentioned conjugates (mouse anti-rabbit IgM-APC-Cy7 and 2dCD4^{WT}-DyLight 680) was performed according to the manufacturer's instructions as follows, 1 µl of modifier reagent was added for every 10 µl of antibody/protein and mixed gently. The total volume (11 µl) of sample mix (modifier reagent and antibody/protein) was added to the lyophilized dye material and used to resuspend the lyophilized fluorescent dye material. The resuspended dye and sample mix were

incubated at room temperature in the dark for 15 minutes to allow for chemical conjugation reaction to take place. Following incubation of the dye and sample mix, 1 µl of quencher reagent was added to this mixture for every 10 µl of antibody/protein used, mixed gently and incubated for four minutes. The conjugates were then ready for use.

The Alexa Fluor™ 647 Microscale Protein Labeling Kit (Thermo Fisher Scientific, Waltham, MA, USA) was used to conjugate 100 µg of $gp140_{GCN4}$ Env and 40.5 µg of Alexa Fluor 647, according to the manufacturer's instructions, as follows: A 1/10 volume of 1 M sodium bicarbonate (pH ~8.3) was added to the $gp140_{GCN4}$ Env, and gently mixed. Ten microliters of dH_2O was added to completely dissolve the Alexa Fluor succinimidyl ester moiety which reacts with the primary amines of the protein forming stable protein-dye conjugates. The reactive dye solution was added to the protein sample mix, and mixed thoroughly by pipetting up and down several times. The reaction mixture was incubated at room temperature in the dark for 15 minutes. Following incubation, the conjugate was purified to remove any unreacted dye solution as follows, 800 µl of a supplied gel resin was added to a spin column and centrifuged at 16,000 ×g for a total of 15 seconds. Fifty microliters of the reaction mixture were added to the centre of the surface of the resin bed, and centrifuged at 16,000 ×g for 1 minute.

2.5.2.2. Preparation of the compensation beads for FACS

To adjust for any fluorescence emission spectral overlap between the selected fluorescent dyes used for labelling, a compensation step was prepared before the antigen-specific B cells were sorted. The BD™ CompBead Anti-Mouse Ig, κ/Negative Control Compensation Particles Set (BD Biosciences, Franklin Lakes, N.J., USA) were prepared by adding one drop of beads in 10 µl of 1×PBS. The anti-rat antibodies were able to bind to the antibody capture beads because of the high homology between the rat and mouse IgG1, IgG2a/b/c constant regions [224], [225].

The prepared antibody capture beads were stained independently. A 1 in 10 dilution of the rat anti-rabbit CD3-Fluoroscein isothiocyanate (FITC) conjugate (GeneTex, Irvine, CA, USA) prepared in a final volume of 40 µl, 3µl of the mouse anti-rabbit IgM-APC-Cy7 conjugate, and 50 µl of the PE mouse anti-rabbit IgG detector (BD Biosciences, Franklin Lakes, N.J., USA) was prepared as recommended by the manufacturer. Instead of using the goat anti-rabbit IgG PE that was used to stain the PBMCs, the PE mouse anti-rabbit IgG detector was used for compensation as it is the correct species for the beads and the antibody was manufactured specifically for testing on

compensation beads. Compensation was not performed for Alexa Fluor 647 and DyLight 680, as these two fluorophores emit light at similar wavelengths (Table: 2.1) with a significant amount of spectral overlap which was not an issue in the current study as both of the antigens ($gp140_{GCN4}$ and $2dCD4^{WT}$) labelled with the respective fluorophores were used to select and sort for the bound antigen-specific fluorophores. Once the fluorescent dyes were added to the compensation beads, the beads were incubated in the dark at room temperature for 60 minutes. Following incubation, 1 ml of 1×PBS were added to the beads to remove any unreactive dye conjugates and centrifuged for 5 minutes at 200 ×g. The supernatant was discarded and the beads were resuspended into a final volume of 500 µl of 1×PBS.

2.5.2.3. Preparation of the purified rabbit PBMCs for FACS

Prior to staining, the purified rabbit PBMCs previously enumerated and stored at 1×10^6 cells/ml, were thawed on ice, and centrifuged at 200 ×g for 5 minutes, and the supernatant was discarded. The PBMCs were washed once with 500 µl of 1×PBS, centrifuged at 200 ×g for 5 minutes, and the supernatant was discarded. The PBMCs were resuspended in final volume of 100 µl in 1×PBS. The cells were stained with 10 µl of Hoechst 33342 (BD Biosciences, Franklin lakes, N.J., USA) (10 µg/ml) as recommended by the manufacturer, 10µl of rat anti-rabbit CD3 IgG – FITC (25 µg), 3µl of mouse anti-rabbit IgM – APC-Cy7, 10 µl of goat anti-rabbit IgG – PE (0.1 mg/ml), 20 µl of $2dCD4^{WT}$ - DyLight 680, and 20 µl of $gp140_{GCN4}$ Env - Alexa Fluor 647. The PBMCs were incubated with the conjugates in the dark for 60 minutes on ice. Following incubation, the cells were washed once with 500 µl 1×PBS to remove any unbound antibody/fluorophore and centrifuged at 200 ×g for 5 minutes. The supernatant was discarded and the cells were resuspended to a final volume of 500 µl. Unstained cell controls were prepared as negative controls and to appropriately set the photomultiplier tubes (PMT) voltages and account for any background autofluorescence.

FACS analysis was performed using the FACS Aria I flow cytometer (BD Biosciences, Franklin Lakes, N.J., USA) and data analyzed using the FACSDiva V6.2 and FlowJo V10.0.1 (TreeStar) software programs. To reduce the number of false positives (cells that are not antigen-specific memory B cells) from being sorted during the experimental procedure, a series of gating events was used to sieve through the pool of PBMCs in order to isolate the antigen-specific memory B cells. Briefly, the first population of cells that were selected for were the single cells, using the

forward scatter height and forward scatter area parameters. From the single cell population, live cells were selected using the forward scatter and negative staining for Hoechst 33342 (a cell viability dye that binds to the cell's double-stranded DNA) parameters. From the live cell population, T cells were identified and discarded using a rat anti-rabbit CD3 IgG antibody conjugated to FITC. From the CD3 negative population, the naïve B cells were identified and discarded as follows: a mouse anti-rabbit IgM antibody conjugated to APC-Cy7 was used to bind the IgM marker on naïve B cells. From the IgM negative population of cells, the memory B cells were selected using a goat anti-rabbit IgG antibody conjugated to PE since IgG is a marker for memory B cells. Cells that showed positive fluorescence in the PE emission spectrum were selected and the antigen-specific memory B cells were identified for sorting based on their binding specificity to $gp140_{GCN4}$ Env trimeric protein conjugated to Alexa Fluor 647 or $2dCD4^{WT}$ protein conjugated to DyLight 680 or memory B cells that demonstrated specificity to both antigens (dual specificity). The gating strategy is explained in more detail in section 3.3. The cells were individually sorted into flat-bottomed 96-well Nunc Polysorp plates (Nunc, Roskilde, Denmark) containing 20 µl of complete reverse transcription buffer (1× RT buffer (Thermo Fisher Scientific, Waltham, MA, USA), 2 U/µl RNAse OUT™ (Thermo Fisher Scientific, Waltham, MA, USA), 1.25 µl of 0.1 M DTT (Thermo Fisher Scientific, Waltham, MA, USA), 0.0625 µl Igepal (Thermo Fisher Scientific, Waltham, MA, USA), DEPC-treated dH_2O (Ambion, Austin, TX, USA) up to final volume of 20 µl). Plates were stored at -80°C until use.

2.6. PCR amplification of the transcriptionally active linear cassette

Transcriptionally active linear expression cassettes were assembled by PCR for the expression of rabbit monoclonal antibodies from isolated antigen specific memory B cells described above. The antigen-specific memory B rabbit cells were lysed and RNA reverse-transcribed using the SuperScript IV (SSIV) enzyme and oligoDTs according to the manufacturer's instructions (Invitrogen, Carlsbad, CA, USA). This method of RNA reverse transcription by the addition of the SSIV enzyme and oligoDTs directly to the cells was preferable to having a separate RNA isolation step due to low quantity of RNA starting material as a result of single B cell isolation and lysis.

All PCRs reactions used the 2× Master Mix Q5 high-fidelity enzyme (New England Biolabs, Ipswich, MA, USA) to avoid PCR-induced errors and DEPC-treated water (Ambion, Austin, TX, USA), unless otherwise stated. Purification of all PCR amplification products were performed

using the GeneJET PCR Purification Kit (Thermo Fisher Scientific, Waltham, MA, USA) according to the manufacturer's instructions.

The primer sequences and corresponding annealing temperatures for each PCR for the heavy- and light-chain fragments are shown in Tables 2.2 and 2.3, respectively. Corresponding heavy- and light-chain variable antibody regions were amplified from the reverse transcribed cDNA using the 5′ and 3′ gene specific primers [223] in a primary PCR, with the 5′ oligonucleotide (oligo) binding to the rabbit variable region leader sequence and the 3′ oligo annealing to either the CH1 (heavy) or Cκ (light) constant regions. A second PCR was performed on all the primary PCR products that yielded both a heavy and a light chain product from the same isolated memory B cell cDNA. The secondary PCR primers sequences [223] are nested within the primary light- and heavy-chain amplicons and contain overlapping nucleotide sequences with HCMV at the 5′ and the heavy- or light-chain antibody constant region on the 3′ end, respectively. These overlapping nucleotide sequences were engineered to facilitate the correct assembly of the transcriptionally active linear cassette following the tertiary PCR (described below). The HCMV promoter was amplified using primers as described in Table 2.2 and 2.3, in a separate PCR reaction using the VRC_4196 plasmid vector as a template (see Appendix A1). The HCMV promoter was not independently amplified to the heavy- or light-chain specifically, and therefore, the same HCMV PCR amplicon was used downstream for both the heavy- and light-chain. Rabbit heavy- and light-chain antibody constant regions, including a poly-adenylation tail sequence (polyA tail), were amplified using primers described in Table 2.2 and 2.3 from constructs generated by GeneArt (Thermo Fisher Scientific, Waltham, MA, USA). These constructs comprised the same rabbit heavy- and light- chain constant sequences available in the pFUSEss-CHIg-rG and pFUSE2ss-CLIg-rK1 vectors, respectively (see Appendix A, supplementary Figure 2 for the heavy- and light-chain constant and polyA fragment inserts). A final PCR (referred to as a tertiary PCR) was performed using primers (Table 2.2 and 2.3) to amplify the final assembled expression cassette comprising (from 5′ to 3′ end) the HCMV promoter, the antibody's variable region and the constant regions containing a polyA sequence at the 3′ end (inclusion of the promoter and constant-polyA fragments in this PCR is necessary). The assembled expression linear cassette ensures it is transcriptionally active for both the heavy- and light-chain genes that can be directly used to co-transfect mammalian cells on a small-scale in order to screen and characterize the IgG-containing supernatant.

Table 2.2: Primers used for the amplification of the transcriptionally active linear expression cassette containing the heavy-chain antibody fragment. The overlapping sequences introduced by the secondary PCR primers are underlined. The red underlining denotes the variable region overlaps, the blue corresponds to the CMV promoter region overlap, and the green underlining corresponds to the constant region overlapping regions.

Primer name	Primer sequence (5′ to 3′ direction)	Annealing temperature
	Primary PCR	
Variable region forward primer	AAGCTTGCCACCATGGAGACTGGGCTGCGCTGGCTTC	50.5℃
Variable region reverse primer	AAGCTTGCCACCATGGACAYGAGGGCCCCACTC	
	Secondary PCR	
Overlap region forward primer	ATCGCGGCCGCTCTAGAGCCACCAAGCTTGCCACCATG	62℃
Overlap region reverse primer	GCAGCAGGGGGCCAGTGGGAAGACTGATGGAG	
	CMV	
Forward primer	CCATTGCATACGTTGTATCC	50℃
Reverse primer	GGTGGCTCTAGAGC	
	Constant and polyA region	
Forward primer	TCGAGTGGGCAACC	50.5℃
Reverse primer	GAATTAATTCCATACCACATTTG	
	Tertiary PCR	
Forward primer	GACATTGATTATTGAC	50℃
Reverse primer	AAGACTGATGGAGCCTTAGGTTGCCC	

Table 2.3: Primers used for the amplification of the transcriptionally active linear expression cassette containing the light-chain antibody fragment. The overlapping sequences introduced by the secondary PCR primers are underlined. The red underlining denotes the variable region overlaps, the blue corresponds to the CMV promoter region overlap, and the green underlining corresponds to the constant region overlapping regions.

Primer name	Primer sequence (5′ to 3′ direction)	Annealing temperature
	Primary PCR	
Variable region forward primer	AAGCTTGCCACCATGGACAYGAGGGCCCCCACTC	50.5℃
Variable region reverse primer	CAGAGTRCTGCTGAGGTTGTAGGTAC	
	Secondary PCR	
Overlap region forward primer	GGCCGCTCTAGAGCCACCAAGCTTGCCACCATG	62℃
Overlap region reverse primer	GGAGGACAGAAGGCGCAACTGGATCCAGAGTRCTGCTGAG	
	CMV	
Forward primer	CCATTGCATACGTTGTATCC	50℃
Reverse primer	GGTGGCTCTAGAGC	
	Constant and polyA region	
Forward primer	GATCCAGTTGCGCCTTC	50.5℃
Reverse primer	CCATACCACATTTGTAGAGG	
	Tertiary PCR	
Forward primer	GACATTGATTATTGAC	48℃
Reverse primer	CCATACCACATTTGTAGAGG	

The PCR reaction mix for the primary, secondary, CMV region, and constant regions (including polyA fragments) was composed of 1.25 µl of 10 mM forward primer, 1.25 µl of 10 mM reverse primer, 1 µl of template DNA, 12.5 µl of 2×Q5 master mix, and dH_2O up to a final volume of 25 µl. The thermocycling procedure was as follows, initial denaturation at 98℃ for 1 min followed by 34 cycles of denaturation at 98℃ for 15 sec, annealing at primer specific temperatures for each

PCR amplification described in Tables 2.2 and 2.3 for 30 sec, and extension at 72℃ for 20 sec. A final extension was done at 72℃ for 2 min.

The final tertiary PCR was a 2-step process [226], where in the first step, the three PCR product constituents (the secondary PCR product, the CMV product, and the constant region and poly-A fragments) at a 1:1:1 molar ratio, respectively, with a total DNA amount of 100 ng was added to a reaction mix composed of 2×Q5 hi-fidelity enzyme and dH_2O to a final volume of 25 µl. The thermocycling process for the first step PCR was implemented under the following conditions; denaturation for 2 min at 98℃, 94℃ for 15 sec, 56℃ for 20 sec, 72℃ for 1 min repeated for 10 cycles, and a final hold at 4℃. The first step denatures and anneals the complimentary overlapping sequences, forming the template of the transcriptionally active linear expression cassette. In the second step the tertiary primers complementary to the 5′ HCMV promoter region and the 3′ polyA signal were used to amplify the assembled transcriptionally active linear cassette (in the first PCR step) for expression studies. For the second step of the PCR, 12 µl of the first step PCR product was added to the reaction mix made up of 2×Q5 hi-fidelity enzyme, 5 µl of 10mM forward primer, 5 µl of 10 mM reverse primer and dH_2O added to a final volume of 100 µl. The second step PCR cycle took place under the following thermocycling conditions; an initial denaturation step at 98℃ for 2 min, 94℃ for 20 sec, annealing at 50℃ and 48℃ for the heavy- and light-chains, respectively, and 72℃ for 2 min 30 sec for 35 cycles, and a final extension of 3 min at 72℃.

For each PCR amplification step, the presence of the amplicon was confirmed by agarose gel electrophoresis. The amplicons were resolved on 0.8% agarose gels (Appendix D1.1 and 1.2) run in a 1× Tris-acetate EDTA (TAE) buffer (Thermo Fisher Scientific, Waltham, MA, USA) and stained with 1× ethidium bromide (Promega, Fitchburg, WI, USA). The stained and resolved bands were detected using the ChemiDoc™ MP imaging system (Bio-Rad, Hercules, CA, USA) and the images were processed using the QuantityOne version 4.6.9 Software Programme (Bio-Rad, Hercules, CA, USA).

2.7. Recombinant protein expression

2.7.1. Small-scale antibody expression studies from the transcriptionally active linear expression cassettes

Using the assembled transcriptionally active linear expression cassettes antibody expression studies were performed on a small scale by transient transfections of HEK 293T cells. The heavy- and light-chain antibody transcriptionally active linear cassettes of five isolated B cells (samples 1, 2, 4, 6, and 7) were used for the transfection studies. The heavy- and light-chain plasmid vectors of the human antibody 2G12 were used as a positive control for the transfection protocol. The HEK 293T cells were maintained as described in section 2.2.2. For the transient transfections, once reaching 70-80% confluency, the cells were re-seeded in 3 ml of complete DMEM at a cell number of 3×10^5 cells/ml in each well of a Nunc™ Nunclon™ Vita 6-Well Multidish (Thermo Fisher Scientific, Waltham, MA, USA). The dish was incubated at 37℃ with 5% CO_2 until the cells reached 80% confluency. Following incubation, the DMEM was discarded and 3 ml of FreeStyle™ serum-free expression media (Thermo Fisher Scientific, Waltham, MA, USA) was added to each well. The transfections were performed using a cationic polymer-based methodology. Briefly, the Polyethylenimine (PEI) Max transfection reagent (Polysciences Inc, Warrington, PA, USA), is a cationic polymer [227] that condenses negatively charged DNA into positively charged particles that are able to bind to anionic cell surfaces, which consequently results in the PEI-DNA complex being taken up in the cells via endocytosis and the DNA is released in the cytoplasm of the cell [228]. Nine micrograms of a 1 mg/ml stock of PEI Max was added to 150 µl of Opti-MEM (Thermo Fisher Scientific, Waltham, MA, USA), and 3 µg of total DNA (equimolar amounts of the DNA of the heavy- and light-chain) was diluted in 150 µl Opti-MEM. The diluted PEI max was added to the diluted DNA and incubated at room temperature for 15 minutes to allow complex formation. The diluted PEI max-DNA mixture was added to each well of the dish. The cells were returned to the 37℃ incubator for 96 hours, and thereafter the supernatants were harvested and clarified of cell debris by centrifugation at 300 ×g for 15 minutes. The supernatants were then filtered using an Acrodisc syringe filter with a 0.2 µm Supor® membrane (PALL Life Sciences, Port Washington, NY, USA) and stored at -20℃ until screening of the antibody expression was performed. An Amicon® Ultra-50kDa (MilliporeSigma, Burlington, MA, USA) centrifugation

filter unit was used to concentrated the harvested protein supernatant six-fold. The concentrated protein was washed with 1×PBS to remove the expression media.

2.7.2. Binding activity of the expressed antibodies to $gp140_{GCN4}$ Env and $2dCD4^{WT}$ using Enzyme Linked Immunosorbent Assay (ELISA)

The presence and binding activity of the expressed antibodies were examined against the immunogen- complex's constituent proteins, namely $gp140_{GCN4}$ Env and 2dCD4, respectively, using an ELISA. For the experimental procedure, $gp140_{GCN4}$ Env or $2dCD4^{WT}$ at a concentration of 2 μg/ml in a total volume of 100 μl in 1×PBS was used to coat each well of the 96-well Nunc Maxisorp Immuno microtiter plates (Nunc, Roskilde, Denmark) overnight at 4 ℃. The microplate was washed 3 times using 300 μl 1× PBS-T (0.05% Tween (Sigma-Aldrich, St Louis, MO, USA)) using the BioTek, ELx 50 automated plate washer (BioTek, Winooski, VT, USA). To eliminate non-specific binding of the protein to the microplate, each well was blocked with 100 μl of 1% BSA in 1×PBS-T and incubated for 1 hour at room temperature. An Amicon® Ultra-50kDa (MilliporeSigma, Burlington, MA, USA) centrifugation filter unit was used to concentrate the harvested protein supernatants six-fold. The concentrated protein was washed with 1×PBS to remove the expression media. The 200 μl of each concentrated transfected cell supernatants were added to the respective wells in duplicate. Two-hundred microliters of the samples or controls (rabbit 24 sera, 2G12 transfection supernatant, a transfection media, and a blank) were added to the 96-well plate and the plate was incubated at room temperature for 1 hour. Sera obtained from rabbit 24 and diluted 1:10,000 in 1×PBS-T was used as a positive control. Following incubation, the plate was washed five times using 1× PBS-T. An HRP-conjugated donkey anti-rabbit IgG (GE Healthcare, Chicago, IL, USA) was used as secondary antibody except for the wells containing 2G12, which received an HRP-conjugated sheep anti-human IgG (GE Healthcare, Chicago, IL, USA) secondary antibody. Both secondary antibodies were used at a 1:2000 dilution. One-hundred microliters of the secondary antibodies were added to the respective wells and the plate was incubated for 1 hour at room temperature. After incubation, the plate was washed five times with 1×PBS-T, and 100 μl of TMB substrate solution (Life Technologies, Carlsbad, CA, USA) was added to each well, thereafter, the plate was incubated in the dark at room temperature for 20 minutes, to allow for the substrate to react with the peroxidase conjugated to the secondary antibodies resulting in a blue colour change. After the 20-minute incubation, 100 μl 2M sulfuric

acid was added to each well as the stopping solution. The absorbance of the reactions was measured at 450 nm using the iMark™ microplate reader (Bio-Rad, Hercules, CA, USA).

2.7.3. Determining monoclonal antibody expression using Sodium dodecyl sulphate-polyacrylamide gel electrophoresis (SDS-PAGE) and western blot

The presence and identity of expressed monoclonal antibodies by transient transfection was determined using SDS-PAGE and western blotting.

2.7.3.1. SDS-PAGE

Purified and concentrated rabbit antibody (rabbit total antibodies were purified from rabbit sera using a standard protein-A chromatography protocol) and the HIV-1 bnAb, human antibody, 10e8, were resolved by SDS-PAGE to observe the banding patterns under non reducing and reducing conditions. The 2g12 transfection control sample and FreeStyle transfection media only control were included in the SDS-PAGE analysis to determine whether non-specific proteins were present in the media. The antibody controls, 2G12 supernatant and media only samples were prepared in 2× Reducing (25% stacking gel buffer (Appendix D2.2), 40% SDS (Merck, Kenilworth, N.J., USA), 20% glycerol, 10% β-mercaptoethanol, 0.02% bromophenol blue, made up to 10 ml with dH_2O) and 2× Non-reducing buffer (25% stacking gel buffer, 40% SDS, 20% glycerol, 0.02% bromophenol blue, made up to 10 ml with dH_2O) and boiled for 5 minutes before being loaded into the wells of the SDS-PAGE gels. A 10% SDS-PAGE gel was prepared as follows: 10% Separating gel (4 ml monomer solution (Appendix D2.1), 3.75 ml separating gel buffer (Appendix B2.2), 150 µl 10% SDS (Merck, Kenilworth, N.J., USA), 7.05 ml dH_2O, 75 µl 10% ammonium persulphate (APS) (Sigma-Aldrich, St. Louis, MO, USA), 15µl TEMED (Sigma-Aldrich, St Louis, MO, USA) and 4% stacking gel, (940 µl monomer solution, 1.75 ml stacking gel buffer (Appendix D2.3) (3 g Tris made up to 50 ml of distilled water, pH 6.8), 70 µl 10% SDS, 4.3 ml dH_2O , 35 µl 10% APS, 15µl TEMED)). The antibody controls and 2g12 and media only samples were resolved on a 10% SDS-page under non-reducing conditions, to analyse the full intact antibodies, and under reducing conditions to observe the separation of the heavy- and light-chain antibody fragments. The Colour Protein Standard Broad Range (Thermo Fisher Scientific, Waltham, MA, USA) molecular weight marker was used to determine the molecular weights of the resolved proteins. The gels were run at a constant voltage of 150V in 1× Tank buffer (10% 10× Tank buffer

(Appendix D2.6) diluted in dH_2O)) until the dye-front reached the end of the gel. Once the controls were resolved on the gels, the gels were stained with 0.025 % Coomassie Blue R250 stain (0.25 g Coomassie® Brilliant Blue R250 (Sigma-Aldrich, St. Louis, MO, USA) dissolved in 50% ml methanol (Sigma-Aldrich, St. Louis, MO, USA), 10% ml acetic acid and dH_2O made up to 1 L) overnight with shaking. The gels were then destained using a 5% acetic acid 7% methanol destaining solution for a minimum of 6 hours or until the bands on the gel could be seen clearly. The SDS-PAGE gels were analysed for the banding pattern of the stained proteins by capturing images using the ChemiDoc™ MP imaging system (Bio-Rad, Hercules, CA, USA) and processed using the QuantityOne version 4.6.9 Software Programme (Bio-Rad, Hercules, CA, USA).

2.7.3.2. Western blotting

Separate western blots were performed for the detection of expressed monoclonal antibodies from rabbit derived samples 1, 2, 4, 6, and 7 and for human 2G12 expression. For each western blot, a 10% SDS-PAGE was run with the samples and controls as described above, and thereafter the SDS-PAGE gels were equilibrated in transfer buffer (20% methanol in 1 L of 1× Tank buffer for approximately 15 minutes. The resolved proteins on the gels were transferred to the nitrocellulose membranes (BioRad, Hercules, CA, USA) at 20V for 30 minutes using the Bio-Rad Trans-Blot® Semi-Dry System (BioRad, Hercules, CA, USA). The nitrocellulose membranes were blocked overnight at 4℃ using 5% blocking solution (5 g fat-free milk powder in 1× TBS-T (10× TBS (10g NaCl, 30 g Tris, 2g KCl, pH 7.4, made up to 1 L in dH_2O) diluted in distilled water, with 0.05% Tween). The blocking solution was discarded and the nitrocellulose membranes were washed three times with TBS-T for five minutes each wash. The presence of expressed antibodies for the samples were compared to the purified rabbit serum positive control and detected using the HRP-conjugated donkey anti-rabbit IgG secondary antibody (GE Healthcare, Chicago, IL, USA). The 2G12 expression was analysed against the 10e8 positive control and was detected using the HRP-conjugated sheep anti-human IgG secondary antibody (GE Healthcare, Chicago, IL, USA). The secondary antibodies were each diluted 1:2000 in TBS-T, and were added to the nitrocellulose membranes and incubated for 1 hour at room temperature. Thereafter, the nitrocellulose membranes were washed three times with TBS-T for 5-minutes per wash. The bound antibodies were detected using the SuperSignal™ West Pico Chemiluminescent Substrate kit (Thermo Fisher Scientific, Waltham, MA, USA) according to the manufacturer's instructions. Images of the banding patterns on the nitrocellulose membranes were detected using the ChemiDoc™ MP

imaging system (Bio-Rad, Hercules, CA, USA) and processed using the QuantityOne version 4.6.9 Software Programme (Bio-Rad, Hercules, CA, USA).

3. Results

3.1. CAP45GCN4 expression and purification

3.1.1. Expression of $gp140_{GCN4}$ Env

Stably transfected 293F cells were successfully grown to express $gp140_{GCN4}$ into the cultured supernatant, as confirmed by SDS-PAGE and western blot analysis (Figure 3.1). The positive control used was a previously expressed and purified sample of $gp140_{GCN4}$ that was available in the laboratory. Resolved and transferred $gp140_{GCN4}$ protein were detected using rabbit serum as the primary antibodies and an HRP-conjugated anti-rabbit secondary antibody and produced a band corresponding to approximately 140 kDa (Figure 3.1).

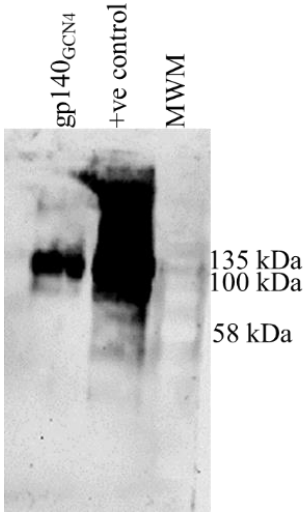


Figure 3.1: Western blot analysis of the expressed HIV-1 $gp140_{GCN4}$ envelope glycoprotein. $gp140_{GCN4}$ protein expression was confirmed by probing the nitrocellulose membrane with a diluted (1: 1000) anti-gp140 rabbit sera primary antibody, and subsequently detecting the primary bound antibody using a diluted (1: 2000) horse radish peroxidase (HRP)-conjugated anti-rabbit secondary antibody. The positive (+ve) control was previously expressed $gp140_{GCN4}$. MWM stands for molecular weight marker corresponding to the pre-stained broad range protein marker (New England Biolabs, MA, USA), shown in kiloDaltons (kDa) on the right.

3.1.2. Purification of trimeric $gp140_{GCN4}$

The trimeric $gp140_{GCN4}$ was separated from the dimeric and monomeric conformations by SEC (Figure 3.2A). Fractions seven to twelve were collected and SDS-PAGE and western blot analysis confirmed the presence of $gp140_{GCN4}$ (Figure 3.2B). Fractions eight to twelve that corresponded to the trimeric Env conformation were pooled and concentrated 10-fold yielding a final concentration of 272.4 µg/ml at a final volume of 1 ml using the BCA assay.

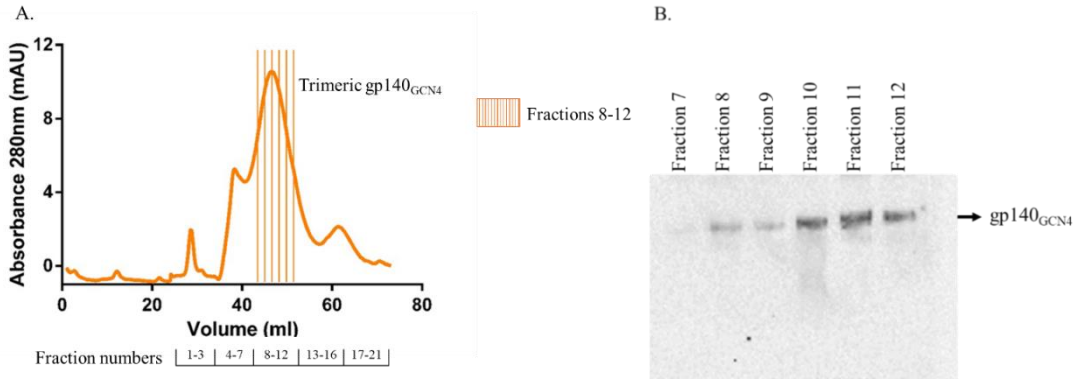


Figure 3.2: The purification of trimeric $gp140_{GCN4}$ using size exclusion chromatography. Following lectin affinity chromatography, the trimeric $gp140_{GCN4}$ conformation was purified using size exclusion chromatography with the HiLoad 16/600 Superdex 200 PG column. Separation of the $gp140_{GCN4}$ Env conformations was monitored by absorbance at 280nm using the Akta FPLC platform. Fractions eight to twelve (indicated by the orange vertical lines) corresponding to the trimeric Env conformation were collected and pooled. (A). Size-exclusion elution fractions seven to twelve were resolved on 10% SDS_PAGE followed by on a western blot to confirm the presence of $gp140_{GCN4}$ using anti-$gp140_{GNC4}$ rabbit sera (1:1000) and secondary, anti-rabbit HRP-linked antibody (1:2000) (B).

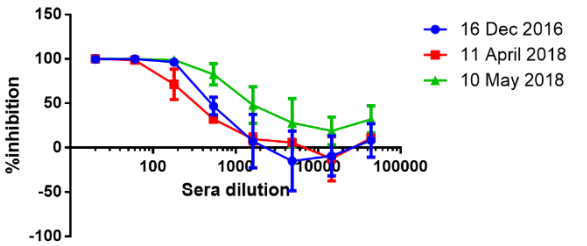
3.2. Confirmation of the $gp140_{GCN4}$ Env/2dCD4^{S60C} neutralising responses

Serum samples obtained from the three rabbits (rabbit ID 24, 31 and 83) at time points B0, B1 and VB1, were each tested for neutralising antibody titres against a heterologous, tier-2 clinically relevant pseudovirus, ZM53M.PB12 using the TZM-bl-based neutralisation assay (Figure. 3.3). The reciprocal of inhibitory dilution to achieve 50% neutralisation (ID_{50}) for each time point was determined.

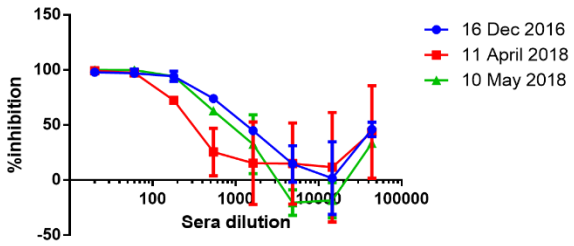
The average neutralisation titres for the three rabbits at B0 was 675.4 and ranged between 540.6 to 909.9, declined on average by 2.6-fold at timepoint B1, and increased on average 2.7-fold in the VB1 serum samples as compared to B1 for all three rabbits, as determined by the ID_{50}s (Figure 3.3D). Most notably the neutralization titres for the rabbit sera 24 and 31 at VB1 were shown to

increase by over three-fold compared to B1 and exceeded or restored the neutralization titres obtained at B0, respectively (Figure 3.3D). Circulating residual neutralising titres were observed two years post the last immunisation, and the neutralising titres improved indicating successful immunization and boosting of the relevant neutralising antibody responses. All three rabbits were thus considered suitable candidates for further antigenic specific memory B cell isolation and characterisation studies.

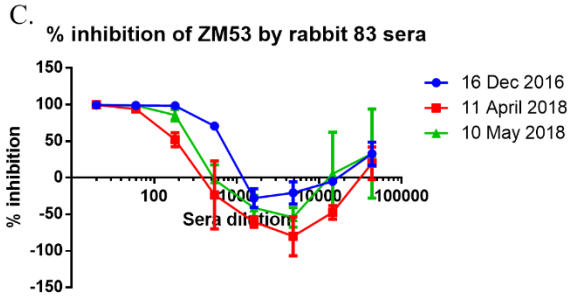
A.



B.



C.



D.

Rabbit sera ID	ID_{50}		
	Titres from the previous study (B0) (16 Dec 2016)	**Titres at the commencement at the current study (B1)** (11 April 2018)	**Titres following the immunisation boost (VB1)** (16 May 2018)
24	**540.6**	**313.2** (↓1.7×)	**1026** (↑3.3×)
31	**909.9**	**219.2** (↓4.2×)	**811.6** (↑3.7×)
83	**575.6**	**237.3** (↓2.4×)	**301.1** (↑1.3×)

ID_{50} Key: > 700 | 700-400 | 400 - 100

Figure 3.3: Determination of elicited HIV-1 neutralising antibody titres in $gp140_{GCN4}$ Env/2dCD4^{S60C} immunised rabbits. The neutralising antibodies titres were confirmed against the tier-2, ZM53M.PB12 (ZM53) HIV-1 pseudovirus using the TZMbl-based neutralisation assay. Rabbit sera isolated from three bleed time points, namely; the last bleed performed by the previous study (16 December 2016; B0), a baseline bleed prior to the initiation of this study (11 April 2018; B1), and a bleed performed post the first boost of this study (10 May 2018; VB1) were evaluated. Percentage inhibition curves for B0, B1 and VB1 sera from rabbit 24 (A), rabbit 31 (B), and rabbit 83 (C) at sera dilutions from 20 to 43,740, tested against tier-2 clinically relevant pseudovirus, ZM53M.PB12. The % inhibition represents the amount of ZM53M.PB12 that is inhibited from infecting cells by the rabbit sera at different dilutions. Neutralisation titres are reported as the reciprocal of inhibitory dilution required to achieve 50% viral neutralisation (ID_{50}) at each time point for each rabbit serum (D).

3.3. Antigen-specific memory B cell isolation

Following the administration of the boosting immunisation and confirmation of HIV-1 neutralising titres in the immunised rabbit sera, the VB1 antigen-specific memory B cells, containing the genetic material required for the expression of the rabbit monoclonal antibodies were isolated using a multi-parameter FACS based protocol. Rabbit immunisations were performed using the HIV-1 $gp140_{GCN4}$ Env/$2dCD4^{S60C}$ complex, however for delineation of the neutralisation antibody responses, selection for either $gp140_{GCN4}$ Env, $2dCD4^{WT}$, or dual-specific (cells demonstrating binding activity to both antigens) antigen-specific memory B cells were performed independently. Figure 3.4 shows the FACS protocol followed for the isolation and single cell sorting of the antigen-specific memory B cells for rabbit 24, and is representative of the protocol followed for each rabbit. The isolated PBMC population were initially subjected to forward scatter (FSC) and side scatter (SSC) analysis to identify the whole population of PBMCs based on the cell size and granularity (Figure. 3.4A). Single cells, which made up 95.1% of the total population of cells, were distinguished from doublets (Figure 3.4B) and the viability of the single-cell-gated population was evaluated and determined to be 93.3% (Figure 3.4C). The CD3 negative cell populations were calculated to comprise 76.4% of the viable cell population (Figure 3.4D). Cells observed to be negative for IgM (naïve B cell) were 33.1% of the previously gated CD3 negative cell population (Figure 3.4E).

Following the elimination of naïve B cells from the cell population, the memory B cells were selected for using an IgG marker conjugated to PE. The cells found to be positive for IgG (which were 28.4% of the remaining gated cell population) were gated and selected for (Figure 3.4F). From this population of cells, the antigen-specific memory B cells were identified using each component of the immunogen complex; the proteins ($gp140_{GCN4}$ or $2dCD4^{WT}$) were conjugated to distinct fluorophores (Alexa Fluor 647, or DyLight 680, respectively) to effectively identify antigen-specific memory B cells. The antigen-specific memory B cells showed distinct populations in all quadrants of the $gp140_{GCN4}$ antigen (representing 34.9% of the gated events), $2dCD4^{WT}$ antigen (representing 26.4% of the gated events), or dual specific targeting of both components of the immunogen complex ($gp140_{GCN4}$ and $2dCD4^{WT}$) (representing 28.4% of the gated events) (Figure 3.4G). From the total population of PBMCs acquired (10,000 events), 2.5%

were $gp140_{GCN4}$ Env antigen-specific, 1.7% were 2dCD4 antigen-specific, and 0.47% were dual antigen-specific memory B cells.

Overall, thirty-two single cells of each gated antigen-specific memory B cell population from each rabbit sera were individually sorted into flat-bottomed 96-well Nunc Polysorp plates containing complete reverse transcription buffer to generate transcriptionally active linear cassettes for the expression of monoclonal antibodies.

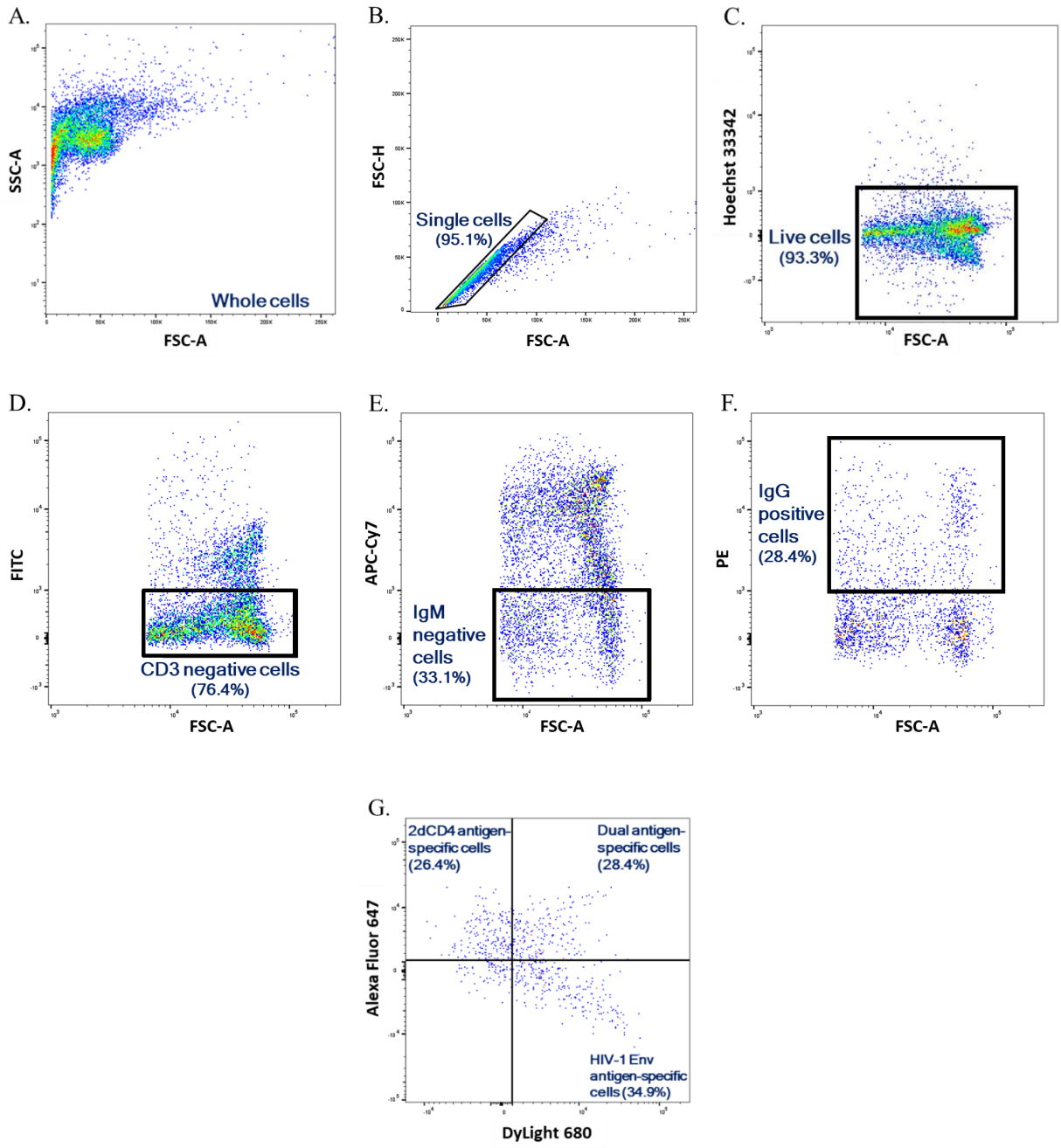


Figure 3.4: The gating strategy for identification of rabbit antigen-specific memory B cells from immunised rabbits. Isolated rabbit PBMCs were analysed using a BD FACS Aria I. The whole PBMC population of was analysed using the FSC and SSC parameters (A). Gates were drawn around single cells (B), live cell-Hoechst 33342 negative cells (C), CD3 – (FITC) negative cells (D), IgM – (APC-Cy7) negative cells (E), IgG – (PE) positive cells (memory B cells) (F), and the antigen-specific memory B cells (2dCD4, $gp140_{GCN4}$ Env, and dual-specific cells) (G). The gated cells from (G) were sorted as single cells into a 96-well plate for PCR amplification of the antibody specific variable regions.

3.4. PCR amplification of the transcriptionally active linear cassette (TAP)

3.4.1. Heavy and light chain antibody variable region amplification

Once individual antigen-specific memory B cells were isolated, the RNA from each cell was reverse transcribed to cDNA. Of the cognate variable regions 18.42% were successfully amplified. Due to time constraints, nine cell samples from rabbit 24 were randomly selected to determine the success of generating the TAPs expressing rabbit derived monoclonal antibodies. Of these, three cells were $gp140_{GCN4}$ Env specific (S1 to S3), three cells were $2dCD4^{WT}$ specific (S4 to S6), and three cells were dual-specific (S7 to S10). The expected 500 bp heavy-chain amplicons were observed for 8 out of 9 isolated antigen specific memory B cells (Figure 3.5A). Similarly, the expected 650 bp light-chain amplicon was observed for 4 of the 9 memory B cells (Figure 3.5B).

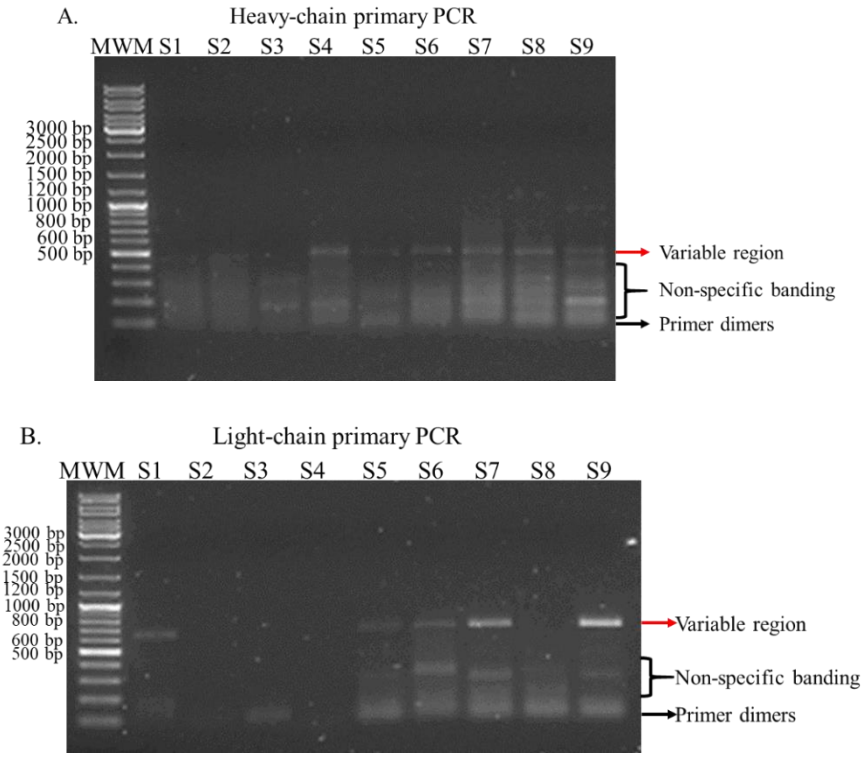


Figure 3.5: PCR amplification of rabbit heavy- and light-chain antibody variable regions. Reversed transcribed cDNA obtained from nine single antigen-specific memory B cells (S1-S9) served as the template for amplification of both heavy- and light-chain antibody variable regions. PCR amplification reactions were resolved on a 0.8% agarose gel and visualised under UV following ethidium bromide staining. Agarose gels showing DNA amplicons from the heavy-chain variable fragment PCR (A) and light-chain PCR (B). The O'Gene Ruler DNA ladder #sm1173 (Thermo Fisher Scientific, Waltham, MA, USA) was used as the reference molecular weight marker (MWM), and the base pairs (bp) of relevant bands making up the marker are indicated on the left of the agarose gel.

Non-specific, lower base pair fragments and smearing were observed for all samples in both the heavy- and light-chain amplification reactions, and were mostly likely due to primer dimers, incompletely/incorrectly amplified fragments, or nucleic acid contamination during the preparation of the reaction. To reduce the non-specific banding patterns, and smearing, the annealing temperature and extension times of the PCR reactions were optimised, different primers were used (Appendix A, supplementary Figure 3A), and fresh DEPC-treated water was used for the reactions. Most of the optimisations did improve the quality of the PCR product, generating bright and distinct banding patterns, however, we were not able to completely eliminate smearing and non-specific banding. Despite the non-specific bands and smears, the bands representing the correct heavy- and light- chain variable regions fragments were prominent enough to indicate successful amplification and enabled us to proceed with the secondary PCR. Additionally, although the heavy chain of S3, and light chains of S2, S3, S4 and S8 were not visible on the agarose gel, the amplification reactions were included in the subsequent analyses.

3.4.2. Amplification of the individual transcriptionally active linear cassette (TAP) constituents

Following amplification of the heavy- and light-chain variable regions in the primary PCR, a secondary PCR was successfully performed to add the complementary CMV promoter region and antibody constant region overhangs to the 5′ and 3’ ends, respectively, of the primary PCR product (Figure 3.6). Distinct bands were observed at approximately 536 bp for the secondary, heavy-chain PCR amplification as expected due to the addition of the complementary overhangs which were 36 bp long in total, with the exception of S3 and S4 (Figure 3.6A). The lack of bands for S3 was expected as no amplification was observed for the primary PCR. Similarly, distinct bands were observed for the light-chain antibody variable regions at the expected size of approximately 683 bp due to the addition of the complimentary overhangs which were 33 bp long in total (Figure 3.6B). There were no bands observed for S2, S3, S4, and S8, suggesting that the light-chain secondary PCR was unsuccessful for these samples which was expected because no amplicons of the light-chain variable regions were visible in the primary PCR.

Non-specific banding of lower base pair fragments and smearing was observed for all samples which may be the result of primer dimers as well as incompletely/incorrectly amplified fragments.

Despite repeated attempts at optimization (Appendix A, supplementary Figure 3B), smearing and non-specific banding were not completely eliminated.

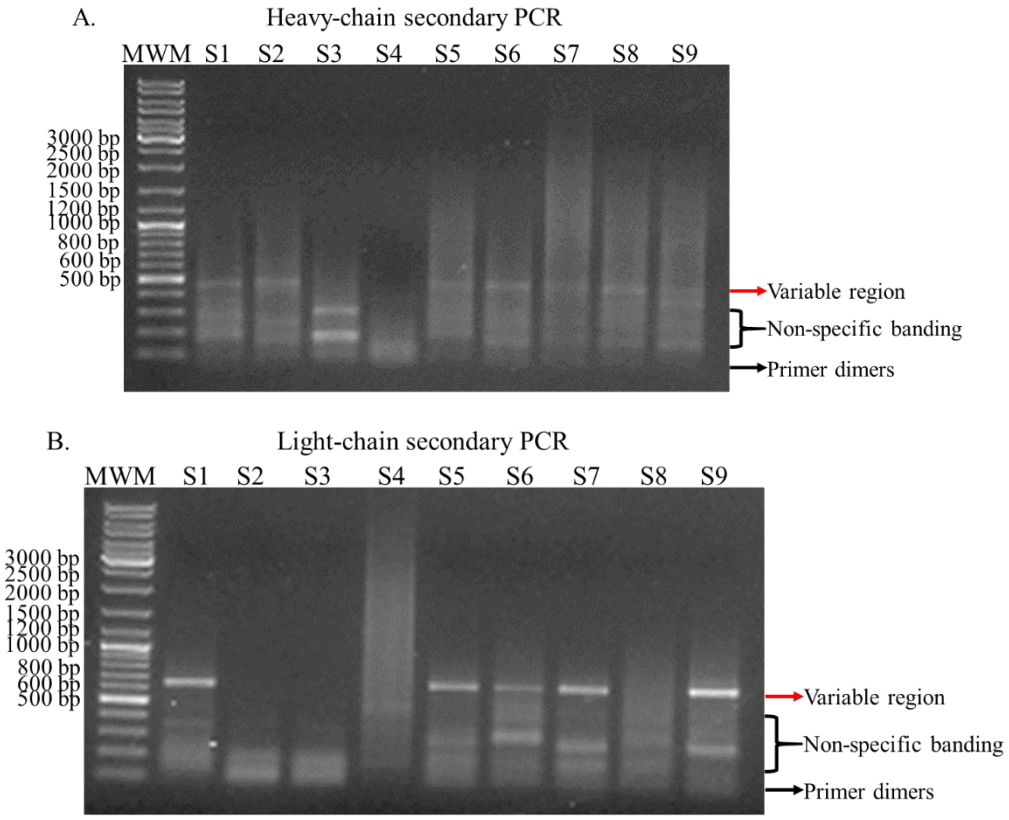


Figure 3.6: PCR amplification of rabbit antibody variable fragments, heavy- and light-chain secondary PCRs. Secondary PCR amplification of the antibody variable heavy-chain (A), and light-chain (B) fragments for samples 1-9 (S1-S9). For the secondary PCR, 1 µl of the primary PCR product was added to the reaction mix. The DNA fragments were resolved on 0.8% agarose gels and visualised under UV light following ethidium bromide staining. The secondary PCR for the heavy- and light-chain antibody variable fragments adds complimenting overhangs for correct genetic assembly of the transcriptionally active linear cassette. The O'Gene Ruler DNA ladder #sm1173 (Thermo Fisher Scientific, Waltham, MA, USA) was used as the reference molecular weight marker (MWM), and the base pairs (bp) are indicated on the left.

The full coding CMV promoter region was amplified from the VRC_4196 expression vector (Appendix A, Supplementary Figure. 1A). The DNA bands for the CMV regions were observed at 1138 bp as anticipated, confirming that the CMV region was successfully amplified (Figure 3.7A). A fainter band of a higher molecular weight was observed following amplification of the CMV region (Figure 3.7A), and therefore the bands of the expected sizes were excised from the agarose gel and purified for the downstream experiments.

The final elements of the transcriptionally active linear cassette, the corresponding heavy- and light-chain antibody constant regions including a polyA region, were successfully PCR amplified from two plasmids obtained from GeneArt. The heavy-chain constant region with the polyA tail (1239 bp) and the light-chain constant including the polyA region (583 bp) are shown in Figure 3.7B.

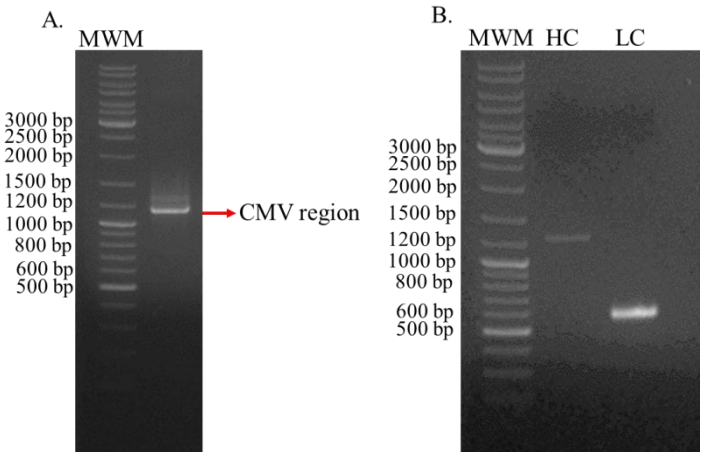


Figure 3.7: PCR amplification of the CMV promotor, and the antibody constant regions including the polyA tail. The DNA fragments were resolved on 0.8% agarose gels and visualised under UV light following ethidium bromide staining. The 1100 bp fragment indicates successful amplification of the CMV promoter region from the VRC_4196 plasmid vector (A). The DNA fragment above the 1200 bp MWM, and at the 600 bp MWM showed successful amplification of the heavy- and light-chain constant and polyA regions respectively (B). HC: heavy-chain constant region fragment containing poly-adenylation sequence, LC: light-chain constant region fragment containing poly-adenylation sequence. The constant and polyA regions were amplified from heavy- and light-chain plasmid vectors synthesized by GeneArt. The O'Gene Ruler DNA ladder #sm1173 (Thermo Fisher Scientific, Waltham, MA, USA) was used as the reference molecular weight marker (MWM), indicated as base pairs (bp) on the left.

3.4.3. Transcriptionally active linear cassette assembly

TAPs comprising the amplified CMV promoter regions, the secondary antibody variable regions (heavy or light chain) and the appropriate antibody light or heavy chain constant region, including the poly A tail were assembled via overlapping complimentary base pairs between individual amplicons (Figure 3.8). Amplicons of the expected molecular weight of the complete antibody heavy-chain cassette (approximately 2700 bp) were not visible, and the brightest bands observed was approximately 2300 bp suggesting that correct assembly of TAP did not occur (Figure 3.8A).

Sample 3 was excluded from the tertiary PCR due to unsuccessful amplification of the heavy- and light-chain variable regions.

Similarly, the expected molecular weight of the complete antibody light-chain cassette was approximately 2400 bp, and bands observed on the agarose gel were lower than the expected size at approximately 1750 bp (Figure 3.8B), which showed that the TAP did not assemble correctly. Samples 2, 4 and 8 were included as "negative controls" for the tertiary PCR since the variable regions of the secondary PCR did not amplify (Figure 3.6). Since the resulting DNA fragment sizes for the "negative controls" were the same as that observed for the test samples, results suggested that the heavy- and light-chain variable region TAP constituents were missing from the assembled cassette (Figure 3.8B).

Despite repeated attempts to optimize the PRC reaction, non-specific banding patterns for the antibodies heavy- and light-chain cassettes could not be eliminated (Appendix A, supplementary Figure 3C). The bands at lower molecular weights than the expected sizes seen in Figure 3.8, may represent the DNA amplicons that failed to assemble correctly. For example, the bands observed at 1000 bp following the heavy-chain tertiary PCR (Figure 3.8A) may represent the CMV promoter that did not assemble, and similarly the bands of DNA at 600 bp for the light-chain tertiary amplification (Figure 3.8B) may represent the secondary variable light chain PCR products that did not assemble.

Since a majority of the heavy- and light-chain TAP products showed similarly sized banding patterns, we decided to continue to evaluate whether these amplified TAP cassettes would express rabbit derived monoclonal antibodies.

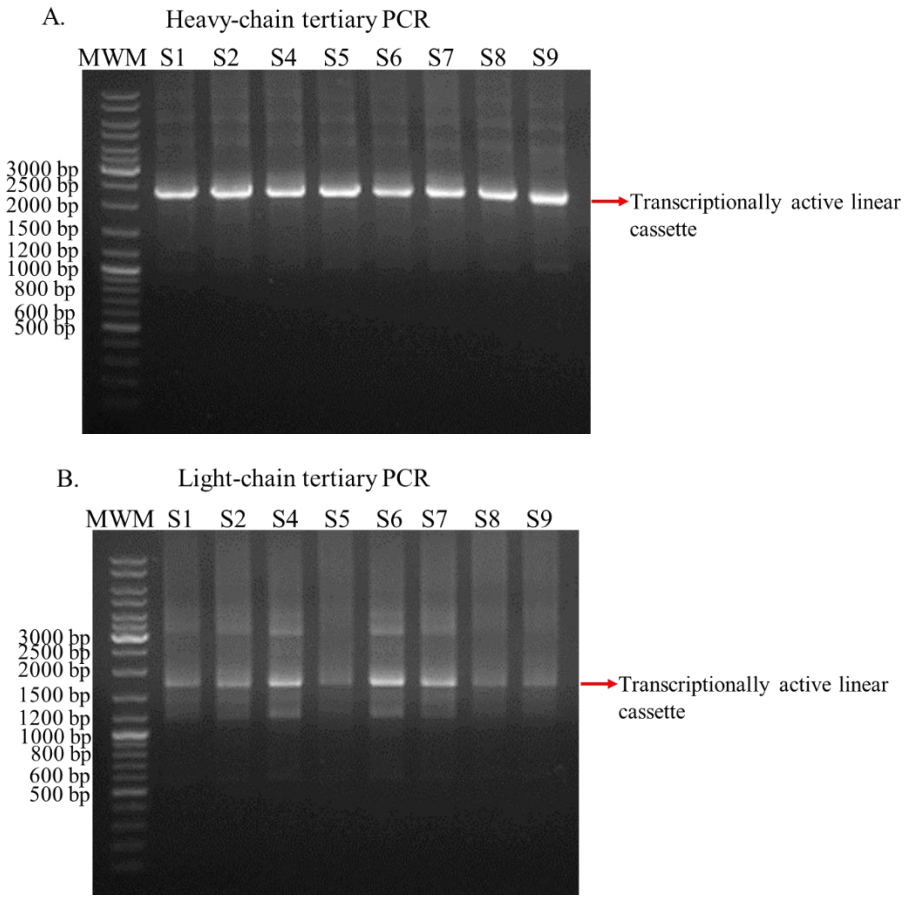


Figure 3.8: Assembled heavy- and light-chain transcriptionally active linear cassettes. The heavy-chain (A), and light-chain (B) transcriptionally active linear cassette amplification for samples 1, 5, 6, 7 and 9 (S1, S5, S6, S7 and S9), and the "negative controls" (Sample 2 (S2), sample 3 (S3), sample 4 (S4) and sample 8 (S8)). The DNA fragments at approximately 2400 bp for the heavy-chain were also observed for the "negative controls" (A), which suggests that the TAP assembly was unsuccessful. The DNA fragments at approximately 1750 bp for the light-chain were also observed for the "negative controls" (B), suggesting that the TAP assembly was not successful. The DNA samples were resolved on a 0.8% agarose gels and visualised under UV light following ethidium bromide staining. The O'Gene Ruler DNA ladder (#sm1173; Thermo Fisher Scientific, Waltham, MA, USA) was used as the reference molecular weight marker (MWM), indicated as base pairs (bp) on the left.

3.5. Evaluation of rabbit monoclonal antibody expression

3.5.1. Enzyme-linked immunosorbent assay (ELISA) for the detection of recombinantly expressed monoclonal antibodies in culture supernatants

Matched linear cassettes pairs (heavy- and light-chains) from rabbit antibody TAP cassettes S1, S2, S4, S6, S7 were co-transfected with HEK 293T cells and tissue culture supernatants were collected, concentrated and evaluated for monoclonal antibody expression. The five concentrated supernatant samples (including a no DNA, expression media only, and transfection media only control samples) were each assayed in duplicate against the respective antigens ($gp140_{GCN4}$ and $2dCD4^{WT}$) in an ELISA (Figure 3.9A and B, respectively). Overall, the positive rabbit sera control was shown to bind to both antigens albeit at varying absorbance readings, the 2G12 anti-human Env antibody which recognises a cluster of high mannose Env residues bound minimally to $gp140_{GCN4}$ and none of the TAP cassettes showed binding activity to either $gp140_{GCN4}$ or $2dCD4^{WT}$ (Figure 3.9). The absorbance readings of the samples were similar to the negative controls, suggesting that either the expressed antibodies did not bind to $gp140_{GCN4}$ and $2dCD4^{WT}$ or little to no antibodies were expressed during transfection.

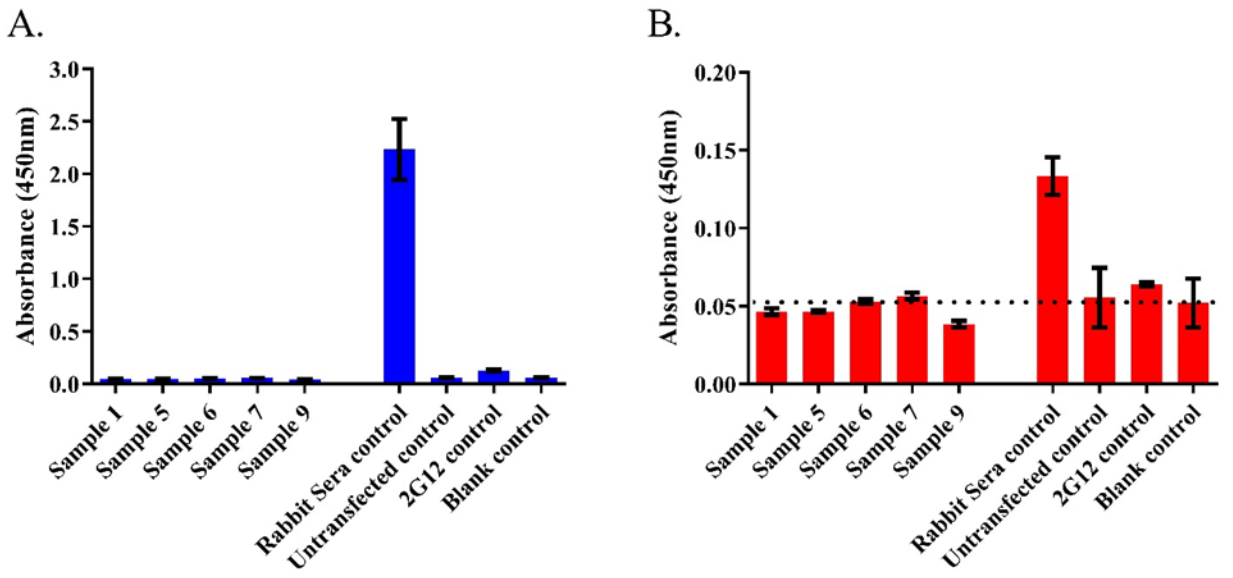


Figure 3.9: Evaluation of the binding activity of the TAP-expressed rabbit antibodies against gp140$_{GCN4}$ and 2dCD4WT using ELISAs. Harvested and concentrated supernatant of each sample was characterised for antibody-binding activity to immobilised antigens gp140$_{GCN4}$ (A) or 2dCD4^{WT} (B) using an ELISAs. The absorbance readings indicate the amount of binding of the antibodies to the antigens. Rabbit sera was used as the positive control, at a 1:10,000, 2G12, a human HIV-1 neutralising antibody, was used as a control to confirm that antibody expression by transfections worked efficiently, and the untransfected cell control and blank (which is secondary antibody only) served as the negative controls. Two replicates of each sample and the respective controls were tested and the average of the two were represented on the graph. The error bars were calculated based on the standard deviation of each sample.

3.5.2. Confirmation of antibody expression by SDS-PAGE and western blot analysis

Concentrated culture samples and 2 µg of purified human bNAb 10e8 were resolved under reducing and non-reducing SDS-PAGE conditions and expressed monoclonal antibodies were visualised by Coomassie staining (Figure.3.10).

The banding patterns observed for the controls under non-reducing conditions were as expected for the purified rabbit antibody and 10e8 samples, distinctly displaying a band at or slightly higher than 150 kDa, indicating the presence of a full antibody conformation (Figure 3.10). In tandem, samples resolved under reducing conditions verified the separation of the corresponding antibody heavy-chains (±50 kDa) from the light-chains (±25 kDa) due to reduction of the inter-chain disulphide linkages. The heavy-chain (±50 kDa) of the purified rabbit and 10e8 antibody controls

were observed under reducing conditions, however, the light-chain fragments (±25 kDa) were not visible on the SDS-PAGE, likely due to incomplete resolution of the lower molecular weight protein bands (Figure 3.10). The high molecular band (±150 kDa) for 2G12 corresponding to the full antibody conformation was not visible on the SDS-PAGE under non-reducing conditions (Figure 3.10). Taken together with the ELISA data, it is likely that 2G12 was not expressed at meaningful concentrations, if at all. As expected, there were no bands observed for the FreeStyle transfection media control, indicating that there were no detectable non-specific proteins in the transfection media.

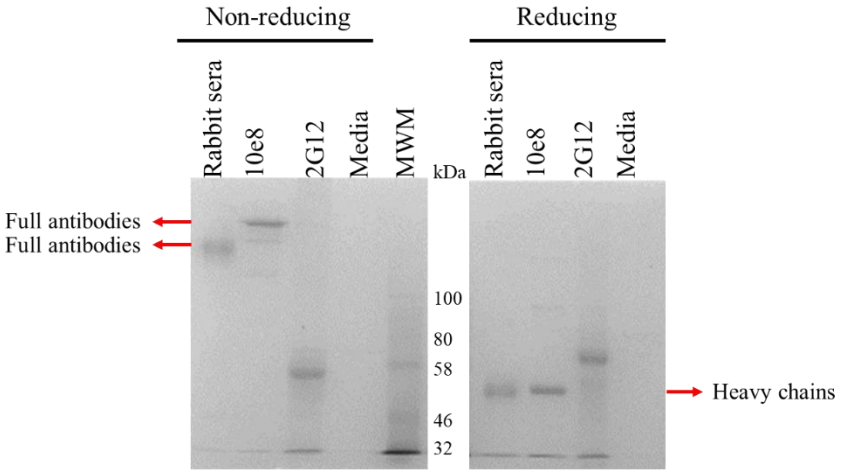


Figure 3.10: Evaluation of the antibody controls used to confirm monoclonal antibody expression by SDS-PAGE. Purified and concentrated samples were resolved on a 10% SDS-PAGE. Protein-A purified rabbit antibodies from rabbit sera and the human antibody 10e8 were used as positive controls. The FreeStyle transfection media was used to determine the presence/absence of non-specific proteins in the transfection media. The full antibodies for the purified rabbit antibodies and 10e8 are observed at or higher than 150 kDa under non-reducing conditions. The heavy-chain of the rabbit sera and 10e8 are observed under reducing conditions. The molecular weight (MWM) marker corresponds to the pre-stained broad range protein marker (New England Biolabs, MA, USA), indicated as kiloDaltons (kDa) between the two gels.

Western blot analysis of samples resolved under reducing and non-reducing conditions and detected using the anti-human HRP linked secondary antibodies confirmed expression of the 2G12 monoclonal antibody in tissue culture supernatant (Figure 3.11). The full antibody conformation was observed at ~150 kDa under non-reducing conditions for the 10e8 positive control and 2G12 culture supernatant (Figure 3.11A and Appendix A, Supplementary Figure 4A). Similarly, under reducing conditions, the heavy-chain fragment was visible at 50 kDa for both the 10e8 antibody

control and 2G12 tissue culture sample (Figure 3.11B and Appendix A, Supplementary Figure 4A), consistent with the SDS-PAGE results shown in Figure. 3.10. No distinct bands were observed for the purified rabbit antibodies control using the anti-human secondary antibody, although some low-level non-specific binding was evident, possibly due to cross reactive residual proteins from the mammalian culture supernatant, since these were not evident in the purified rabbit sera controls (Figure 3.11B).

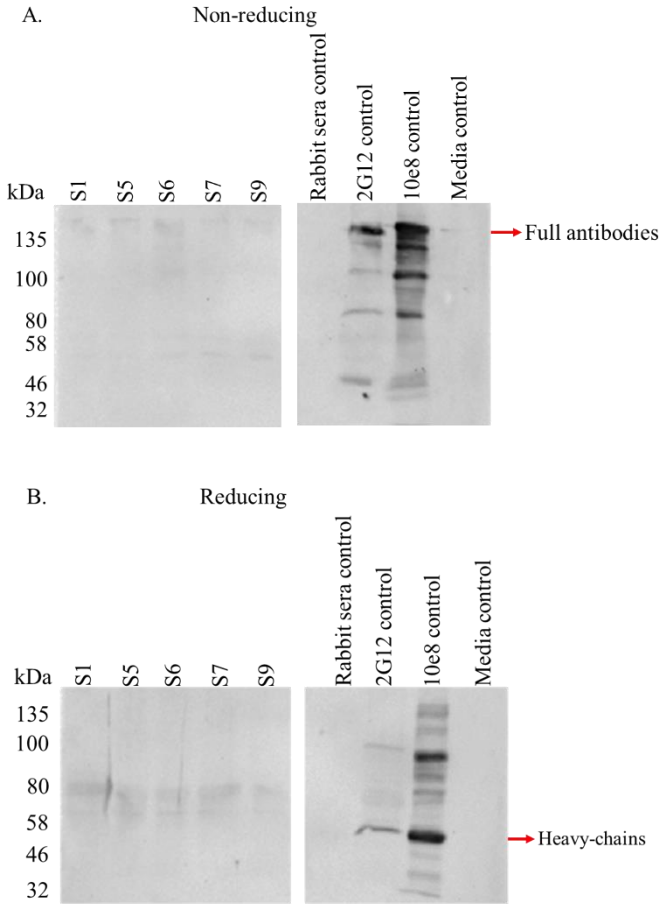


Figure 3.11: Confirmation of the 2G12 antibody expression by western blot. The antibody, 10e8, was used as a positive control to confirm that the western blot detection using the anti-human antibody was successful. The transfection media (media control) was used to determine the presence/absence of non-specific proteins in the transfection media. The antibody expression by the samples (S1, S5, S6, S7 and S9) and 2G12 was determined under non-reducing (A) and reducing (B) conditions. The secondary antibody used to detect the antibody expression was an anti-human antibody used at a 1:2000 dilution. The molecular weight marker (MWM) corresponds to the pre-stained broad range protein marker (New England Biolabs, MA, USA), and are shown in kiloDaltons (kDa) on the left.

Similarly, to confirm expression of the rabbit monoclonal antibodies from the generated TAP cassettes following transient transfection of HEK 293T cells, the resolved supernatant samples were subjected to Western blot analysis and probed with an anti-rabbit HRP- linked antibody (Figure 3.12). As expected, visible bands from protein-A purified rabbit sera (positive control) were observed at ±150 kDa under non-reducing conditions (Figure 3.12A and Appendix A, Supplementary Figure 4B), and at ±58 kDa under reducing conditions (Figure 3.12B and Appendix A, Supplementary Figure 4B), corresponding to the findings in Figure 3.10.

Probing of the five TAP cassette tissue culture samples resolved under non-reducing conditions produced a similar banding pattern to the purified rabbit antibody control samples, however under reducing conditions the patterns were different (Figure 3.12A and B respectively). Additionally, faint bands were detected under non-reducing and reducing conditions for the human antibodies, 2G12, and 10e8, suggesting a high background of non-specific binding, or cross reactivity of the rabbit and human antibodies.

Overall, taken together the ELISA, SDS-PAGE and western blot analyses indicate that rabbit monoclonal antibody expression in HEK 293T cells did not occur, which is supported by Figure 3.8, showing that the heavy- and light-chain variable regions did not assemble into the correctly sized TAP cassette, which may have resulted in the low level expression of incorrectly sized proteins.

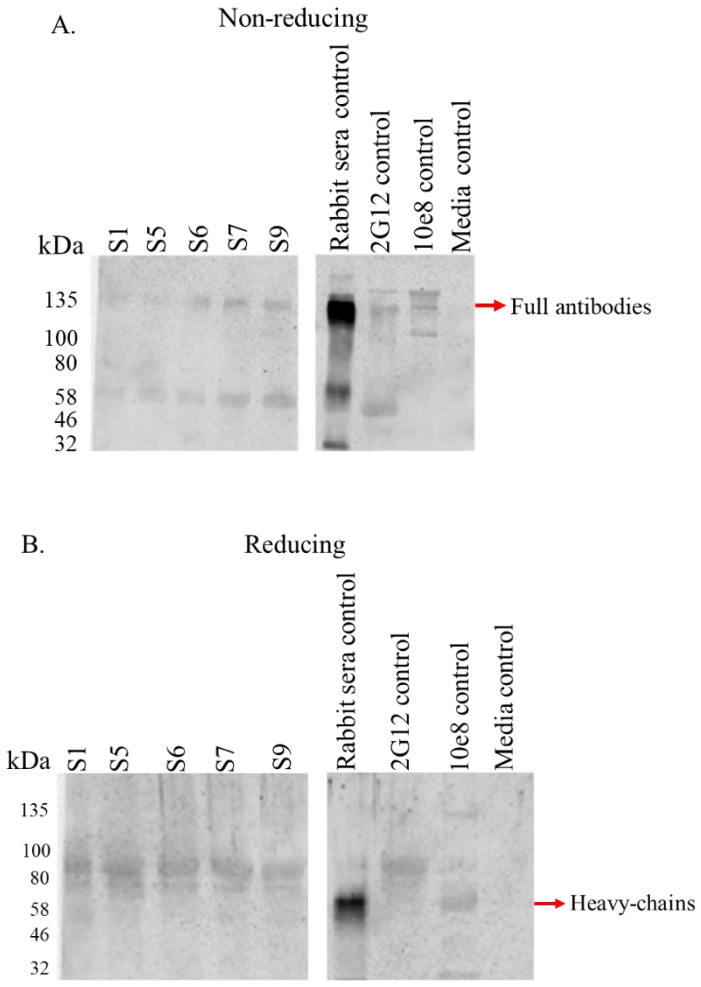


Figure 3.12: Evaluation of the rabbit monoclonal antibody expression by western blot analysis. Protein A purified antibodies from rabbit sera was used as a positive control. The transfection media (media control) was used to determine the presence/absence of non-specific proteins in the transfection media. The antibody expression by the samples (S1, S5, S6, S7 and S9) and 2G12 was determined by western blot analysis under non-reducing (A) and reducing (B) conditions. The secondary antibody used to detect the antibody expression was an anti-rabbit antibody used at a 1:2000 dilution. The molecular weight marker (MWM), kiloDaltons (kDa; indicated in the left) corresponds to the pre-stained broad range protein marker (New England Biolabs, MA, USA).

4. Discussion

The ultimate goal in the development of an effective prophylactic HIV-1 vaccine is the ability of the vaccine to facilitate the elicitation of a bNAb response. Vaccine studies have utilized the HIV-1 Env as the target, as it is the only virally-encoded protein on the virus surface, responsible for viral entry and ultimately infection, and susceptible to neutralization by bNAbs [20], [113]. The elicitation of bNAbs in natural human infections have been mapped to epitopes on the HIV-1 Env [184], indicating that Env is a target for bNAbs and significant for the generation of the bNAbs. Env-based subunit vaccines are non-replicating inactivated vaccines and are therefore safer than previous traditional vaccine strategies, as the recombinant proteins used in these vaccine cannot replicate in the vaccinated host and pose no risk of causing disease (reviewed in [229]). The testing of effective vaccines by previous human clinical trials have been unsuccessful because the immunogens have failed to elicit protective immunity, and this may be due to the many challenges of HIV-1 vaccine design including the high genetic variability of the virus (reviewed in [230], [231]), the high degree of glycan shielding of critical Env epitopes [172], [194], [212] and conformation-dependent exposure of critical epitopes such as CD4i epitopes that are exposed during the open Env conformation as a result of Env and CD4 binding [232]. Previous studies provide evidence that early exposure of critical epitopes is essential for engaging the relevant B cell repertoires and driving the somatic evolution required for high affinity maturation of antibodies required for the elicitation of bNAb immune responses in humans [173]. HIV-1 Env bound to CD4 promotes conformational changes in the Env leading to the exposure of CD4-induced epitopes which has been shown to provide improved bNAb responses [204], [205], [210].

A previous study done by our laboratory showed that the recombinant 2dCD4^{S60C} variant binds to gp120 through a intermolecular disulphide exchange and stabilizes the gp120-CD4 interaction effectively resulting in a potent antiviral effect *in vitro* [218]. In addition our group demonstrated that the cleaved gp140$_{GCN4}$ Env complexed to 2dCD4^{S60C}, when used to immunise NZW rabbits, elicited broad and potent neutralizing titres against clinically relevant, HIV-1 tier 2 pseudoviruses [217]. The current study described here was aimed at delineating the neutralizing antibodies generated in response to this gp140$_{GCN4}$ Env/2dCD4^{S60C} immunogen complex by isolating and characterizing the monoclonal antibodies present in the immunized rabbit sera.

4.1. Confirmation of the elicitation of broadly neutralizing responses by the HIV-1 $gp140_{GCN4}$ Env/2dCD4^{S60C} immunogen complex

The first objective of the current study was to confirm the elicitation of neutralizing antibody responses generated in rabbits that received the $gp140_{GCN4}$ Env/2dCD4^{S60C} immunization as previously reported in the preliminary study [217]. In addition, we examined the neutralization responses following boosting immunizations and compared them to sera samples taken two years prior. Two years prior to the initiation of this study, rabbits were immunized four times at four-week intervals and the isolated sera demonstrated neutralization responses against eight clinically relevant, heterologous, tier-2, genetically diverse HIV-1 pseudoviruses [217]. The isolated sera used in both the preliminary study and the current study were also capable of neutralising the subtype C ZM53M.PB12 pseudovirus which is representative of heterologous tier-2 pseudovirus (Figure 3.3). We confirmed the presence of neutralizing antibodies in the rabbit sera two years after the last immunization, however at a decreased level. Studies have shown that antibodies elicited in response to an immunogen should be long lasting due to the activation of the adaptive immune response, but that these antibody responses waned over time due to a low concentration of the circulating antigen and self-regulatory systems of the immune system (reviewed in [233], [234]). A study that supported these findings explored binding and autologous neutralising responses in South African individuals that previously participated in the HVTN 073 [235], HVTN 086 [236] and HVTN 204 [237] trials, demonstrated immunogenic responses following vaccination, however 18 months post vaccination, the antibody responses waned [238]. These antibody responses were observed in previous studies and the current study, however, vaccinations are known to elicit long-lasting memory B cell responses that are capable of restoring sera antibody titres following boosting vaccinations with the same antigens [239]. Following the boosting immunisations, the neutralizing responses increased to approximately double the ID_{50} (ID_{50} = 1026) observed for rabbit 24 two years prior to the study (ID_{50} = 540.6) (Figure 3.3A), and a similar ID_{50} observed two years prior (ID_{50} = 909.9) was obtained for rabbit 31 after the boosting immunization (ID_{50} = 811.6) (Figure 3.3B). This clearly demonstrates that the boosting immunization slightly improved the neutralizing titres against HIV-1. In contrast, the calculated ID_{50} after the boosting immunization (ID_{50} = 301.1) for rabbit 83 did not return to the value observed for the bleed performed two years prior to this study (ID_{50} = 575.6) (Figure 3.3C),

however an increase in the neutralizing titre from the baseline bleed (ID_{50} = 237.7) was noted. We are not sure why, following the boosting immunization, rabbit 83 failed to generate similar neutralising titres to the immunisations two years prior to the study, however, a study has shown that longer periods between immunisations, where they immunized rabbits eight times over a seventy-three week period, may have an effect on the ability of rabbits to generate neutralizing antibody responses and the magnitude of the neutralizing responses against HIV-1 Env may be affected [240]. The genetic factors of the rabbit antibody repertoire [241] and factors that influence humoral immunity such as age [241], [242], and the appropriate intestinal microflora which affects the well-being of the gut-associated lymphoid tissue (GALT) [242], [243], may have all contributed to the lower neutralizing antibody titre observed when comparing the boosting immunization to the serum sample obtained two years prior to the study. Nonetheless all three rabbits were considered for antigen specific memory B cell isolation and characterization experiments, as all three rabbits elicited neutralizing titres against a tier 2, clinically relevant, heterologous HIV-1 pseudovirus.

4.2. Antigen-specific rabbit memory B-cell isolation

Once the neutralizing titres were confirmed, we used a multiparameter flow cytometry method for the isolation of antigen-specific memory B cells from isolated PBMCs of immunized rabbits, a method described in a study by Starkie, *et al* [223]. Both B cells and non-B cells present in the PBMCs were identified through cell surface marker-targeted antibody staining to ensure that a highly purified population of antigen-specific B cells were identified and selected for. The sequential approach described in the methods and materials in section 2.5.2. for identifying and sorting the antigen-specific memory B cells helps to enrich a pure, positive population of sorted cells [223], [244]. The protocol for the sequential approach was adapted from that described by Starkie *et al* [223], however, we optimised the fluorophore panel to account for fluorescent spectrum spillover. In the study by Starkie *et al*, the CD4 marker was used to identify and discard T cells [223], however, for this study, CD3 was the cell marker used to identify and discard the T cells, in order to avoid the possibility of the anti-CD4 antibody used to bind the T cells from inadvertently targeting the surface-bound 2dCD4 antigen on memory B cells. This may have resulted in a decrease in the identification and subsequent isolation of 2dCD4 antigen specific memory B cells within the final isolated memory B cells population. Overall, a low number of

IgG+ memory B cells was observed at 6.37% of the total events acquired (isolated PBMC fraction). This was slightly higher than the IgG+ memory B cell population reported by Starkie *et al.,* which was found to be 2.67% of the total events [223].

Following the cell sorting and to determine the success of isolating antigen-specific memory B cells, TAPs were engineered for downstream antibody expression. The transcriptionally active linear expression cassettes (TAPs) allow for direct mammalian transfections following PCR amplification, eliminating the time-consuming traditional cloning and subsequent DNA plasmid purification methods and thus are more amenable to high throughput screening methodologies. High throughput screening is advantageous for isolating antibodies from a diverse population using various antigenic targets, they provide the ability of direct screening for antigen-specific antibodies, and efficient determination of both antibody binding and function. These high throughout methodologies make it possible to determine the antibodies generated as a result of the immune response to the vaccine, and provide more information on possible advances to vaccine design.

We successfully amplified the cognate variable antibody regions using the primary PCR primer set, and in this study, we demonstrate nine, randomly selected cell samples from rabbit 24, to determine the generation of the TAPs and the downstream expression of the rabbit monoclonal antibodies. From the nine selected cell samples we successfully amplified 5/9 cognate heavy- and light-chain variable region pairs. The success of the amplification of the heavy- and light-chain variable regions in the primary PCR was confirmed to be rabbit antibody variable regions using Sanger sequencing and NCBI-Blast (data not shown). On average, from a full 96-well plate of sorted cells, 18.42% of the cell samples resulted in successful amplification of variable region cognate pairs, which was comparable to the 18% of variable region cognate pairs obtained by the study by Starkie *et al* [225]. For the unsuccessfully amplified variable regions, we hypothesized that the lack of bands on the agarose gels for the primary PCR, may have been due to, an unsuccessful RT-PCR for the above-mentioned cell samples, or a low quantity of template cDNA present following RT-PCR of the single cells. Although only five of the nine cell samples tested successfully resulted in the amplification of cognate pairs of variable regions, previous studies have also been shown to produce a low efficiency of variable heavy- and light-chain pairs from sorting for single cells using flow cytometry [223]. Starkie *et al*, reported that sorting three antigen-specific memory B cells per well increased the antibody variable region pairs amplification

efficiency [223], however, we opted not to do this as we were concerned of the possibility of mixing non-cognate heavy- and light-chain variable pairs that may impact on downstream antibody assembly and characterisation studies.

To complete the generation of the transcriptionally active linear expression cassette, the CMV promoter, secondary PCR products and respective heavy- and light-chain constant and polyA regions were successfully amplified. The CMV promoter is required to activate and enhance transcription of the downstream genes required for antibody expression [245] and the polyA fragment at the tail end of the constant region sequence is responsible for polyadenylation of the 3′ end of the mRNA which indicates the end of translation for protein production [246].

Following successful amplification of the individual TAP constituents (the heavy- and light-chain secondary amplicons (Figure 3.6), the CMV promoter (Figure 3.7A), and the constant and polyA regions (Figure 3.7B), these were combined into a single reaction and transcriptionally active linear cassettes amplified using the tertiary PCR primer set and protocol previously described in section 2.6. In our previous optimization attempts at the tertiary PCR, we optimized for the annealing temperatures of the second PCR step, the thermal cycling extension times, different cycling protocols, different high-fidelity enzymes, and altered the amounts of DNA template used in the reactions. Following optimization, we performed the tertiary PCR on eight of the cell samples, excluding sample 3, as a negative result was obtained for both the heavy- and light-chain secondary PCRs. Despite samples 2, 4, and 8 displaying inconsistent results showing unsuccessful light-chain secondary PCR amplification, we used these samples as negative controls because these samples did not amplify and continued with the tertiary PCR to observe whether assembly of the input DNA fragments (secondary PCR amplicons, CMV promoter, and constant region including the polyA tail) would occur. After careful analysis of the resolved tertiary amplicons denoting the transcriptionally active linear expression cassettes for both the heavy- and light-chains, the observed sizes including those obtained for the negative control samples (2, 4 and 8) suggests that incorporation of the variable antibody regions in the expression cassette did not occur. Thus, the tertiary amplicons most likely comprised exclusively of the CMV promoter and the respective constant region and accounts for the approximate ~400/600 bp difference for the heavy- and light-chain variable regions, respectively (Figure 3.8). The annealing temperature may have favoured the annealing of the CMV promoter to the constant and polyA regions, therefore to further optimize the tertiary PCR, the annealing temperature of the first step of the PCR could have

been altered, the number of cycles for the first step of the tertiary PCR could have been increased, and a decreased equimolar amount of the DNA fragments could have been used for the first step of the tertiary PCR.

It is unclear as to why this may have occurred, as the CMV promoter and heavy- and light-chain constant and polyA regions do not have the necessary complementary, overlapping sequences. Amplification using the tertiary primer set should have only occurred if there was complete fragment assembly of all three TAPs constituents. The results suggest that assembly of the CMV promoter and the constant including the polyA fragment regions occurred, allowing for amplification using the tertiary primers set and ultimately excluding the light and heavy chain variable regions. To confirm this hypothesis, further characterisation and sequencing of the expression cassette would be required. However, following critical analysis of the optimisation results, and since we had obtained sufficiently pure PCR products, we decided to proceed with TAPs-mediated transfection and expression studies in mammalian cells.

4.3. Antibody expression of transcriptionally active linear cassettes

Following the generation of the transcriptionally active linear expression cassettes, heavy- and light-chain expression cassettes were used in equimolar amounts to express the rabbit monoclonal antibodies using transient co-transfections. To ensure that the transfections were successful, we co-transfected mammalian cells with heavy-chain and light-chain plasmid vectors for the expression of the human anti-HIV-1 bNAb 2G12, [176]. The 2G12 bNAb recognizes the highly conserved cluster of oligomannose residues on the glycan shield of gp120 subunit of Env [178], [247]–[249]. Only five of the cell samples were selected for monoclonal antibody expression studies, these being samples 1, 5, 6, 7 and 9. Samples 2, 4, and 8 were excluded from the expression studies due to unsuccessful secondary PCR amplification (Figure 3.6B).

Rabbit sera obtained from rabbit 24 following the boosting immunisation used in the study was used as a positive control, and showed that the sera had activity against both immunogen components (i.e. $gp140_{GCN4}$ and $2dCD4^{WT}$). The 2G12 transfection supernatant control was shown not to bind to immobilized $gp140_{GCN4}$ Env and $2dCD4^{WT}$ antigens. This was expected since 2G12 is a subtype B derived anti-HIV-1 antibody [176] that has a low binding affinity for subtype C Env [250], [251] as subtype C Env lacks crucial N-linked glycan at position 295 on Env required for the formation of the 2G12 epitope [178]. In addition, no off-target binding of 2G12 to $2dCD4^{WT}$

was noted consistent with its specificity for HIV-1 Env. Unfortunately, no binding was observed for the samples suggesting unsuccessful antibody expression by the TAPs which is most likely due to the missing variable regions in TAPs cassette, which are critical for the formation of the antibody paratope. Although less likely in this instance, the lack of antibody binding activity in the ELISA may also be as a result of the low recovery rate (18%) of the paired variable regions obtained following FACS combined with the observation that, only three quarters of these resulted in the expression of antigen-specific antibodies [223]. Therefore, given the low number of cell samples used in the current study, considering similar inefficiencies to that of Starkie *et al*., reported above, ultimately more samples are required to be screened.

To determine whether rabbit monoclonal antibodies were expressed we used SDS-PAGE and western blot analysis. SDS-PAGE was performed to analyse the banding patterns produced by the positive and negative controls for confirmation of antibody expression (Figure 3.10). Western blots (Figure 3.11 & 3.12) were performed to analyse antibody expression in the TAPs expressed samples as it was expected that the expression yields would be too low to be visualize exclusively by SDS-PAGE and Coomassie blue staining of the resolved protein bands. The banding patterns observed for transiently expressed 2G12 sample resolved on the SDS-PAGE gels and visualized with Coomassie blue staining, did not correspond to that observed for the 10e8 antibody positive control which targets gp41 and the MPER of HIV-1 Env [252], [253]. This may have been due to the presence of residual BSA which has a molecular weight of 66.5 kDa from the media used during the transfection procedure. Under-reducing conditions, the lack of light-chain fragments observed for the 10e8 and purified rabbit antibody controls was as a result of the lower percentage gel, which can also be observed for the protein marker, as all of the bands are not resolved with the last resolved band of the molecular weight marker at 32 kDa (Figure 3.10).

To confirm 2G12 expression, an HRP-conjugated anti-human secondary antibody was used for detection of the resolved antibody samples on the nitrocellulose membranes (western blot). The 10e8 antibody served as the positive control for the western blot used to determine 2G12 expression. Similarly to the 10e8 antibody, the full antibody conformation band was observed for the 2G12 transfection sample under non-reducing conditions, and a corresponding heavy-chain band under reducing conditions. We concluded that the expressed 2G12 antibody concentration was below the detection sensitivity of Coomassie-stained SDS-PAGE analysis, this despite

concentrating the 2G12 sample, as the recommended amount of protein required in a sample to be visualized by Coomassie staining is ±30 ng. We were able to confirm 2G12 antibody expression, albeit at a low level, indicating that the transient co-transfections of the mammalian cells were successful, however non-specific banding was observed. No cross reactivity was observed with the protein-A purified rabbit antibody control further confirming that the antibody banding patterns observed are human antibodies.

Expression of the rabbit monoclonal antibodies was detected by an HRP-conjugated anti-rabbit secondary antibody using western blot analysis (Figure 3.12). Under non-reducing conditions, a high molecular weight band at ±150 kDa was observed for the samples corresponding to the full antibody fragment for the protein-A purified rabbit antibodies from sera control, providing an indication of full antibody expression (Fig. 3.12A). Under reducing conditions, the heavy-chain band was observed for the purified rabbit antibody control at the expected size of at ±58 kDa, indicating correct resolution of the heavy-chain fragment (Figure 3.12B). However, under reducing conditions, a higher molecular weight band to that of the heavy-chain band, was observed for the samples, in comparison to the purified rabbit antibody control (Figure 3.12B), and corresponds to the similar molecular weight band observed for the 2G12 transfection supernatant control, suggesting the presence and detection of non-specific proteins. The lack of light-chain fragments observed under reducing conditions is due to the low resolution of the casted gel that was unable to resolve the lower molecular weight proteins bands. Cross reactivity of the anti-rabbit secondary antibody with the human antibodies (10e8 and 2G12) was observed, with the high molecular weight band of ±150 kDa detected under non-reducing conditions, although at a much lower intensity than previously observed (Figure 11) and in comparison, to the purified rabbit antibody control (Figure 12). This further supports our hypothesis that the banding patterns observed for the samples under reducing conditions was indeed the detection of non-specific proteins. Combined, these results indicate that antibody expression from the TAPs did not occur which was not surprising as we hypothesized that the variable regions may have been missing from the assembled transcriptionally active linear cassettes which would result in truncated protein expression or no expression at all since the heavy- and light-chain variable regions are required for recombinant monoclonal antibody expression.

4.4. Conclusion and future work

The Env_{GCN4}/2dCD4^{S60C} immunogen complex is a promising immunogen for the elicitation of HIV-1 specific bNAbs. We were able to confirm the persistence of circulating neutralizing antibody responses two years after the last immunization. In addition, we demonstrate that these specific neutralization titres could once again be elevated following a single booster immunization. Using the multi-parameter FACS protocol, rabbit antigen-specific B cells were successfully sorted, however, the amplification of the generated transcriptionally active linear expression cassettes was unsuccessful and would require further optimisation in order to add the variable regions into the TAPs.

The lack of binding activity observed for the samples against 2dCD4^{WT} and/or $gp140_{GCN4}$ Env, and the expression screening analysis (SDS-PAGE and western blotting) confirms that expression of rabbit monoclonal antibodies by the TAPs were unsuccessful. The hypothesized, incomplete assembly of the transcriptionally active linear expression cassette may have resulted is the most likely explanation for the lack of monoclonal antibody expression.

To successfully express and characterize the rabbit monoclonal antibodies, in order to delineate the neutralizing response elicited by the HIV-1 $gp140_{GCN4}$ Env/2dCD4^{S60C} immunogen complex, future work is required. The future work would include; generating transcriptionally active linear expression cassettes for all paired variable regions of the single sorted antigen-specific memory B cells for antibody expression as this increases the likelihood of generating a monoclonal antibody because not all cognate pairs of expression cassettes have been shown to successfully express antigen-specific antibodies. Alternatively, the variable region regions could be cloned into a suitable dual plasmid vector system to facilitate expression studies. Sequencing of the Fab regions of selected candidates should be done to characterise their genetic make-up and lineage. In addition, the evaluation of neutralisation activity of the antibodies against a panel of HIV-1 pseudovirions in a luciferase reporter gene-based neutralising assays should be performed as this will allow us to figure out the individual contribution of each antibody to the serum breadth.

References

[1] HIV.gov, 'What Are HIV and AIDS?', *HIV.gov*, Jun. 17, 2019. https://www.hiv.gov/hiv-basics/overview/about-hiv-and-aids/what-are-hiv-and-aids (accessed Jan. 26, 2020).

[2] UNAIDS, 'Global HIV & AIDS statistics — 2019 fact sheet'. 2019, Accessed: Jan. 26, 2020. [Online]. Available: https://www.unaids.org/sites/default/files/media_asset/UNAIDS_FactSheet_en.pdf.

[3] S. P. Buchbinder, 'Antiretroviral use for prevention and other factors affecting the course of the HIV-1 epidemic', *Top. Antivir. Med.*, vol. 20, no. 2, pp. 32–40, 2012.

[4] M. S. Cohen *et al.*, 'Prevention of HIV-1 Infection with Early Antiretroviral Therapy', *N. Engl. J. Med.*, vol. 365, no. 6, pp. 493–505, Jul. 2011, doi: 10.1056/NEJMoa1105243.

[5] T. J. Coates, L. Richter, and C. Caceres, 'Behavioural strategies to reduce HIV transmission: how to make them work better', *The Lancet*, vol. 372, no. 9639, pp. 669–684, Aug. 2008, doi: 10.1016/S0140-6736(08)60886-7.

[6] UNAIDS, 'Combination HIV Prevention: Tailoring and Coordinating Biomedical, Behavioural and Structural Strategies to Reduce New HIV Infections'. Sep. 2010.

[7] Avert, 'HIV PREVENTION PROGRAMMES OVERVIEW', *Avert*, Oct. 10, 2019. https://www.avert.org/professionals/hiv-programming/prevention/overview#footnote58_awc0iot (accessed Feb. 19, 2020).

[8] A. E. Kurth, C. Celum, J. M. Baeten, S. H. Vermund, and J. N. Wasserheit, 'Combination HIV Prevention: Significance, Challenges, and Opportunities', *Curr. HIV/AIDS Rep.*, vol. 8, no. 1, pp. 62–72, Mar. 2011, doi: 10.1007/s11904-010-0063-3.

[9] UNAIDS, 'Voluntary medical male circumcision—4.1 million performed in 2018', *UNAIDS*. https://www.unaids.org/en/resources/presscentre/featurestories/2019/october/20191021_vmmc (accessed Feb. 19, 2020).

[10] J. B. Reed *et al.*, 'Voluntary medical male circumcision: an HIV prevention priority for PEPFAR', *J. Acquir. Immune Defic. Syndr. 1999*, vol. 60 Suppl 3, no. 0 3, pp. S88–S95, Aug. 2012, doi: 10.1097/QAI.0b013e31825cac4e.

[11] M. L. McNairy and W. M. El-Sadr, 'Antiretroviral therapy for the prevention of HIV transmission: what will it take?', *Clin. Infect. Dis. Off. Publ. Infect. Dis. Soc. Am.*, vol. 58, no. 7, pp. 1003–1011, Apr. 2014, doi: 10.1093/cid/ciu018.

[12] W. M. El-Sadr, M. Affrunti, T. Gamble, and A. Zerbe, 'Antiretroviral therapy: a promising HIV prevention strategy?', *J. Acquir. Immune Defic. Syndr. 1999*, vol. 55 Suppl 2, no. Suppl 2, pp. S116–S121, Dec. 2010, doi: 10.1097/QAI.0b013e3181fbca6e.

[13] S. C. Kim *et al.*, 'Planning for pre-exposure prophylaxis to prevent HIV transmission: challenges and opportunities', *J. Int. AIDS Soc.*, vol. 13, no. 1, p. 24, Jul. 2010, doi: 10.1186/1758-2652-13-24.

[14] M. S. Cohen *et al.*, 'HIV Treatment As Prevention: How Scientific Discovery Occurred And Translated Rapidly Into Policy For The Global Response', *Health Aff. (Millwood)*, vol. 31, no. 7, pp. 1439–1449, Jul. 2012, doi: 10.1377/hlthaff.2012.0250.

[15] R. G. Wamai *et al.*, 'Male circumcision for HIV prevention: current evidence and implementation in sub-Saharan Africa', *J. Int. AIDS Soc.*, vol. 14, pp. 49–49, Oct. 2011, doi: 10.1186/1758-2652-14-49.

[16] I. Cremin, R. Alsallaq, M. Dybul, P. Piot, G. Garnett, and T. B. Hallett, 'The new role of antiretrovirals in combination HIV prevention: a mathematical modelling analysis.', *AIDS Lond. Engl.*, vol. 27, no. 3, pp. 447–458, Jan. 2013, doi: 10.1097/QAD.0b013e32835ca2dd.
[17] R. O'Connell, J. Kim, L. Corey, and N. Michael, 'Human Immunodeficiency Virus Vaccine Trials', *Cold Spring Harb. Perspect. Med.*, vol. 2, Dec. 2012, doi: 10.1101/cshperspect.a007351.
[18] J.-P. Julien *et al.*, 'Crystal structure of a soluble cleaved HIV-1 envelope trimer.', *Science*, vol. 342, no. 6165, pp. 1477–1483, Dec. 2013, doi: 10.1126/science.1245625.
[19] G. M. Orloff, S. L. Orloff, M. S. Kennedy, P. J. Maddon, and J. S. McDougal, 'Penetration of CD4 T cells by HIV-1. The CD4 receptor does not internalize with HIV, and CD4-related signal transduction events are not required for entry.', *J. Immunol. Baltim. Md 1950*, vol. 146, no. 8, pp. 2578–2587, Apr. 1991.
[20] C. B. Wilen, J. C. Tilton, and R. W. Doms, 'HIV: cell binding and entry', *Cold Spring Harb. Perspect. Med.*, vol. 2, no. 8, p. a006866, Aug. 2012, doi: 10.1101/cshperspect.a006866.
[21] M. A. Checkley, B. G. Luttge, and E. O. Freed, 'HIV-1 envelope glycoprotein biosynthesis, trafficking, and incorporation.', *J. Mol. Biol.*, vol. 410, no. 4, pp. 582–608, Jul. 2011, doi: 10.1016/j.jmb.2011.04.042.
[22] A. Harris *et al.*, 'Trimeric HIV-1 glycoprotein gp140 immunogens and native HIV-1 envelope glycoproteins display the same closed and open quaternary molecular architectures', *Proc. Natl. Acad. Sci.*, vol. 108, no. 28, p. 11440, Jul. 2011, doi: 10.1073/pnas.1101414108.
[23] F. Kirchhoff, 'HIV Life Cycle: Overview', 2013, pp. 1–9.
[24] AIDS info, 'The HIV Life Cycle', *AIDS info*, Jan. 07, 2019. https://aidsinfo.nih.gov/understanding-hiv-aids/fact-sheets/19/73/the-hiv-life-cycle (accessed Feb. 19, 2020).
[25] W.-S. Hu and S. H. Hughes, 'HIV-1 reverse transcription', *Cold Spring Harb. Perspect. Med.*, vol. 2, no. 10, p. a006882, Oct. 2012, doi: 10.1101/cshperspect.a006882.
[26] R. Craigie, 'The molecular biology of HIV integrase', *Future Virol.*, vol. 7, no. 7, pp. 679–686, Jul. 2012, doi: 10.2217/FVL.12.56.
[27] S. Y. Kim, R. Byrn, J. Groopman, and D. Baltimore, 'Temporal aspects of DNA and RNA synthesis during human immunodeficiency virus infection: evidence for differential gene expression', *J. Virol.*, vol. 63, no. 9, pp. 3708–3713, Sep. 1989.
[28] E. O. Freed, 'HIV-1 assembly, release and maturation.', *Nat. Rev. Microbiol.*, vol. 13, no. 8, pp. 484–496, Aug. 2015, doi: 10.1038/nrmicro3490.
[29] S. Hallenberger, V. Bosch, H. Angliker, E. Shaw, H. D. Klenk, and W. Garten, 'Inhibition of furin-mediated cleavage activation of HIV-1 glycoprotein gp160.', *Nature*, vol. 360, no. 6402, pp. 358–361, Nov. 1992, doi: 10.1038/360358a0.
[30] S. 'Assessment of P. T. by B. German Advisory Committee Blood (Arbeitskreis Blut), 'Human Immunodeficiency Virus (HIV)', *Transfus. Med. Hemotherapy Off. Organ Dtsch. Ges. Transfusionsmedizin Immunhamatologie*, vol. 43, no. 3, pp. 203–222, May 2016, doi: 10.1159/000445852.
[31] P. Dorr *et al.*, 'Maraviroc (UK-427,857), a Potent, Orally Bioavailable, and Selective Small-Molecule Inhibitor of Chemokine Receptor CCR5 with Broad-Spectrum Anti-Human Immunodeficiency Virus Type 1 Activity', *Antimicrob. Agents Chemother.*, vol. 49, no. 11, p. 4721, Nov. 2005, doi: 10.1128/AAC.49.11.4721-4732.2005.

[32] B. P. Kearney, J. F. Flaherty, and J. Shah, ‘Tenofovir Disoproxil Fumarate’, *Clin. Pharmacokinet.*, vol. 43, no. 9, pp. 595–612, Aug. 2004, doi: 10.2165/00003088-200443090-00003.
[33] A. Hughes, T. Barber, and M. Nelson, ‘New treatment options for HIV salvage patients: An overview of second generation PIs, NNRTIs, integrase inhibitors and CCR5 antagonists’, *Focus HIVAIDS*, vol. 57, no. 1, pp. 1–10, Jul. 2008, doi: 10.1016/j.jinf.2008.05.006.
[34] N. Y. Rakhmanina and J. N. van den Anker, ‘Efavirenz in the therapy of HIV infection’, *Expert Opin. Drug Metab. Toxicol.*, vol. 6, no. 1, pp. 95–103, Jan. 2010, doi: 10.1517/17425250903483207.
[35] J.-F. Mouscadet and L. Tchertanov, ‘Raltegravir: molecular basis of its mechanism of action’, *Eur. J. Med. Res.*, vol. 14 Suppl 3, no. Suppl 3, pp. 5–16, Nov. 2009, doi: 10.1186/2047-783x-14-s3-5.
[36] R. S. Cvetkovic and K. L. Goa, ‘Lopinavir/Ritonavir’, *Drugs*, vol. 63, no. 8, pp. 769–802, Apr. 2003, doi: 10.2165/00003495-200363080-00004.
[37] S. B. Joseph, R. Swanstrom, A. D. Kashuba, and M. S. Cohen, ‘Bottlenecks in HIV-1 transmission: insights from the study of founder viruses’, *Nat. Rev. Microbiol.*, vol. 13, no. 7, pp. 414–425, 2015.
[38] A. J. McMichael, P. Borrow, G. D. Tomaras, N. Goonetilleke, and B. F. Haynes, ‘The immune response during acute HIV-1 infection: clues for vaccine development’, *Nat. Rev. Immunol.*, vol. 10, no. 1, pp. 11–23, 2010.
[39] J. M. Brenchley *et al.*, ‘CD4+ T cell depletion during all stages of HIV disease occurs predominantly in the gastrointestinal tract’, *J. Exp. Med.*, vol. 200, no. 6, pp. 749–759, 2004.
[40] R. S. Veazey *et al.*, ‘Dynamics of CCR5 expression by CD4+ T cells in lymphoid tissues during simian immunodeficiency virus infection’, *J. Virol.*, vol. 74, no. 23, pp. 11001–11007, 2000.
[41] S. Mehandru *et al.*, ‘Primary HIV-1 infection is associated with preferential depletion of CD4+ T lymphocytes from effector sites in the gastrointestinal tract’, *J. Exp. Med.*, vol. 200, no. 6, pp. 761–770, 2004.
[42] T. B. Geijtenbeek *et al.*, ‘DC-SIGN, a dendritic cell–specific HIV-1-binding protein that enhances trans-infection of T cells’, *Cell*, vol. 100, no. 5, pp. 587–597, 2000.
[43] S. Moir *et al.*, ‘B cells of HIV-1–infected patients bind virions through CD21–complement interactions and transmit infectious virus to activated T cells’, *J. Exp. Med.*, vol. 192, no. 5, pp. 637–646, 2000.
[44] Z. Grossman, M. Meier-Schellersheim, W. E. Paul, and L. J. Picker, ‘Pathogenesis of HIV infection: what the virus spares is as important as what it destroys’, *Nat. Med.*, vol. 12, no. 3, pp. 289–295, 2006.
[45] M. Guadalupe *et al.*, ‘Severe CD4+ T-cell depletion in gut lymphoid tissue during primary human immunodeficiency virus type 1 infection and substantial delay in restoration following highly active antiretroviral therapy’, *J. Virol.*, vol. 77, no. 21, pp. 11708–11717, 2003.
[46] L. J. Picker and D. I. Watkins, ‘HIV pathogenesis: the first cut is the deepest’, *Nat. Immunol.*, vol. 6, no. 5, pp. 430–432, 2005.
[47] J. Dinoso *et al.*, ‘Treatment intensification does not reduce residual HIV-1 viremia in patients on highly active antiretroviral therapy’, *Proc. Natl. Acad. Sci.*, vol. 106, no. 23, pp. 9403–9408, 2009.

[48] T. W. Schacker, J. P. Hughes, T. Shea, R. W. Coombs, and L. Corey, 'Biological and virologic characteristics of primary HIV infection', *Ann. Intern. Med.*, vol. 128, no. 8, pp. 613–620, 1998.
[49] G. Pantaleo *et al.*, 'Major expansion of CD8+ T cells with a predominant Vβ usage during the primary immune response to HIV', *Nature*, vol. 370, no. 6489, pp. 463–467, 1994.
[50] P. Borrow, H. Lewicki, B. H. Hahn, G. M. Shaw, and M. Oldstone, 'Virus-specific CD8+ cytotoxic T-lymphocyte activity associated with control of viremia in primary human immunodeficiency virus type 1 infection.', *J. Virol.*, vol. 68, no. 9, pp. 6103–6110, 1994.
[51] D. D. Ho, A. U. Neumann, A. S. Perelson, W. Chen, J. M. Leonard, and M. Markowitz, 'Rapid turnover of plasma virions and CD4 lymphocytes in HIV-1 infection', *Nature*, vol. 373, no. 6510, pp. 123–126, 1995.
[52] E. S. Ford, C. E. Puronen, and I. Sereti, 'Immunopathogenesis of asymptomatic chronic HIV Infection: the calm before the storm', *Curr. Opin. HIV AIDS*, vol. 4, no. 3, p. 206, 2009.
[53] L. J. Picker, 'Immunopathogenesis of acute AIDS virus infection', *Curr. Opin. Immunol.*, vol. 18, no. 4, pp. 399–405, 2006.
[54] J. M. Brenchley *et al.*, 'Microbial translocation is a cause of systemic immune activation in chronic HIV infection', *Nat. Med.*, vol. 12, no. 12, pp. 1365–1371, 2006.
[55] A. Boasso and G. M. Shearer, 'Chronic innate immune activation as a cause of HIV-1 immunopathogenesis', *Clin. Immunol.*, vol. 126, no. 3, pp. 235–242, 2008.
[56] Z. Grossman, M. Meier-Schellersheim, A. E. Sousa, R. M. Victorino, and W. E. Paul, 'CD4+ T-cell depletion in HIV infection: are we closer to understanding the cause?', *Nat. Med.*, vol. 8, no. 4, pp. 319–323, 2002.
[57] D. C. Douek *et al.*, 'Changes in thymic function with age and during the treatment of HIV infection', *Nature*, vol. 396, no. 6712, pp. 690–695, 1998.
[58] D. C. Douek, L. J. Picker, and R. A. Koup, 'T cell dynamics in HIV-1 infection', *Annu. Rev. Immunol.*, vol. 21, no. 1, pp. 265–304, 2003.
[59] J. D. Estes *et al.*, 'Simian immunodeficiency virus-induced lymphatic tissue fibrosis is mediated by transforming growth factor β1-positive regulatory T cells and begins in early infection', *J. Infect. Dis.*, vol. 195, no. 4, pp. 551–561, 2007.
[60] S. M. Alam *et al.*, 'Human immunodeficiency virus type 1 gp41 antibodies that mask membrane proximal region epitopes: antibody binding kinetics, induction, and potential for regulation in acute infection', *J. Virol.*, vol. 82, no. 1, pp. 115–125, 2008.
[61] B. He *et al.*, 'HIV-1 envelope triggers polyclonal Ig class switch recombination through a CD40-independent mechanism involving BAFF and C-type lectin receptors', *J. Immunol.*, vol. 176, no. 7, pp. 3931–3941, 2006.
[62] A. Rustagi and M. Gale, 'Innate Antiviral Immune Signaling, Viral Evasion and Modulation by HIV-1', *Antivir. Innate Immun. Part II*, vol. 426, no. 6, pp. 1161–1177, Mar. 2014, doi: 10.1016/j.jmb.2013.12.003.
[63] D. B. Stetson and R. Medzhitov, 'Type I Interferons in Host Defense', *Immunity*, vol. 25, no. 3, pp. 373–381, Sep. 2006, doi: 10.1016/j.immuni.2006.08.007.
[64] S. Jost and M. Altfeld, 'Control of human viral infections by natural killer cells.', *Annu. Rev. Immunol.*, vol. 31, pp. 163–194, 2013, doi: 10.1146/annurev-immunol-032712-100001.
[65] C. Vilches and P. Parham, 'KIR: diverse, rapidly evolving receptors of innate and adaptive immunity.', *Annu. Rev. Immunol.*, vol. 20, pp. 217–251, 2002, doi: 10.1146/annurev.immunol.20.092501.134942.

[66] R. A. Koup *et al.*, ‘Temporal association of cellular immune responses with the initial control of viremia in primary human immunodeficiency virus type 1 syndrome.’, *J. Virol.*, vol. 68, no. 7, pp. 4650–4655, Jul. 1994.
[67] B. Rodriguez *et al.*, ‘Predictive value of plasma HIV RNA level on rate of CD4 T-cell decline in untreated HIV infection.’, *JAMA*, vol. 296, no. 12, pp. 1498–1506, Sep. 2006, doi: 10.1001/jama.296.12.1498.
[68] P. J. R. Goulder and B. D. Walker, ‘HIV and HLA class I: an evolving relationship.’, *Immunity*, vol. 37, no. 3, pp. 426–440, Sep. 2012, doi: 10.1016/j.immuni.2012.09.005.
[69] A. Schneidewind *et al.*, ‘Escape from the dominant HLA-B27-restricted cytotoxic T-lymphocyte response in Gag is associated with a dramatic reduction in human immunodeficiency virus type 1 replication.’, *J. Virol.*, vol. 81, no. 22, pp. 12382–12393, Nov. 2007, doi: 10.1128/JVI.01543-07.
[70] H. Crawford *et al.*, ‘Evolution of HLA-B*5703 HIV-1 escape mutations in HLA-B*5703-positive individuals and their transmission recipients.’, *J. Exp. Med.*, vol. 206, no. 4, pp. 909–921, Apr. 2009, doi: 10.1084/jem.20081984.
[71] J. L. Prince *et al.*, ‘Role of transmitted Gag CTL polymorphisms in defining replicative capacity and early HIV-1 pathogenesis.’, *PLoS Pathog.*, vol. 8, no. 11, p. e1003041, 2012, doi: 10.1371/journal.ppat.1003041.
[72] P. A. Goepfert *et al.*, ‘Transmission of HIV-1 Gag immune escape mutations is associated with reduced viral load in linked recipients.’, *J. Exp. Med.*, vol. 205, no. 5, pp. 1009–1017, May 2008, doi: 10.1084/jem.20072457.
[73] A. Grakoui *et al.*, ‘HCV persistence and immune evasion in the absence of memory T cell help.’, *Science*, vol. 302, no. 5645, pp. 659–662, Oct. 2003, doi: 10.1126/science.1088774.
[74] M. Lichterfeld *et al.*, ‘Loss of HIV-1-specific CD8+ T cell proliferation after acute HIV-1 infection and restoration by vaccine-induced HIV-1-specific CD4+ T cells.’, *J. Exp. Med.*, vol. 200, no. 6, pp. 701–712, Sep. 2004, doi: 10.1084/jem.20041270.
[75] J. J. Mattapallil, D. C. Douek, B. Hill, Y. Nishimura, M. Martin, and M. Roederer, ‘Massive infection and loss of memory CD4+ T cells in multiple tissues during acute SIV infection.’, *Nature*, vol. 434, no. 7037, pp. 1093–1097, Apr. 2005, doi: 10.1038/nature03501.
[76] D. C. Douek *et al.*, ‘HIV preferentially infects HIV-specific CD4+ T cells.’, *Nature*, vol. 417, no. 6884, pp. 95–98, May 2002, doi: 10.1038/417095a.
[77] H. Streeck, M. P. D’Souza, D. R. Littman, and S. Crotty, ‘Harnessing CD4(+) T cell responses in HIV vaccine development.’, *Nat. Med.*, vol. 19, no. 2, pp. 143–149, Feb. 2013, doi: 10.1038/nm.3054.
[78] D. Z. Soghoian *et al.*, ‘HIV-specific cytolytic CD4 T cell responses during acute HIV infection predict disease outcome.’, *Sci. Transl. Med.*, vol. 4, no. 123, p. 123ra25, Feb. 2012, doi: 10.1126/scitranslmed.3003165.
[79] D. Ramduth *et al.*, ‘Immunodominant HIV-1 Cd4+ T cell epitopes in chronic untreated clade C HIV-1 infection.’, *PloS One*, vol. 4, no. 4, p. e5013, 2009, doi: 10.1371/journal.pone.0005013.
[80] W. Liao, J.-X. Lin, and W. J. Leonard, ‘Interleukin-2 at the crossroads of effector responses, tolerance, and immunotherapy.’, *Immunity*, vol. 38, no. 1, pp. 13–25, Jan. 2013, doi: 10.1016/j.immuni.2013.01.004.
[81] B. D. Walker and D. R. Burton, ‘Toward an AIDS Vaccine’, *Science*, vol. 320, no. 5877, p. 760, May 2008, doi: 10.1126/science.1152622.

[82] P. D. Kwong and J. R. Mascola, ‘Human antibodies that neutralize HIV-1: identification, structures, and B cell ontogenies’, *Immunity*, vol. 37, no. 3, pp. 412–425, 2012.
[83] N. A. Doria-Rose *et al.*, ‘Frequency and phenotype of human immunodeficiency virus envelope-specific B cells from patients with broadly cross-neutralizing antibodies’, *J. Virol.*, vol. 83, no. 1, pp. 188–199, 2009.
[84] E. S. Gray *et al.*, ‘The neutralization breadth of HIV-1 develops incrementally over four years and is associated with CD4+ T cell decline and high viral load during acute infection’, *J. Virol.*, vol. 85, no. 10, pp. 4828–4840, 2011.
[85] E. S. Gray *et al.*, ‘Isolation of a monoclonal antibody that targets the alpha-2 helix of gp120 and represents the initial autologous neutralizing-antibody response in an HIV-1 subtype C-infected individual’, *J. Virol.*, vol. 85, no. 15, pp. 7719–7729, 2011.
[86] I. Mikell, D. N. Sather, S. A. Kalams, M. Altfeld, G. Alter, and L. Stamatatos, ‘Characteristics of the earliest cross-neutralizing antibody response to HIV-1’, *PLoS Pathog.*, vol. 7, no. 1, 2011.
[87] X. Wu *et al.*, ‘Rational design of envelope identifies broadly neutralizing human monoclonal antibodies to HIV-1.’, *Science*, vol. 329, no. 5993, pp. 856–861, Aug. 2010, doi: 10.1126/science.1187659.
[88] S. Crotty, ‘Follicular helper CD4 T cells (TFH).’, *Annu. Rev. Immunol.*, vol. 29, pp. 621–663, 2011, doi: 10.1146/annurev-immunol-031210-101400.
[89] N. Fazilleau, L. J. McHeyzer-Williams, H. Rosen, and M. G. McHeyzer-Williams, ‘The function of follicular helper T cells is regulated by the strength of T cell antigen receptor binding’, *Nat. Immunol.*, vol. 10, no. 4, p. 375, 2009.
[90] D. Breitfeld *et al.*, ‘Follicular B helper T cells express CXC chemokine receptor 5, localize to B cell follicles, and support immunoglobulin production’, *J. Exp. Med.*, vol. 192, no. 11, pp. 1545–1552, 2000.
[91] D. Zotos *et al.*, ‘IL-21 regulates germinal center B cell differentiation and proliferation through a B cell–intrinsic mechanism’, *J. Exp. Med.*, vol. 207, no. 2, pp. 365–378, 2010.
[92] J. Rolf, K. Fairfax, and M. Turner, ‘Signaling pathways in T follicular helper cells’, *J. Immunol.*, vol. 184, no. 12, pp. 6563–6568, 2010.
[93] G. D. Victora and M. C. Nussenzweig, ‘Germinal centers’, *Annu. Rev. Immunol.*, vol. 30, pp. 429–457, 2012.
[94] K. L. Good-Jacobson and M. J. Shlomchik, ‘Plasticity and heterogeneity in the generation of memory B cells and long-lived plasma cells: the influence of germinal center interactions and dynamics’, *J. Immunol.*, vol. 185, no. 6, pp. 3117–3125, 2010.
[95] C. C. Goodnow, C. G. Vinuesa, K. L. Randall, F. Mackay, and R. Brink, ‘Control systems and decision making for antibody production’, *Nat. Immunol.*, vol. 11, no. 8, p. 681, 2010.
[96] M. McHeyzer-Williams, S. Okitsu, N. Wang, and L. McHeyzer-Williams, ‘Molecular programming of B cell memory’, *Nat. Rev. Immunol.*, vol. 12, no. 1, pp. 24–34, 2012.
[97] S. G. Tangye and D. M. Tarlinton, ‘Memory B cells: Effectors of long-lived immune responses’, *Eur. J. Immunol.*, vol. 39, no. 8, pp. 2065–2075, 2009.
[98] J.-L. Excler, G. D. Tomaras, and N. D. Russell, ‘Novel directions in HIV-1 vaccines revealed from clinical trials’, *Curr. Opin. HIV AIDS*, vol. 8, no. 5, p. 421, 2013.
[99] J. I. Lai *et al.*, ‘Divergent antibody subclass and specificity profiles but not protective HLA-B alleles are associated with variable antibody effector function among HIV-1 controllers’, *J. Virol.*, vol. 88, no. 5, pp. 2799–2809, 2014.

[100] M. Lindqvist *et al.*, 'Expansion of HIV-specific T follicular helper cells in chronic HIV infection', *J. Clin. Invest.*, vol. 122, no. 9, pp. 3271–3280, 2012.
[101] M. Perreau *et al.*, 'Follicular helper T cells serve as the major CD4 T cell compartment for HIV-1 infection, replication, and production', *J. Exp. Med.*, vol. 210, no. 1, pp. 143–156, 2013.
[102] E. A. Boritz *et al.*, 'Multiple origins of virus persistence during natural control of HIV infection', *Cell*, vol. 166, no. 4, pp. 1004–1015, 2016.
[103] R. Banga *et al.*, 'PD-1+ and follicular helper T cells are responsible for persistent HIV-1 transcription in treated aviremic individuals', *Nat. Med.*, vol. 22, no. 7, p. 754, 2016.
[104] R. A. Cubas *et al.*, 'Inadequate T follicular cell help impairs B cell immunity during HIV infection', *Nat. Med.*, vol. 19, no. 4, p. 494, 2013.
[105] S. Pallikkuth *et al.*, 'Interleukin-21 administration to rhesus macaques chronically infected with simian immunodeficiency virus increases cytotoxic effector molecules in T cells and NK cells and enhances B cell function without increasing immune activation or viral replication', *Vaccine*, vol. 29, no. 49, pp. 9229–9238, 2011.
[106] M. Vaccari and G. Franchini, 'T cell subsets in the germinal center: lessons from the macaque model', *Front. Immunol.*, vol. 9, p. 348, 2018.
[107] J. Learmont *et al.*, 'Long-term symptomless HIV-1 infection in recipients of blood products from a single donor.', *Lancet Lond. Engl.*, vol. 340, no. 8824, pp. 863–867, Oct. 1992, doi: 10.1016/0140-6736(92)93281-q.
[108] M. D. Daniel, F. Kirchhoff, S. C. Czajak, P. K. Sehgal, and R. C. Desrosiers, 'Protective effects of a live attenuated SIV vaccine with a deletion in the nef gene.', *Science*, vol. 258, no. 5090, pp. 1938–1941, Dec. 1992, doi: 10.1126/science.1470917.
[109] T. W. Baba *et al.*, 'Live attenuated, multiply deleted simian immunodeficiency virus causes AIDS in infant and adult macaques.', *Nat. Med.*, vol. 5, no. 2, pp. 194–203, Feb. 1999, doi: 10.1038/5557.
[110] Y. Gao, P. F. McKay, and J. F. S. Mann, 'Advances in HIV-1 Vaccine Development', *Viruses*, vol. 10, no. 4, p. 167, Apr. 2018, doi: 10.3390/v10040167.
[111] J. Zhuang *et al.*, 'Human immunodeficiency virus type 1 recombination: rate, fidelity, and putative hot spots.', *J. Virol.*, vol. 76, no. 22, pp. 11273–11282, Nov. 2002, doi: 10.1128/jvi.76.22.11273-11282.2002.
[112] B. C. Ramirez, E. Simon-Loriere, R. Galetto, and M. Negroni, 'Implications of recombination for HIV diversity.', *Virus Res.*, vol. 134, no. 1–2, pp. 64–73, Jun. 2008, doi: 10.1016/j.virusres.2008.01.007.
[113] Y. Geiss and U. Dietrich, 'Catch Me If You Can--The Race Between HIV and Neutralizing Antibodies.', *AIDS Rev.*, vol. 17, no. 2, pp. 107–113, Jun. 2015.
[114] R. W. Sanders *et al.*, 'A Next-Generation Cleaved, Soluble HIV-1 Env Trimer, BG505 SOSIP.664 gp140, Expresses Multiple Epitopes for Broadly Neutralizing but Not Non-Neutralizing Antibodies', *PLOS Pathog.*, vol. 9, no. 9, p. e1003618, Sep. 2013, doi: 10.1371/journal.ppat.1003618.
[115] R. W. Sanders *et al.*, 'Stabilization of the soluble, cleaved, trimeric form of the envelope glycoprotein complex of human immunodeficiency virus type 1.', *J. Virol.*, vol. 76, no. 17, pp. 8875–8889, Sep. 2002, doi: 10.1128/jvi.76.17.8875-8889.2002.
[116] S. W. de Taeye, J. P. Moore, and R. W. Sanders, 'HIV-1 Envelope Trimer Design and Immunization Strategies To Induce Broadly Neutralizing Antibodies.', *Trends Immunol.*, vol. 37, no. 3, pp. 221–232, Mar. 2016, doi: 10.1016/j.it.2016.01.007.

[117] N. Schülke *et al.*, 'Oligomeric and conformational properties of a proteolytically mature, disulfide-stabilized human immunodeficiency virus type 1 gp140 envelope glycoprotein', *J. Virol.*, vol. 76, no. 15, pp. 7760–7776, 2002.
[118] N. M. Flynn, D. N. Forthal, C. D. Harro, F. N. Judson, K. H. Mayer, and M. F. Para, 'Placebo-controlled phase 3 trial of a recombinant glycoprotein 120 vaccine to prevent HIV-1 infection.', *J. Infect. Dis.*, vol. 191, no. 5, pp. 654–665, Mar. 2005, doi: 10.1086/428404.
[119] P. Pitisuttithum *et al.*, 'Randomized, double-blind, placebo-controlled efficacy trial of a bivalent recombinant glycoprotein 120 HIV-1 vaccine among injection drug users in Bangkok, Thailand.', *J. Infect. Dis.*, vol. 194, no. 12, pp. 1661–1671, Dec. 2006, doi: 10.1086/508748.
[120] S. Rerks-Ngarm *et al.*, 'Vaccination with ALVAC and AIDSVAX to prevent HIV-1 infection in Thailand.', *N. Engl. J. Med.*, vol. 361, no. 23, pp. 2209–2220, Dec. 2009, doi: 10.1056/NEJMoa0908492.
[121] A. J. Gartland *et al.*, 'Analysis of HLA A*02 association with vaccine efficacy in the RV144 HIV-1 vaccine trial.', *J. Virol.*, vol. 88, no. 15, pp. 8242–8255, Aug. 2014, doi: 10.1128/JVI.01164-14.
[122] B. F. Haynes *et al.*, 'Immune-correlates analysis of an HIV-1 vaccine efficacy trial.', *N. Engl. J. Med.*, vol. 366, no. 14, pp. 1275–1286, Apr. 2012, doi: 10.1056/NEJMoa1113425.
[123] R.-P. Sekaly, 'The failed HIV Merck vaccine study: a step back or a launching point for future vaccine development?', *J. Exp. Med.*, vol. 205, no. 1, pp. 7–12, Jan. 2008, doi: 10.1084/jem.20072681.
[124] J. K. Mann and T. Ndung'u, 'HIV-1 vaccine immunogen design strategies', *Virol. J.*, vol. 12, no. 1, p. 3, Jan. 2015, doi: 10.1186/s12985-014-0221-0.
[125] J. Brown, J.-L. Excler, and J. H. Kim, 'New prospects for a preventive HIV-1 vaccine', *J. Virus Erad.*, vol. 1, no. 2, pp. 78–88, Apr. 2015.
[126] M. Altfeld *et al.*, 'HLA Alleles Associated with Delayed Progression to AIDS Contribute Strongly to the Initial CD8(+) T Cell Response against HIV-1.', *PLoS Med.*, vol. 3, no. 10, p. e403, Oct. 2006, doi: 10.1371/journal.pmed.0030403.
[127] T. Harrer *et al.*, 'Strong cytotoxic T cell and weak neutralizing antibody responses in a subset of persons with stable nonprogressing HIV type 1 infection.', *AIDS Res. Hum. Retroviruses*, vol. 12, no. 7, pp. 585–592, May 1996, doi: 10.1089/aid.1996.12.585.
[128] B. Emu *et al.*, 'HLA class I-restricted T-cell responses may contribute to the control of human immunodeficiency virus infection, but such responses are not always necessary for long-term virus control.', *J. Virol.*, vol. 82, no. 11, pp. 5398–5407, Jun. 2008, doi: 10.1128/JVI.02176-07.
[129] S. P. Buchbinder *et al.*, 'Efficacy assessment of a cell-mediated immunity HIV-1 vaccine (the Step Study): a double-blind, randomised, placebo-controlled, test-of-concept trial.', *Lancet Lond. Engl.*, vol. 372, no. 9653, pp. 1881–1893, Nov. 2008, doi: 10.1016/S0140-6736(08)61591-3.
[130] G. E. Gray *et al.*, 'Safety and efficacy of the HVTN 503/Phambili study of a clade-B-based HIV-1 vaccine in South Africa: a double-blind, randomised, placebo-controlled test-of-concept phase 2b study.', *Lancet Infect. Dis.*, vol. 11, no. 7, pp. 507–515, Jul. 2011, doi: 10.1016/S1473-3099(11)70098-6.
[131] G. E. Gray *et al.*, 'Recombinant adenovirus type 5 HIV gag/pol/nef vaccine in South Africa: unblinded, long-term follow-up of the phase 2b HVTN 503/Phambili study.', *Lancet Infect. Dis.*, vol. 14, no. 5, pp. 388–396, May 2014, doi: 10.1016/S1473-3099(14)70020-9.

[132] M. Rolland *et al.*, 'Genetic impact of vaccination on breakthrough HIV-1 sequences from the STEP trial.', *Nat. Med.*, vol. 17, no. 3, pp. 366–371, Mar. 2011, doi: 10.1038/nm.2316.
[133] S. M. Hammer *et al.*, 'Efficacy trial of a DNA/rAd5 HIV-1 preventive vaccine.', *N. Engl. J. Med.*, vol. 369, no. 22, pp. 2083–2092, Nov. 2013, doi: 10.1056/NEJMoa1310566.
[134] A. C. deCamp *et al.*, 'Sieve analysis of breakthrough HIV-1 sequences in HVTN 505 identifies vaccine pressure targeting the CD4 binding site of Env-gp120.', *PloS One*, vol. 12, no. 11, p. e0185959, 2017, doi: 10.1371/journal.pone.0185959.
[135] J. H. Kim, J.-L. Excler, and N. L. Michael, 'Lessons from the RV144 Thai phase III HIV-1 vaccine trial and the search for correlates of protection.', *Annu. Rev. Med.*, vol. 66, pp. 423–437, 2015, doi: 10.1146/annurev-med-052912-123749.
[136] UNAIDS, 'HVTN 702 clinical trial of an HIV vaccine stopped', *UNAIDS*. https://www.unaids.org/en/resources/presscentre/pressreleaseandstatementarchive/2020/february/20200204_vaccine.
[137] T. Bradley *et al.*, 'Pentavalent HIV-1 vaccine protects against simian-human immunodeficiency virus challenge', *Nat. Commun.*, vol. 8, pp. 15711–15711, Jun. 2017, doi: 10.1038/ncomms15711.
[138] C. Morgan *et al.*, 'The Use of Nonhuman Primate Models in HIV Vaccine Development', *PLOS Med.*, vol. 5, no. 8, p. e173, Aug. 2008, doi: 10.1371/journal.pmed.0050173.
[139] R. M. Lynch, T. Yamamoto, and A. B. McDermott, 'HIV vaccine research and discovery in the nonhuman primates model: a unified theory in acquisition prevention and control of SIV infection', *Curr. Opin. HIV AIDS*, vol. 8, no. 4, pp. 288–294, Jul. 2013, doi: 10.1097/COH.0b013e328361cfe8.
[140] M. B. McChesney and C. J. Miller, 'New directions for HIV vaccine development from animal models', *Curr. Opin. HIV AIDS*, vol. 8, no. 5, pp. 376–381, Sep. 2013, doi: 10.1097/COH.0b013e328363d3a2.
[141] C. A. Derdeyn, P. L. Moore, and L. Morris, 'Development of broadly neutralizing antibodies from autologous neutralizing antibody responses in HIV infection.', *Curr. Opin. HIV AIDS*, vol. 9, no. 3, pp. 210–216, May 2014, doi: 10.1097/COH.0000000000000057.
[142] A. Piantadosi *et al.*, 'Breadth of neutralizing antibody response to human immunodeficiency virus type 1 is affected by factors early in infection but does not influence disease progression.', *J. Virol.*, vol. 83, no. 19, pp. 10269–10274, Oct. 2009, doi: 10.1128/JVI.01149-09.
[143] B. D. Weitzner, R. L. Dunbrack Jr, and J. J. Gray, 'The origin of CDR H3 structural diversity', *Struct. Lond. Engl. 1993*, vol. 23, no. 2, pp. 302–311, Feb. 2015, doi: 10.1016/j.str.2014.11.010.
[144] T. Mohan, Z. Berman, S.-M. Kang, and B.-Z. Wang, 'Sequential immunizations with a panel of HIV-1 Env virus-like particles coach immune system to make broadly neutralizing antibodies', *Sci. Rep.*, vol. 8, no. 1, pp. 7807–7807, May 2018, doi: 10.1038/s41598-018-25960-1.
[145] S. A. Brown *et al.*, 'Heterologous Prime-Boost HIV-1 Vaccination Regimens in Pre-Clinical and Clinical Trials', *Viruses*, vol. 2, no. 2, pp. 435–467, Feb. 2010, doi: 10.3390/v2020435.
[146] D. C. Malherbe *et al.*, 'Sequential immunization with a subtype B HIV-1 envelope quasispecies partially mimics the in vivo development of neutralizing antibodies', *J. Virol.*, vol. 85, no. 11, pp. 5262–5274, Jun. 2011, doi: 10.1128/JVI.02419-10.
[147] BioCell, 'Antibody Strucure', *Bio Cell*. https://bxcell.com/antibody-structure/.

[148] E. Kabat, T. T. Wu, and H. Bilofsky, ‘Unusual distributions of amino acids in complementarity determining (hypervariable) segments of heavy and light chains of immunoglobulins and their possible roles in specificity of antibody-combining sites’, *J. Biol. Chem.*, vol. 252, no. 19, pp. 6609–6616, 1977.
[149] K. Elgert D., *Immunology: Understanding the immune system.*, 2nd ed. Virginia: Wliley Blackwell, 1996.
[150] M. Dondelinger *et al.*, ‘Understanding the Significance and Implications of Antibody Numbering and Antigen-Binding Surface/Residue Definition’, *Front. Immunol.*, vol. 9, pp. 2278–2278, Oct. 2018, doi: 10.3389/fimmu.2018.02278.
[151] L. E. McCoy and D. R. Burton, ‘Identification and specificity of broadly neutralizing antibodies against HIV.’, *Immunol. Rev.*, vol. 275, no. 1, pp. 11–20, Jan. 2017, doi: 10.1111/imr.12484.
[152] X. Wu *et al.*, ‘Maturation and Diversity of the VRC01-Antibody Lineage over 15 Years of Chronic HIV-1 Infection’, *Cell*, vol. 161, no. 3, pp. 470–485, Apr. 2015, doi: 10.1016/j.cell.2015.03.004.
[153] M. Caskey *et al.*, ‘Viraemia suppressed in HIV-1-infected humans by broadly neutralizing antibody 3BNC117.’, *Nature*, vol. 522, no. 7557, pp. 487–491, Jun. 2015, doi: 10.1038/nature14411.
[154] M. Bonsignori *et al.*, ‘Antibody-virus co-evolution in HIV infection: paths for HIV vaccine development’, *Immunol. Rev.*, vol. 275, no. 1, pp. 145–160, Jan. 2017, doi: 10.1111/imr.12509.
[155] J.-P. Julien *et al.*, ‘Ablation of the complementarity-determining region H3 apex of the anti-HIV-1 broadly neutralizing antibody 2F5 abrogates neutralizing capacity without affecting core epitope binding’, *J. Virol.*, vol. 84, no. 9, pp. 4136–4147, 2010.
[156] E. M. Scherer, D. P. Leaman, M. B. Zwick, A. J. McMichael, and D. R. Burton, ‘Aromatic residues at the edge of the antibody combining site facilitate viral glycoprotein recognition through membrane interactions’, *Proc. Natl. Acad. Sci.*, vol. 107, no. 4, pp. 1529–1534, 2010.
[157] G. Ofek *et al.*, ‘Relationship between antibody 2F5 neutralization of HIV-1 and hydrophobicity of its heavy chain third complementarity-determining region’, *J. Virol.*, vol. 84, no. 6, pp. 2955–2962, 2010.
[158] S. M. Alam *et al.*, ‘Role of HIV membrane in neutralization by two broadly neutralizing antibodies’, *Proc. Natl. Acad. Sci.*, vol. 106, no. 48, pp. 20234–20239, 2009.
[159] T. M. Reichart *et al.*, ‘Trimerization of the HIV transmembrane domain in lipid bilayers modulates broadly neutralizing antibody binding’, *Angew. Chem. Int. Ed.*, vol. 55, no. 8, pp. 2688–2692, 2016.
[160] B. Chakrabarti *et al.*, ‘Direct antibody access to the HIV-1 membrane-proximal external region positively correlates with neutralization sensitivity’, *J. Virol.*, vol. 85, no. 16, pp. 8217–8226, 2011.
[161] G. Frey, H. Peng, S. Rits-Volloch, M. Morelli, Y. Cheng, and B. Chen, ‘A fusion-intermediate state of HIV-1 gp41 targeted by broadly neutralizing antibodies’, *Proc. Natl. Acad. Sci.*, vol. 105, no. 10, pp. 3739–3744, 2008.
[162] R. P. Lai *et al.*, ‘A fusion intermediate gp41 immunogen elicits neutralizing antibodies to HIV-1’, *J. Biol. Chem.*, vol. 289, no. 43, pp. 29912–29926, 2014.
[163] L. D. Williams *et al.*, ‘Potent and broad HIV-neutralizing antibodies in memory B cells and plasma’, *Sci. Immunol.*, vol. 2, no. 7, p. eaal2200, Jan. 2017, doi: 10.1126/sciimmunol.aal2200.

[164] J. Huang *et al.*, 'Broad and potent HIV-1 neutralization by a human antibody that binds the gp41-gp120 interface', *Nature*, vol. 515, no. 7525, pp. 138–142, Nov. 2014, doi: 10.1038/nature13601.
[165] D. Pinto *et al.*, 'Structural Basis for Broad HIV-1 Neutralization by the MPER-Specific Human Broadly Neutralizing Antibody LN01', *Cell Host Microbe*, vol. 26, no. 5, pp. 623-637.e8, Nov. 2019, doi: 10.1016/j.chom.2019.09.016.
[166] A. M. Trama *et al.*, 'HIV-1 envelope gp41 antibodies can originate from terminal ileum B cells that share cross-reactivity with commensal bacteria', *Cell Host Microbe*, vol. 16, no. 2, pp. 215–226, 2014.
[167] H.-X. Liao *et al.*, 'Initial antibodies binding to HIV-1 gp41 in acutely infected subjects are polyreactive and highly mutated', *J. Exp. Med.*, vol. 208, no. 11, pp. 2237–2249, 2011.
[168] D. R. Burton and L. Hangartner, 'Broadly neutralizing antibodies to HIV and their role in vaccine design', *Annu. Rev. Immunol.*, vol. 34, pp. 635–659, 2016.
[169] J. M. McCune *et al.*, 'Endoproteolytic cleavage of gp160 is required for the activation of human immunodeficiency virus.', *Cell*, vol. 53, no. 1, pp. 55–67, Apr. 1988, doi: 10.1016/0092-8674(88)90487-4.
[170] E. Falkowska *et al.*, 'Broadly neutralizing HIV antibodies define a glycan-dependent epitope on the prefusion conformation of gp41 on cleaved envelope trimers', *Immunity*, vol. 40, no. 5, pp. 657–668, 2014.
[171] C. Blattner *et al.*, 'Structural delineation of a quaternary, cleavage-dependent epitope at the gp41-gp120 interface on intact HIV-1 Env trimers', *Immunity*, vol. 40, no. 5, pp. 669–680, 2014.
[172] P. D. Kwong, R. Wyatt, J. Robinson, R. W. Sweet, J. Sodroski, and W. A. Hendrickson, 'Structure of an HIV gp120 envelope glycoprotein in complex with the CD4 receptor and a neutralizing human antibody.', *Nature*, vol. 393, no. 6686, pp. 648–659, Jun. 1998, doi: 10.1038/31405.
[173] H.-X. Liao *et al.*, 'Co-evolution of a broadly neutralizing HIV-1 antibody and founder virus.', *Nature*, vol. 496, no. 7446, pp. 469–476, Apr. 2013, doi: 10.1038/nature12053.
[174] X. Wu, T. Zhou, S. O'Dell, R. T. Wyatt, P. D. Kwong, and J. R. Mascola, 'Mechanism of human immunodeficiency virus type 1 resistance to monoclonal antibody B12 that effectively targets the site of CD4 attachment', *J. Virol.*, vol. 83, no. 21, pp. 10892–10907, Nov. 2009, doi: 10.1128/JVI.01142-09.
[175] L. Kong *et al.*, 'Supersite of immune vulnerability on the glycosylated face of HIV-1 envelope glycoprotein gp120', *Nat. Struct. Mol. Biol.*, vol. 20, no. 7, p. 796, 2013.
[176] A. Trkola *et al.*, 'Human monoclonal antibody 2G12 defines a distinctive neutralization epitope on the gp120 glycoprotein of human immunodeficiency virus type 1.', *J. Virol.*, vol. 70, no. 2, pp. 1100–1108, Feb. 1996.
[177] A. Trkola *et al.*, 'Cross-clade neutralization of primary isolates of human immunodeficiency virus type 1 by human monoclonal antibodies and tetrameric CD4-IgG.', *J. Virol.*, vol. 69, no. 11, pp. 6609–6617, 1995.
[178] R. W. Sanders *et al.*, 'The Mannose-Dependent Epitope for Neutralizing Antibody 2G12 on Human Immunodeficiency Virus Type 1 Glycoprotein gp120', *J. Virol.*, vol. 76, no. 14, p. 7293, Jul. 2002, doi: 10.1128/JVI.76.14.7293-7305.2002.
[179] C. Wibmer, P. Moore, and L. Morris, 'HIV broadly neutralizing antibody targets', *Curr. Opin. HIV AIDS*, vol. 10, Mar. 2015, doi: 10.1097/COH.0000000000000153.

[180] D. Lyumkis *et al.*, 'Cryo-EM structure of a fully glycosylated soluble cleaved HIV-1 envelope trimer.', *Science*, vol. 342, no. 6165, pp. 1484–1490, Dec. 2013, doi: 10.1126/science.1245627.
[181] A. Bartesaghi, A. Merk, M. J. Borgnia, J. L. S. Milne, and S. Subramaniam, 'Prefusion structure of trimeric HIV-1 envelope glycoprotein determined by cryo-electron microscopy.', *Nat. Struct. Mol. Biol.*, vol. 20, no. 12, pp. 1352–1357, Dec. 2013, doi: 10.1038/nsmb.2711.
[182] J. S. McLellan *et al.*, 'Structure of HIV-1 gp120 V1/V2 domain with broadly neutralizing antibody PG9.', *Nature*, vol. 480, no. 7377, pp. 336–343, Nov. 2011, doi: 10.1038/nature10696.
[183] N. A. Doria-Rose *et al.*, 'Developmental pathway for potent V1V2-directed HIV-neutralizing antibodies.', *Nature*, vol. 509, no. 7498, pp. 55–62, May 2014, doi: 10.1038/nature13036.
[184] L. M. Walker *et al.*, 'Broad and potent neutralizing antibodies from an African donor reveal a new HIV-1 vaccine target.', *Science*, vol. 326, no. 5950, pp. 285–289, Oct. 2009, doi: 10.1126/science.1178746.
[185] J.-P. Julien *et al.*, 'Asymmetric recognition of the HIV-1 trimer by broadly neutralizing antibody PG9.', *Proc. Natl. Acad. Sci. U. S. A.*, vol. 110, no. 11, pp. 4351–4356, Mar. 2013, doi: 10.1073/pnas.1217537110.
[186] R. Loving, M. Sjoberg, S.-R. Wu, J. M. Binley, and H. Garoff, 'Inhibition of the HIV-1 spike by single-PG9/16-antibody binding suggests a coordinated-activation model for its three protomeric units.', *J. Virol.*, vol. 87, no. 12, pp. 7000–7007, Jun. 2013, doi: 10.1128/JVI.00530-13.
[187] N. A. Doria-Rose *et al.*, 'A short segment of the HIV-1 gp120 V1/V2 region is a major determinant of resistance to V1/V2 neutralizing antibodies.', *J. Virol.*, vol. 86, no. 15, pp. 8319–8323, Aug. 2012, doi: 10.1128/JVI.00696-12.
[188] S. C. Harrison, 'Viral membrane fusion.', *Nat. Struct. Mol. Biol.*, vol. 15, no. 7, pp. 690–698, Jul. 2008, doi: 10.1038/nsmb.1456.
[189] P. M. Colman and M. C. Lawrence, 'The structural biology of type I viral membrane fusion.', *Nat. Rev. Mol. Cell Biol.*, vol. 4, no. 4, pp. 309–319, Apr. 2003, doi: 10.1038/nrm1076.
[190] R. Kong *et al.*, 'Fusion peptide of HIV-1 as a site of vulnerability to neutralizing antibody.', *Science*, vol. 352, no. 6287, pp. 828–833, May 2016, doi: 10.1126/science.aae0474.
[191] M. Pancera *et al.*, 'Structure and immune recognition of trimeric pre-fusion HIV-1 Env.', *Nature*, vol. 514, no. 7523, pp. 455–461, Oct. 2014, doi: 10.1038/nature13808.
[192] Y. D. Kwon *et al.*, 'Crystal structure, conformational fixation and entry-related interactions of mature ligand-free HIV-1 Env.', *Nat. Struct. Mol. Biol.*, vol. 22, no. 7, pp. 522–531, Jul. 2015, doi: 10.1038/nsmb.3051.
[193] B. Korber *et al.*, 'Timing the ancestor of the HIV-1 pandemic strains.', *Science*, vol. 288, no. 5472, pp. 1789–1796, Jun. 2000, doi: 10.1126/science.288.5472.1789.
[194] R. Wyatt *et al.*, 'The antigenic structure of the HIV gp120 envelope glycoprotein.', *Nature*, vol. 393, no. 6686, pp. 705–711, Jun. 1998, doi: 10.1038/31514.
[195] D. C. Douek, P. D. Kwong, and G. J. Nabel, 'The rational design of an AIDS vaccine', *Cell*, vol. 124, no. 4, pp. 677–681, 2006.
[196] P. D. Kwong, J. R. Mascola, and G. J. Nabel, 'Rational design of vaccines to elicit broadly neutralizing antibodies to HIV-1', *Cold Spring Harb. Perspect. Med.*, vol. 1, no. 1, pp. a007278–a007278, Sep. 2011, doi: 10.1101/cshperspect.a007278.

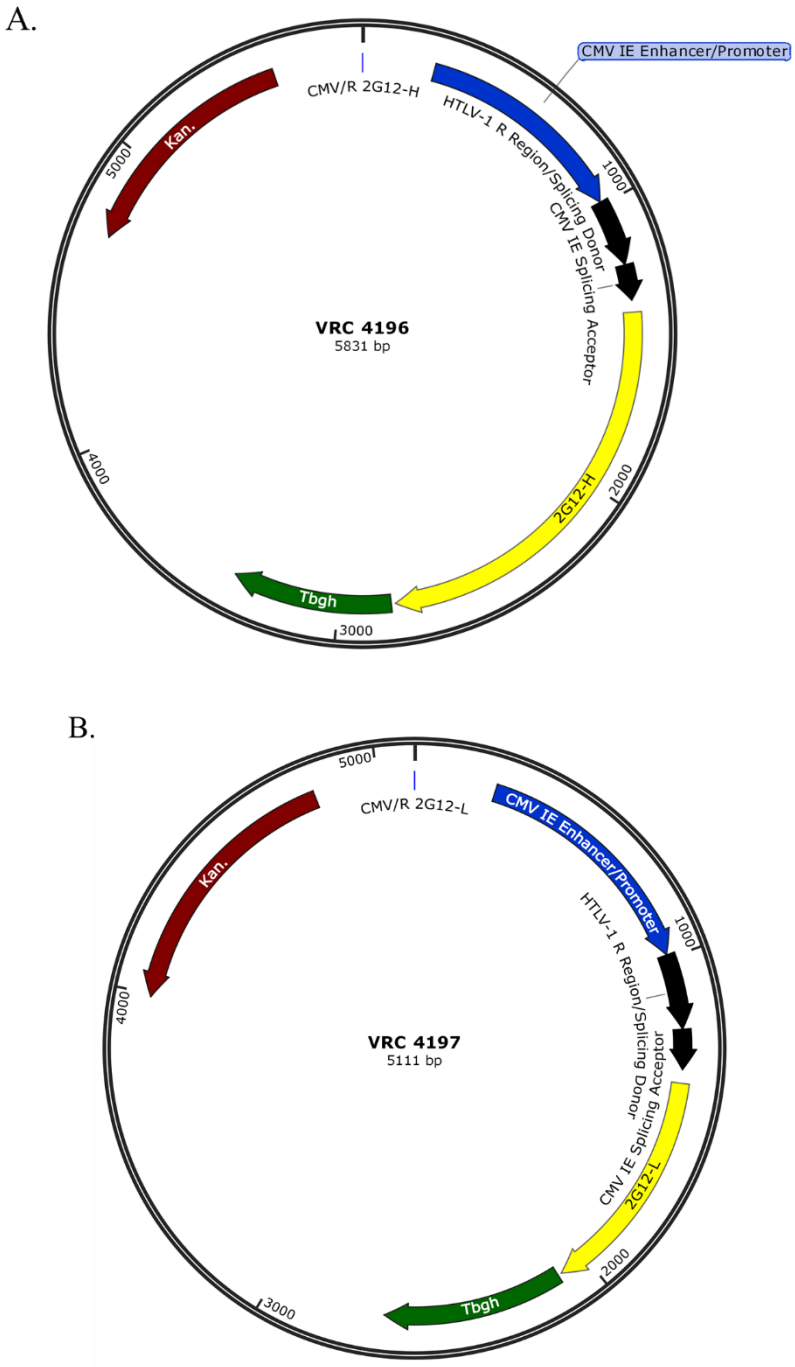
[197] J. M. Binley *et al.*, 'A recombinant human immunodeficiency virus type 1 envelope glycoprotein complex stabilized by an intermolecular disulfide bond between the gp120 and gp41 subunits is an antigenic mimic of the trimeric virion-associated structure', *J. Virol.*, vol. 74, no. 2, pp. 627–643, 2000.
[198] R. W. Sanders *et al.*, 'Variable-loop-deleted variants of the human immunodeficiency virus type 1 envelope glycoprotein can be stabilized by an intermolecular disulfide bond between the gp120 and gp41 subunits', *J. Virol.*, vol. 74, no. 11, pp. 5091–5100, 2000.
[199] R. Khayat *et al.*, 'Structural characterization of cleaved, soluble HIV-1 envelope glycoprotein trimers.', *J. Virol.*, vol. 87, no. 17, pp. 9865–9872, Sep. 2013, doi: 10.1128/JVI.01222-13.
[200] A. B. Ward and I. A. Wilson, 'The HIV-1 envelope glycoprotein structure: Nailing down a moving target', *Immunol. Rev.*, vol. 275, no. 1, pp. 21–32, 2017.
[201] K. Sliepen *et al.*, 'Presenting native-like HIV-1 envelope trimers on ferritin nanoparticles improves their immunogenicity.', *Retrovirology*, vol. 12, p. 82, Sep. 2015, doi: 10.1186/s12977-015-0210-4.
[202] R. W. Sanders *et al.*, 'HIV-1 neutralizing antibodies induced by native-like envelope trimers', *Science*, vol. 349, no. 6244, p. aac4223, Jul. 2015, doi: 10.1126/science.aac4223.
[203] M. Pauthner *et al.*, 'Elicitation of robust tier 2 neutralizing antibody responses in nonhuman primates by HIV envelope trimer immunization using optimized approaches', *Immunity*, vol. 46, no. 6, pp. 1073–1088, 2017.
[204] L. Devico *et al.*, 'Monoclonal antibodies raised against covalently crosslinked complexes of human immunodeficiency virus type 1 gp120 and CD4 receptor identify a novel complex-dependent epitope on gp120', *Virology*, vol. 211, no. 2, pp. 583–588, 1995.
[205] A. DeVico *et al.*, 'Antibodies to CD4-induced sites in HIV gp120 correlate with the control of SHIV challenge in macaques vaccinated with subunit immunogens', *Proc. Natl. Acad. Sci.*, vol. 104, no. 44, pp. 17477–17482, 2007.
[206] T. Fouts *et al.*, 'Crosslinked HIV-1 envelope-CD4 receptor complexes elicit broadly cross-reactive neutralizing antibodies in rhesus macaques', *Proc. Natl. Acad. Sci. U. S. A.*, vol. 99, no. 18, pp. 11842–11847, Sep. 2002, doi: 10.1073/pnas.182412199.
[207] T. R. Fouts *et al.*, 'Expression and characterization of a single-chain polypeptide analogue of the human immunodeficiency virus type 1 gp120-CD4 receptor complex.', *J. Virol.*, vol. 74, no. 24, pp. 11427–11436, Dec. 2000, doi: 10.1128/jvi.74.24.11427-11436.2000.
[208] G. Martin *et al.*, 'Stabilization of HIV-1 envelope in the CD4-bound conformation through specific cross-linking of a CD4 mimetic.', *J. Biol. Chem.*, vol. 286, no. 24, pp. 21706–21716, Jun. 2011, doi: 10.1074/jbc.M111.232272.
[209] R. Varadarajan *et al.*, 'Characterization of gp120 and its single-chain derivatives, gp120-CD4D12 and gp120-M9: implications for targeting the CD4i epitope in human immunodeficiency virus vaccine design', *J. Virol.*, vol. 79, no. 3, pp. 1713–1723, Feb. 2005, doi: 10.1128/JVI.79.3.1713-1723.2005.
[210] A. K. Dey *et al.*, 'Elicitation of neutralizing antibodies directed against CD4-induced epitope (s) using a CD4 mimetic cross-linked to a HIV-1 envelope glycoprotein', *PLoS One*, vol. 7, no. 1, 2012.
[211] E. T. Crooks *et al.*, 'Vaccine-Elicited Tier 2 HIV-1 Neutralizing Antibodies Bind to Quaternary Epitopes Involving Glycan-Deficient Patches Proximal to the CD4 Binding Site.', *PLoS Pathog.*, vol. 11, no. 5, p. e1004932, May 2015, doi: 10.1371/journal.ppat.1004932.

[212] X. Wei *et al.*, 'Antibody neutralization and escape by HIV-1.', *Nature*, vol. 422, no. 6929, pp. 307–312, Mar. 2003, doi: 10.1038/nature01470.
[213] J. M. Decker *et al.*, 'Antigenic conservation and immunogenicity of the HIV coreceptor binding site.', *J. Exp. Med.*, vol. 201, no. 9, pp. 1407–1419, May 2005, doi: 10.1084/jem.20042510.
[214] K. Salzwedel, E. D. Smith, B. Dey, and E. A. Berger, 'Sequential CD4-coreceptor interactions in human immunodeficiency virus type 1 Env function: soluble CD4 activates Env for coreceptor-dependent fusion and reveals blocking activities of antibodies against cryptic conserved epitopes on gp120.', *J. Virol.*, vol. 74, no. 1, pp. 326–333, Jan. 2000, doi: 10.1128/jvi.74.1.326-333.2000.
[215] S.-H. Xiang, N. Doka, R. K. Choudhary, J. Sodroski, and J. E. Robinson, 'Characterization of CD4-induced epitopes on the HIV type 1 gp120 envelope glycoprotein recognized by neutralizing human monoclonal antibodies', *AIDS Res. Hum. Retroviruses*, vol. 18, no. 16, pp. 1207–1217, 2002.
[216] C. D. Rizzuto *et al.*, 'A conserved HIV gp120 glycoprotein structure involved in chemokine receptor binding', *Science*, vol. 280, no. 5371, pp. 1949–1953, 1998.
[217] M. A. Killick, M. L. Grant, N. M. Cerutti, A. Capovilla, and M. A. Papathanasopoulos, 'Env–2dCD4S60C complexes act as super immunogens and elicit potent, broadly neutralizing antibodies against clinically relevant human immunodeficiency virus type 1 (HIV-1)', *Vaccine*, vol. 33, no. 46, pp. 6298–6306, Nov. 2015, doi: 10.1016/j.vaccine.2015.09.056.
[218] N. Cerutti *et al.*, 'Stabilization of HIV-1 gp120-CD4 receptor complex through targeted interchain disulfide exchange', *J. Biol. Chem.*, vol. 285, no. 33, pp. 25743–25752, Aug. 2010, doi: 10.1074/jbc.M110.144121.
[219] M. Killick, A. Capovilla, and M. A. Papathanasopoulos, 'Generation and characterization of an HIV-1 subtype C transmitted and early founder virus consensus sequence', *AIDS Res. Hum. Retroviruses*, vol. 30, no. 10, pp. 1001–1005, Oct. 2014, doi: 10.1089/AID.2014.0042.
[220] T. Moshette, S. A. Ali, M. A. Killick, and M. A. Papathanasopoulos, 'Engineering and characterising a novel, highly potent bispecific antibody iMab-CAP256 that targets HIV-1.', *Retrovirology.*, vol. 16, no. 1, p. 31, Nov. 2019, doi: 10.1186/s12977-019-0493-y.
[221] F. Wegmann *et al.*, 'The Carbomer-Lecithin Adjuvant Adjuplex Has Potent Immunoactivating Properties and Elicits Protective Adaptive Immunity against Influenza Virus Challenge in Mice', *Clin. Vaccine Immunol.*, vol. 22, no. 9, p. 1004, Sep. 2015, doi: 10.1128/CVI.00736-14.
[222] D. Montefiori C., 'Standardized Assessments of Neutralizing Antibodies for HIV/AIDS Vaccine Development.', *Los Alamos HIV Database*. https://www.hiv.lanl.gov/content/nab-reference-strains/html/home.htm.
[223] D. O. Starkie, J. E. Compson, S. Rapecki, and D. J. Lightwood, 'Generation of Recombinant Monoclonal Antibodies from Immunised Mice and Rabbits via Flow Cytometry and Sorting of Antigen-Specific IgG+ Memory B Cells', *PloS One*, vol. 11, no. 3, pp. e0152282–e0152282, Mar. 2016, doi: 10.1371/journal.pone.0152282.
[224] M. Bruggemann, J. Free, A. Diamond, J. Howard, S. Cobbold, and H. Waldmann, 'Immunoglobulin heavy chain locus of the rat: striking homology to mouse antibody genes.', *Proc. Natl. Acad. Sci. U. S. A.*, vol. 83, no. 16, pp. 6075–6079, Aug. 1986, doi: 10.1073/pnas.83.16.6075.
[225] M. Bruggemann, 'Evolution of the rat immunoglobulin gamma heavy-chain gene family.', *Gene*, vol. 74, no. 2, pp. 473–482, Dec. 1988, doi: 10.1016/0378-1119(88)90180-1.

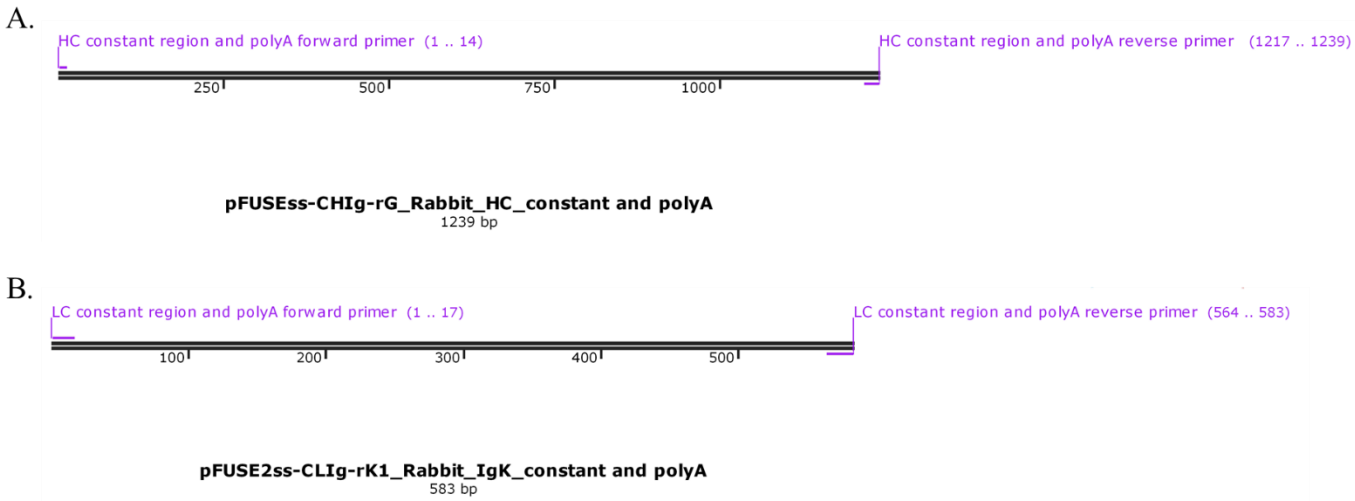
[226] N. A. Shevchuk, A. V. Bryksin, Y. A. Nusinovich, F. C. Cabello, M. Sutherland, and S. Ladisch, 'Construction of long DNA molecules using long PCR-based fusion of several fragments simultaneously', *Nucleic Acids Res.*, vol. 32, no. 2, pp. e19–e19, Jan. 2004, doi: 10.1093/nar/gnh014.
[227] O. Boussif *et al.*, 'A versatile vector for gene and oligonucleotide transfer into cells in culture and in vivo: polyethylenimine.', *Proc. Natl. Acad. Sci. U. S. A.*, vol. 92, no. 16, pp. 7297–7301, Aug. 1995, doi: 10.1073/pnas.92.16.7297.
[228] N. D. Sonawane, F. C. J. Szoka, and A. S. Verkman, 'Chloride accumulation and swelling in endosomes enhances DNA transfer by polyamine-DNA polyplexes.', *J. Biol. Chem.*, vol. 278, no. 45, pp. 44826–44831, Nov. 2003, doi: 10.1074/jbc.M308643200.
[229] N.-H. Lee, J.-A. Lee, S.-Y. Park, C.-S. Song, I.-S. Choi, and J.-B. Lee, 'A review of vaccine development and research for industry animals in Korea', *Clin. Exp. Vaccine Res.*, vol. 1, no. 1, pp. 18–34, Jul. 2012, doi: 10.7774/cevr.2012.1.1.18.
[230] B. D. Walker and B. T. Korber, 'Immune control of HIV: the obstacles of HLA and viral diversity.', *Nat. Immunol.*, vol. 2, no. 6, pp. 473–475, Jun. 2001, doi: 10.1038/88656.
[231] B. Gaschen *et al.*, 'Diversity considerations in HIV-1 vaccine selection.', *Science*, vol. 296, no. 5577, pp. 2354–2360, Jun. 2002, doi: 10.1126/science.1070441.
[232] Y. Li *et al.*, 'Broad HIV-1 neutralization mediated by CD4-binding site antibodies.', *Nat. Med.*, vol. 13, no. 9, pp. 1032–1034, Sep. 2007, doi: 10.1038/nm1624.
[233] C. DeLisi and J. R. Hiernaux, *Regulation of Immune Response Dynamics*, vol. 1. CRC Press, 2019.
[234] M. K. Slifka and I. J. Amanna, 'Role of Multivalency and Antigenic Threshold in Generating Protective Antibody Responses', *Front. Immunol.*, vol. 10, pp. 956–956, May 2019, doi: 10.3389/fimmu.2019.00956.
[235] G. E. Gray *et al.*, 'Subtype C gp140 Vaccine Boosts Immune Responses Primed by the South African AIDS Vaccine Initiative DNA-C2 and MVA-C HIV Vaccines after More than a 2-Year Gap', *Clin. Vaccine Immunol. CVI*, vol. 23, no. 6, pp. 496–506, Jun. 2016, doi: 10.1128/CVI.00717-15.
[236] G. Churchyard *et al.*, 'Sequential Immunization with gp140 Boosts Immune Responses Primed by Modified Vaccinia Ankara or DNA in HIV-Uninfected South African Participants', *PLOS ONE*, vol. 11, no. 9, p. e0161753, Sep. 2016, doi: 10.1371/journal.pone.0161753.
[237] G. J. Churchyard *et al.*, 'A phase IIA randomized clinical trial of a multiclade HIV-1 DNA prime followed by a multiclade rAd5 HIV-1 vaccine boost in healthy adults (HVTN204).', *PloS One*, vol. 6, no. 8, p. e21225, 2011, doi: 10.1371/journal.pone.0021225.
[238] Z. Ditse *et al.*, 'Effect of HIV Envelope Vaccination on the Subsequent Antibody Response to HIV Infection', *mSphere*, vol. 5, no. 1, pp. e00738-19, Feb. 2020, doi: 10.1128/mSphere.00738-19.
[239] P. Spearman *et al.*, 'Rapid Boosting of HIV-1 Neutralizing Antibody Responses in Humans Following a Prolonged Immunologic Rest Period', *J. Infect. Dis.*, vol. 219, no. 11, pp. 1755–1765, Jan. 2019, doi: 10.1093/infdis/jiz008.
[240] P. J. Klasse *et al.*, 'Sequential and Simultaneous Immunization of Rabbits with HIV-1 Envelope Glycoprotein SOSIP.664 Trimers from Clades A, B and C', *PLoS Pathog.*, vol. 12, no. 9, pp. e1005864–e1005864, Sep. 2016, doi: 10.1371/journal.ppat.1005864.
[241] D. Sehgal, H. Obiakor, and R. G. Mage, 'Distinct Clonal Ig Diversification Patterns in Young Appendix Compared to Antigen-Specific Splenic Clones', *J. Immunol.*, vol. 168, no. 11, p. 5424, Jun. 2002, doi: 10.4049/jimmunol.168.11.5424.

[242] D. Lanning, P. Sethupathi, K. J. Rhee, S. K. Zhai, and K. L. Knight, 'Intestinal microflora and diversification of the rabbit antibody repertoire.', *J. Immunol. Baltim. Md 1950*, vol. 165, no. 4, pp. 2012–2019, Aug. 2000, doi: 10.4049/jimmunol.165.4.2012.
[243] K.-J. Rhee, P. J. Jasper, P. Sethupathi, M. Shanmugam, D. Lanning, and K. L. Knight, 'Positive selection of the peripheral B cell repertoire in gut-associated lymphoid tissues', *J. Exp. Med.*, vol. 201, no. 1, pp. 55–62, Jan. 2005, doi: 10.1084/jem.20041849.
[244] S. E. Townsend, C. C. Goodnow, and R. J. Cornall, 'Single epitope multiple staining to detect ultralow frequency B cells.', *J. Immunol. Methods*, vol. 249, no. 1–2, pp. 137–146, Mar. 2001, doi: 10.1016/s0022-1759(00)00352-5.
[245] M. F. Stinski and H. Isomura, 'Role of the cytomegalovirus major immediate early enhancer in acute infection and reactivation from latency', *Med. Microbiol. Immunol. (Berl.)*, vol. 197, no. 2, pp. 223–231, Jun. 2008, doi: 10.1007/s00430-007-0069-7.
[246] P. D. Ray and R. C. Fry, 'Chapter 2 - The Cell: The Fundamental Unit in Systems Biology', in *Systems Biology in Toxicology and Environmental Health*, R. C. Fry, Ed. Boston: Academic Press, 2015, pp. 11–42.
[247] A. Buchacher *et al.*, 'Generation of human monoclonal antibodies against HIV-1 proteins; electrofusion and Epstein-Barr virus transformation for peripheral blood lymphocyte immortalization.', *AIDS Res. Hum. Retroviruses*, vol. 10, no. 4, pp. 359–369, Apr. 1994, doi: 10.1089/aid.1994.10.359.
[248] C. N. Scanlan *et al.*, 'The Broadly Neutralizing Anti-Human Immunodeficiency Virus Type 1 Antibody 2G12 Recognizes a Cluster of α1→2 Mannose Residues on the Outer Face of gp120', *J. Virol.*, vol. 76, no. 14, p. 7306, Jul. 2002, doi: 10.1128/JVI.76.14.7306-7321.2002.
[249] D. A. Calarese *et al.*, 'Antibody Domain Exchange Is an Immunological Solution to Carbohydrate Cluster Recognition', *Science*, vol. 300, no. 5628, p. 2065, Jun. 2003, doi: 10.1126/science.1083182.
[250] E. S. Gray, T. Meyers, G. Gray, D. C. Montefiori, and L. Morris, 'Insensitivity of Paediatric HIV-1 Subtype C Viruses to Broadly Neutralising Monoclonal Antibodies Raised against Subtype B', *PLOS Med.*, vol. 3, no. 7, p. e255, Jul. 2006, doi: 10.1371/journal.pmed.0030255.
[251] R. Bures *et al.*, 'Regional clustering of shared neutralization determinants on primary isolates of clade C human immunodeficiency virus type 1 from South Africa', *J. Virol.*, vol. 76, no. 5, pp. 2233–2244, 2002.
[252] A. Irimia *et al.*, 'Lipid interactions and angle of approach to the HIV-1 viral membrane of broadly neutralizing antibody 10E8: Insights for vaccine and therapeutic design', *PLoS Pathog.*, vol. 13, no. 2, p. e1006212, 2017.
[253] E. Rujas *et al.*, 'Structural basis for broad neutralization of HIV-1 through the molecular recognition of 10E8 helical epitope at the membrane interface', *Sci. Rep.*, vol. 6, p. 38177, 2016.

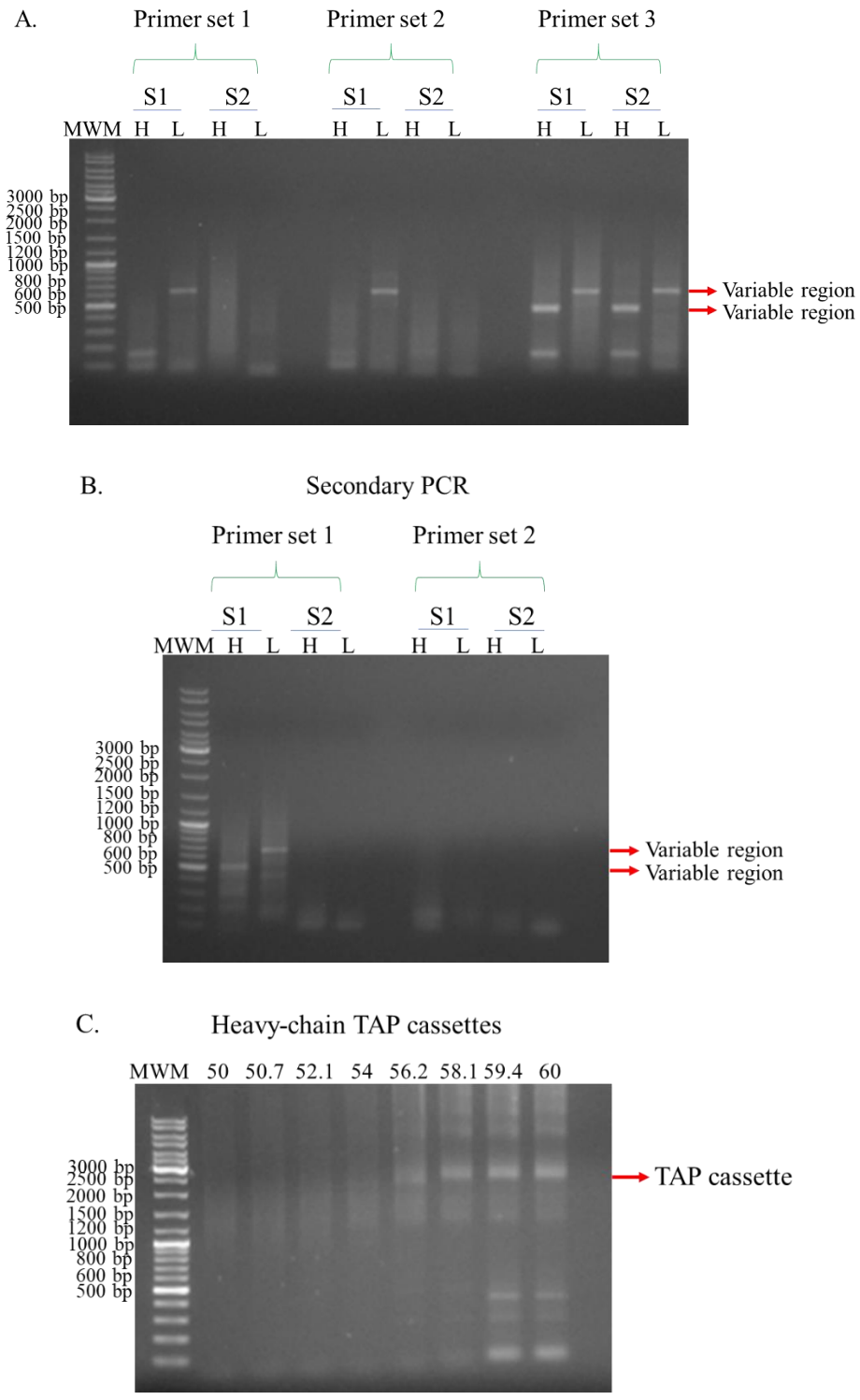
Appendix A: Supplementary figures



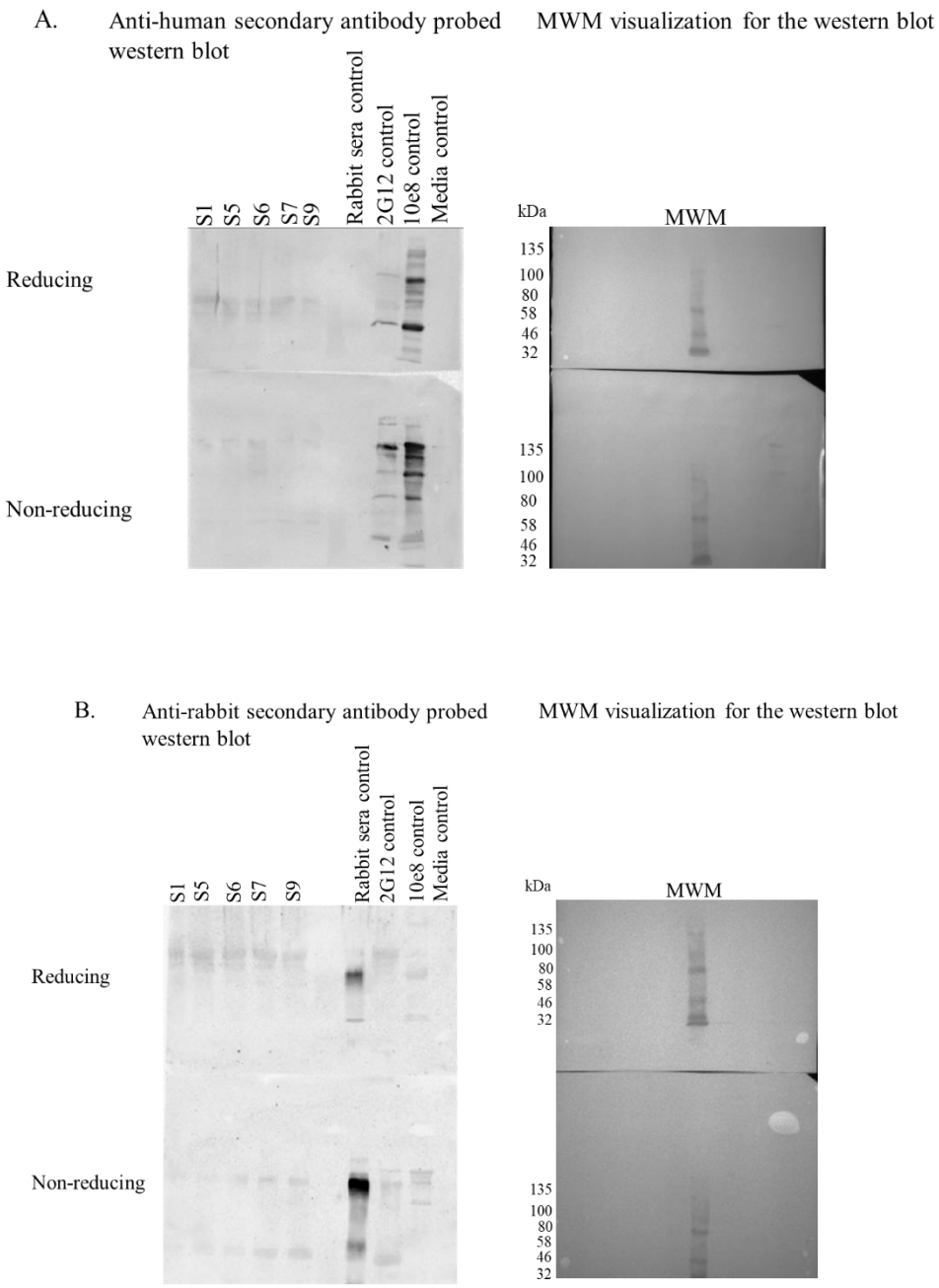
Supplementary Figure 1: The VRC_4196 and VRC_4197 plasmid vector maps. The VRC_4196 plasmid vector used for the expression of the 2g12 antibody heavy-chain (A), and VRC_4197 for the expression of 2g12 antibody light-chain (B). These plasmid vectors were used for the expression of 2g12 antibodies by mammalian co-transfections.



Supplementary Figure 2: The heavy- and light-chain constant and polyA fragments inserts for the plasmid vectors. The rabbit heavy-chain constant and polyA fragments (A), and the rabbit light-chain constant and poly A fragments (B), were synthesized into plasmid vectors by GeneArt.



Supplementary Figure 3: Optimisation of PCR protocols for the primary PCR reaction. Different primer sets were used to determine which would successfully amplify the variable regions in the primary PCR (A). One of the optimizations for the secondary PCR was to determine which primer sets would work best (B). A gradient PCR was performed for the tertiary PCR for the optimization of the annealing temperature (degrees Celsius ℃) (C). Multiple optimization steps were followed for each PCR step for the generation of the best possible PCR product.



Supplementary Figure 4: Western blots used for confirmation of antibody expression. The reducing and non-reducing western blots probed with the anti-human secondary antibody for the detection of 2G12 expression and the respective MWM visualized under white light (A). The western blots probed with an anti-rabbit secondary antibody under reducing and non-reducing conditions for the detection of rabbit monoclonal antibody expression by the TAP cassettes, and the respective MWM visualized under white light (B). The molecular weight marker (MWM) corresponds to the pre-stained broad range protein marker (New England Biolabs, MA, USA). Sizes are indicated in kiloDaltons (kDa).

Appendix B: Human Ethics waiver

UNIVERSITY OF THE WITWATERSRAND, JOHANNESBURG

HUMAN RESEARCH ETHICS COMMITTEE (MEDICAL

Human Research Ethics Committee (Medical)

Research Office Secretariat:
Faculty of Health Sciences, Phillip Tobias Building, 3rd Floor, Office 301/2/4, 29 Princess of Wales Terrace, Parktown, 2193
Tel +27 (0)11-717-1252 /1234/2656/2700
Private Bag 3, Wits 2050
Office email: HREC-Medical.ResearchOffice@wits.ac.za
Website: www.wits.ac.za/research/about-our-research/ethics-and-research-integrity/

Ref: W-CBP-180802-2 02/08/2018

TO WHOM IT MAY CONCERN:

Waiver: This certifies that the following research does not require clearance from the Human Research Ethics Committee (Medical)

Investigator: Miss Simone Smith (student no. 806594)

Supervisor: Prof Maria Papathanasopoulos

Department: Molecular Medicine and Haematology

Project title: Isolation and characterization of HIV-1-specific monoclonal antibodies from immunized rabbits

Reason: Laboratory analysis. The research will include extraction of antibodies from rabbit blood cells. The proteins will be expressed in mammalian cell lines. No human participants will be involved in the study.

CB Penny

Professor CB Penny

Chairperson: Human Research Ethics Committee (Medical)

Copy – HREC (Medical) Secretariat: Zanele Ndlovu, Charmaine Khumalo and Rhulani Mkansi.

Appendix C: Animal ethics approval

AESC 2017 M&E

Please note that only typewritten applications will be accepted.

UNIVERSITY OF THE WITWATERSRAND

ANIMAL ETHICS SCREENING COMMITTEE
MODIFICATIONS AND EXTENSIONS TO EXPERIMENTS

a. Name: Maria Papathanasopoulos

b. Department: Molecular Medicine and Haematology

c. Experiment to be modified / extended

		AESC NO		
Original AESC number	2014	51	B	
Other M&Es : Approved 27 November 2014, additional 6 animals Approved 8 April 2015, Re-allocation of 3 rabbits Approved 25 October 2017, extension of project for isolation of antibodies				3

d. Project Title: Immunogenicity of novel Indian and South African HIV-1 vaccine immunogens in New Zealand White rabbits and evaluation of anti HIV-1 immune responses.

		No.	Species
e.	Number and species of animals originally approved:	48	*New Zealand White Rabbits*
f.	Number of additional animals previously allocated on M&Es:	6	New Zealand White Rabbits
g.	Total number of animals allocated to the experiment to date:	54	New Zealand White Rabbits
h.	Number of animals used to date:	51	New Zealand White Rabbits

i. Specific modification / extension requested:

Appointment of additional co-workers on the project:

Miss Simone Smith – MSc Student – student number 806584

Mrs Nancy Meulenberg – Wits Staff member – staff number A0045584

j. Motivation for modification / extension:

Motivational for additional co-workers:

The proposed work on the three remaining rabbits will form part of Miss Simone Smith's MSc project, entitled "Isolation and characterization of novel, broadly neutralizing antibodies from rabbits immunized with the HIV-1 Env/2dCD4^{S60C} immune complex." Miss Smith will be co-supervised by Mrs Nancy Meulenberg (request for inclusion as an additional co-worker in this application), Dr Mark Killick and myself.

AESC 2017 M&E

Date: 8 March 2018

Signature:

RECOMMENDATIONS

Date: 9th MARCH 2018

Signature:

Chairman, AESC

References

(Seeber et al., 2014, Starkie et al., 2016)SEEBER, S., ROS, F., THOREY, I., TIEFENTHALER, G., KALUZA, K., LIFKE, V., FISCHER, J. A., KLOSTERMANN, S., ENDL, J., KOPETZKI, E., PASHINE, A., SIEWE, B., KALUZA, B., PLATZER, J. & OFFNER, S. 2014. A robust high throughput platform to generate functional recombinant monoclonal antibodies using rabbit B cells from peripheral blood. *PLoS One,* 9, e86184.

STARKIE, D. O., COMPSON, J. E., RAPECKI, S. & LIGHTWOOD, D. J. 2016. Generation of Recombinant Monoclonal Antibodies from Immunised Mice and Rabbits via Flow Cytometry and Sorting of Antigen-Specific IgG+ Memory B Cells. *PLoS One,* 11, e0152282.

AESC 2017 M&E

Please note that only typewritten applications will be accepted.

UNIVERSITY OF THE WITWATERSRAND

ANIMAL ETHICS SCREENING COMMITTEE

MODIFICATIONS AND EXTENSIONS TO EXPERIMENTS

a. Name: Maria Papathanasopoulos

b. Department: Molecular Medicine and Haematology

c. Experiment to be modified / extended

			AESC NO
Original AESC number	**2014**	**51**	**B**
Other M&Es : Approved 27 November 2014, additional 6 animals Approved 8 April 2015, Re-allocation of 3 rabbits Approved 29 June 2016, Additional immunizations and blood collections Approved 25 October 2017, extension of project for isolation of antibodies Approved 9th March 2018, Addition of co-workers			5

d. Project Title: Immunogenicity of novel Indian and South African HIV-1 vaccine immunogens in New Zealand White rabbits and evaluation of anti HIV-1 immune responses.

		No.	**Species**
e.	Number and species of animals originally approved:	48	*New Zealand White Rabbits*
f.	Number of additional animals previously allocated on M&Es:	6	New Zealand White Rabbits
g.	Total number of animals allocated to the experiment to date:	54	New Zealand White Rabbits
h.	Number of animals used to date:	51	New Zealand White Rabbits

i. Specific modification / extension requested:

Request for time extension on existing M&E approved 25 October 2017

We would like to apply for time extension on the existing M&E approved on the 25 October 2017, until the end of this year (21 December 2018) for the isolation and characterisation of HIV-1 neutralizing antibodies from these three rabbits. The protocol is unchanged from that proposal in the said M&E and methodology excerpt is included below:

"the antibody titre in the three remaining rabbits may need to boosted by additional vaccination. Rabbits will be immunized using the identical immunogen and immunization protocol briefly; 40 µg of CAP45 gp140GCN4(+)/2dCD4S60C complex, formulated in Adjuplex/PBS suspension and administered intramuscularly (Final volume 500 µl). Approximately 10mls of blood (EDTA tube) will be drawn 2 weeks post immunization, sera will be screened in vitro for the presence of HIV-1 neutralizing antibodies. Depending of the neutralization titres obtained we may need to perform additional immunizations as required (Maximum of 3 immunizations, followed by 10 ml blood draw after 2 weeks). Once neutralization titres have been confirmed, additional blood samples will be drawn from the ear (1 x 10ml EDTA) for PBMC isolation and memory B-cell interrogation. If we are successful at isolating the appropriate B-cell lineage after one blood draw, then the experiment can be terminated. If unsuccessful, we would require additional blood draws (maximum 2 times)."

j. Motivation for modification / extension:

AESC 2017 M&E

Motivation for time extension

Several delays were incurred during the initial phase of this project. The FACS ARIA instrument required for the B-Cell sorting required upgrading before training could commence. A week long training course was conducted by the BD technicians on 26 March 2018. Having received adequate training on the instrument, each rabbit received a single boosting immunisation and the anti HIV-1 neutralization titres were confirmed in our in-house *in vitro,* neutralization assay. We isolated Rabbit PBMCs and are currently optimizing the single B cell sorting methodology on the BD FACS Aria instrument and subsequent rabbit antibody variable region PCR amplification. As this was a new project, considerable time was required for the optimisation of the above protocols and thus overran the time allocated on the current M&E (Expired 30 June 2018). We would like to perform the additional blood draws and immunizations required (provision for two additional immunizations, plus two 10ml blood draws for PBMC isolation following each immunization from the previous M&E) for isolation of PBMC and subsequent antibodies. However, our major concern is for the welfare of the rabbits as this study has been ongoing since 2014. Assessment of the three rabbits was conducted by Dr Jardine (her report is attached to this application). She confirmed that there were no clinical manifestations present that would prohibit their inclusion in the study if the time extension was awarded.

Date: 25 August 2018 Signature:

RECOMMENDATIONS

Date: 14TH SEPTEMBER 2018 Signature:

Chairman, AESC

References

(Seeber et al., 2014, Starkie et al., 2016)SEEBER, S., ROS, F., THOREY, I., TIEFENTHALER, G., KALUZA, K., LIFKE, V., FISCHER, J. A., KLOSTERMANN, S., ENDL, J., KOPETZKI, E., PASHINE, A., SIEWE, B., KALUZA, B., PLATZER, J. & OFFNER, S. 2014. A robust high throughput platform to generate functional recombinant monoclonal antibodies using rabbit B cells from peripheral blood. *PLoS One,* 9, e86184.

STARKIE, D. O., COMPSON, J. E., RAPECKI, S. & LIGHTWOOD, D. J. 2016. Generation of Recombinant Monoclonal Antibodies from Immunised Mice and Rabbits via Flow Cytometry and Sorting of Antigen-Specific IgG+ Memory B Cells. *PLoS One,* 11, e0152282.

Appendix D: Recipes

B1) Agarose gel electrophoresis

B1.1) Preparation of 0.8% agarose gels

0.8 % agarose gels were made by adding 0.8 g of agarose powder (Sigma-Aldrich, St. Louis, MO, USA) to 100 ml of 1 × TAE buffer (Thermo Fisher Scientific, Waltham, MA, USA). The mixture was heated to dissolve the agarose powder, and ethidium bromide (Promega, Fitchburg, WI, USA) was added to the mixture at a final concentration of 0.5 µg/ml. The gels were poured into a Bio-Rad gel Chamber System (Bio-Rad, Hercules, CA, USA) and allowed to set at room temperature.

B1.2) Agarose gel electrophoresis procedure

The set agarose gels were placed in the Bio-Rad Gel Tank System (Bio-Rad, Hercules, CA, USA) containing 1 × TAE buffer to allow for even current during DNA migration through the gel. The DNA samples, and controls were mixed with 6x Orange DNA Loading Dye (Thermo Fisher Scientific, Waltham, MA, USA). The mixed samples, controls and the O'Gene Ruler DNA Ladder mix, Ready-to-use (Thermo Fisher Scientific, Waltham, MA, USA) were loaded into respective wells of the gels. The gels were run at 80 V for 45 to 60 minutes, or until the samples were adequately resolved. DNA bands on the gels were visualised and images captured under UV light using the ChemiDoc™ MP imaging system from Bio-Rad (Bio-Rad, Hercules, CA, USA) and the QuantityOne version 4.6.9 Software Programme (Bio-Rad, Hercules, CA, USA).

B2) SDS-PAGE

B2.1) Monomer Solution: 30% Acrylamide/ 0.8% Bisacrylamide

30 g of acrylamide (Sigma-Aldrich, St. Louis, MO, USA) and 0.8 g of bisacrylamide (N, N'-methylenebisacrylamide) (Sigma-Aldrich, St. Louis, MO, USA) were dissolved in dH_2O to a final volume of 100 ml and stored in the dark at 4℃ until needed.

B2.2) Stacking Gel Buffer: 4X Tris-HCl, pH 6.8 (0.5 M Tris)

6.05 g Tris (USB, Cleveland, OH, USA) was dissolved in dH_2O to a volume of 40 ml. The pH was adjusted to 6.8 and made up to a final volume of 100 ml and was stored in the dark at 4℃ until needed.

B2.3) Separating Gel Buffer: 4X Tris-HCl, pH 8.8 (1.5 M Tris)

91 g Tris was dissolved in dH_2O to a volume of 300 ml. The pH was adjusted to 8.8 and made up to a final volume of 500 ml with dH_2O and was stored in the dark at 4℃ until needed.

B2.5) 10% Ammonium Persulphate (APS)

0.1 g of APS (Sigma-Aldrich, St. Louis, MO, USA) was dissolved in dH_2O to a final volume of 1 ml. A fresh solution was made up each time.

B2.6) 10×Tank Buffer

30.28 g Tris-HCl, 144.13 g of glycine, 10 g SDS dissolved in dH_2O to a final volume of 1 L.

Appendix E: Plagiarism form

UNIVERSITY OF THE WITWATERSRAND, JOHANNESBURG

FACULTY OF HEALTH SCIENCES

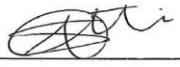
PLAGIARISM DECLARATION TO BE SIGNED BY ALL HIGHER DEGREE STUDENTS

SENATE PLAGIARISM POLICY: APPENDIX ONE

I Simone Ashleigh Smith (Student number: 806594) am a student registered for the degree of MSc (Med) in the academic year 2020.

I hereby declare the following:

- I am aware that plagiarism (the use of someone else's work without their permission and/or without acknowledging the original source) is wrong.
- I confirm that the work submitted for assessment for the above degree is my own unaided work except where I have explicitly indicated otherwise.
- I have followed the required conventions in referencing the thoughts and ideas of others.
- I understand that the University of the Witwatersrand may take disciplinary action against me if there is a belief that this is not my own unaided work or that I have failed to acknowledge the source of the ideas or words in my writing.
- I have included as an appendix a report from "Turnitin" (or other approved plagiarism detection) software indicating the level of plagiarism in my research document.

Signature:  Date: 27/03/2020